# HYDROGEOMORPHOLOGICAL CONTROLS ON STREAM CHEMISTRY AND AQUATIC BIOTA IN THE CATSKILL MOUNTAINS, NEW YORK STATE

A Dissertation

Presented to the Faculty of the Graduate School

of Cornell University

In Partial Fulfillment of the Requirements for the Degree of

Doctor of Philosophy

by

Adrian Adam Harpold

May 2010

# HYDROGEOMORPHOLOGICAL CONTROLS ON STREAM CHEMISTRY AND AQUATIC BIOTA IN THE CATSKILL MOUNTAINS, NEW YORK STATE

Adrian Adam Harpold, Ph.D.

Cornell University 2010

Traditional Darcy-based models have not been providing satisfactory answers for watershed scientists working in complex landscapes and new methods are thus being developed. Ideally these new methods would characterize discharge patterns, estimate stream chemistry, and can be transferrable between complex and heterogeneous watersheds. In this dissertation, we develop two such methods by relating hydrologic and geomorphologic (or 'hydrogeomorphologic') properties to stream chemistry, biota and (preferential) flow patterns. The research is carried out in two different, well-studied watersheds in the Catskill Mountains, New York State: Neversink River and Town Brook.

The 176 $km^2$ Neversink River watershed has a detailed discharge, chemistry, and biotic data for nested sub-watersheds (0.2 to 160 $km^2$) that are affected by acid rain. The results from the Neversink River watershed showed that baseflow stream acid buffering chemistry (ANC values and $Ca^{2+}$ concentrations) was reduced in subwatersheds

that were steeper or had more stream channels. Although speculative, we believe that long-term flushing of base cations from the shallow soils during storm runoff events reduces the acid buffering chemistry during baseflow. A simple geomorphologic relationship, based on mean slope and stream channels per area, was

strongly correlated to populations of aquatic biota (macroinvertebrate, periphytic diatom, and fish) in 'ungaged' sub-watersheds where discharge was not measured.

Town Brook watershed (2.5 $km^2$) was investigated to determine the sources and flowpaths of water during nine rainfall events from April 2007 to October 2007. A combination of hydrometric, chemical, and isotopic data sets was measured and surface saturation maps were developed. The results suggested that during precipitation events greater than 1 cm, hill side saturation areas caused by groundwater springs and soil pipes were a significant runoff source. The properties commonly used to infer surface saturation areas in Town Brook (i.e. slope, upslope area, and/or soil transmissivity) predicted general spatial patterns, but were insufficient to estimate surface saturation at the smallest scales measured (<100 $m^2$).

The success of hydrogeomorphologic properties in estimating stream acid buffering chemistry and watershed saturation patterns in the two Catskill watersheds suggest that simple alternatives to traditional Darcy-based predictions may be applicable under certain conditions.

## BIOGRAPHICAL SKETCH

Adrian Adam Harpold was born in Seattle, Washington to Mindy Nichols and Hal Harpold in 1981. Most of his childhood was spent in western Washington exploring the woods and streams behind his house. His father's job took them to North Carolina, where he finished high school in Winston-Salem. His undergraduate years were spent as a Hokie at Virginia Tech. This was a very expanding period for Adrian's career interests in academia. Adrian completed his Masters in 2003 and matriculated to Cornell University shortly thereafter. His first position after his doctorate was at the University of Arizona Hydrology and Water Resources department.

# ACKNOWLEDGMENTS

There are many people that need to be thanked and acknowledged for their help in this effort. First I would like to acknowledge the friends and family that supported me during the final stage of my dissertation writing. My mother and father have been incredibly helpful and supportive during some of the most difficult times. My friend Adam Blakney let me use his office space for more than a year (for free), without which I may not have been able to finish. All of my friends have been incredibly supportive and patient when I could never visit or take time off.

Next, I would like to thank all of my collaborators and partners in this work. Particularly I would like to thank Mike McHale from the USGS who helped me get key data and visited Town Brook multiple times. It is important to thank my collaborators Steve Shaw of Cornell, who was my most consistent resource. I would also acknowledge Steve Lyon of the University of Stockholm, who is always motivated to do something new. Finally, Peter Troch of the University of Arizona for running the water isotope samples from Town Brook.

Lastly, I would like to thank my academic advisers, all of which have shaped my view of research and hydrology. My mentors from Virginia Tech continue to be important friends and mentors, Tess Wynn and Saied Mostaghimi. My advisers at Cornell were extremely influential in the last four years. Todd Walter has taught me how to enjoy what you do and to do what you enjoy, an important learning experience for any young scientist. Doug Burns has research interests most similar to my own, and thus it has been extremely rewarding to work and learn from him. Finally, Tammo Steenhuis has be my main adviser throughout this process, even when it wasn't clear how I was going to finish, he trusted that I could get it done.

TABLE OF CONTENTS

LIST OF FIGURES

LIST OF TABLES

# CHAPTER 1

# INTRODUCTION

Watershed hydrology is a puzzle with many pieces. When viewed together, these pieces can explain the sources, ages, and flowpaths water takes from the point it lands as precipitation to when it leaves a watershed. Collectively this information is also needed to help predict stream chemistry and aquatic habitat. However, the explicit mapping of the heterogeneous properties is impractical, even in small research watersheds (Beven and Feyen, 2002; McDonnell et al., 2007). It is even more difficult to predict how these properties change across spatial scales, which is critical to effectively managing water resources in larger areas (NRC, 1991; McDonnell et al., 2007).

The Catskill Mountains are the water supply for New York City's population of 8 million people. The Catskills are also a mixed land-use area, necessitating management for water quality issues to protect drinking water supplies and freshwater ecology. The dominant concerns for local water management agencies are water-borne pathogens, sediment, and nutrients (NRC, 2000), who sources are typically related to agriculture, urban/suburban development, and/or other natural processes. . A wide range of governmental and citizen groups work to protect and manage the water resources of the Catskills (Galusha, 2002).

The glacially-derived soils and heterogeneous geohydrology of the Catskills (Rich, 1934; Kirkland, 1973; Ozvarth, 1985) result in complicated spatial variability; this limits the prediction of stream chemistry (i.e. Wolock et al. 1997) and aquatic biota (i.e. Baldigo and Lawrence, 2001). The goal of this dissertation was thus to

evaluate whether 'hydrogeomorphologic' properties can be effective predictors of stream chemistry and aquatic biota in two Catskill watersheds. Town Brook sub-watershed is 2.5 $km^2$ and characterized by relatively short, steep forested hill sides and very-wide agricultural valley-bottoms with thick glacial deposits and shallow perched water tables. In contrast, the Neversink River watershed is much larger (176 $km^2$) and dominated by steep, forested hill sides with shallow till soils and narrow valley bottoms with minimal thick glacial deposits.

## 1.1 Summary of Chapters

The next two chapters in this dissertation explore the hydrological, chemical, and ecological response of the Neversink. Chapter 2 improves previous speculation as to why adjacent Neversink sub-watersheds have strongly varying acid buffering chemistry (acid neutralizing capacity ANC and calcium $Ca^{2+}$). The complex hydrology of the Neversink inhibits some distributed models for explaining the variable stream chemistry (i.e. Wolock et al., 1997), thus a simple regression analysis is employed using numerous widely-available hydrogeomorphologic properties. The hydrogeomorphologic relationship developed in Chapter 2 is then correlated to the populations of aquatic biota (fish, diatom, and macroinvertebrate inventories) in Chapter 3.

Town Brook sub-watershed (2.5 $km^2$) is investigated in more detail in Chapter 4 to determine the dominant hydrological flowpaths and source areas at smaller, more detailed scales. These investigations use hydrometric, chemical, and isotopic measurements to detail runoff sources during nine storm events. The hydrometric measurements include detailed mapping of saturated areas, which help to validate conventional distributed geomorphologic properties at the hillslope-scale. Finally,

Chapter 5 synthesizes the dissertation results and speculates on how and when hydrogeomorphologic properties could be used to improve predictions of stream chemistry and aquatic biota in the Catskill Mountains.

REFERENCES

Baldigo, B.P. and G.B. Lawrence. 2001. Effects of stream acidification and habitat on fish populations of a North American river. Aquatic Sciences. 63: 196-222.

Beven, K. and J. Feyen. 2002. The Future of Distributed Modeling. Hydrological Processes. 16: 169-172.

Galusha, D. 2002. In Liquid Assets: A History of New York City's Water System. 303 pp. Purple Mountain Press: Fleischmanns, NY.

Kirkland, J.T. 1973. Glacial geology of the western Catskills. State University of Binghamton. Doctoral dissertation. 104p.

McDonnell, J.J., M. Sivapalan. K. Vache, S. Dunn, G. Grant, R. Haggerty, C. Hinz, R. Hooper, J. Kirchner, M.L. Roderick, J. Selker, and M. Weiler. 2007. Moving beyond heterogeneity and process complexity: A new vision for watershed hydrology. Water Resources Research. 43. W07301. Doi:10.1029/2006 WR005467.

National Research Council (US). 1991. Opportunities in the Hydrologic Sciences. National Academy Press: Washington DC.

National Research Council (US). 2000. Watershed management for potable water supply: Assessing the New York City strategy. National Academy Press: Washington D.C.

Ozvarth, D.L. 1985. Glacial geomorphology and the late Wisconsinsian deglaciation of the western Catskill Mountains. State University of New York at Binghamton, Doctoral Dissertation. 181p.

Rich, J.L. 1934. Glacial Geology of the Catskills. New York State Bulletin, 299. University of the State of New York, Albany. 180 pp.

Wolock, D.M., J. Fan, and G.B. Lawrence. 1997. Effects of basin size on low-flow stream chemistry and subsurface contact time in the Neversink River Watershed, New York. Hydrological Processes. 11:1273-1286.

Chapter 2

# RELATING HYDROGEOMORPHOLOGIC PROPERTIES TO STREAM BUFFERING CHEMISTRY IN THE NEVERSINK RIVER WATERSHED, NEW YORK STATE, USA

## 2.1 Abstract

Monitoring the effects of acidic deposition on aquatic ecosystems in the Northeastern U.S. has generally required regular measurements of stream buffering chemistry (i.e. acid neutralizing capacity ANC and calcium $Ca^{2+}$), which can be expensive and time consuming. The goal of this paper was to develop a simple method for predicting baseflow buffering chemistry based on the hydrogeomorphologic properties of ten nested watersheds in the Neversink River basin (2.0 to 176.0 $km^2$), an acid-sensitive basin in the Catskill Mountains, New York State. The tributaries and main reach watersheds have strongly contrasting mean baseflow ANC values and $Ca^{2+}$ concentrations, despite rather homogeneous vegetation, bedrock geology, and soils. A stepwise regression was applied to relate thirteen hydrogeomorphologic properties to the mean baseflow ANC values and $Ca^{2+}$ concentrations. The regression analysis showed that watersheds with lower ANC values had a higher mean ratio of 'quickflow' runoff to precipitation during twenty non-snowmelt runoff events (referred to as mean *Runoff Ratio*). The mean *Runoff Ratio* could explain at least 80% of the variability in mean baseflow ANC values and $Ca^{2+}$ concentrations among the ten watersheds. Greater mean *Runoff Ratios* also correlated with steeper slopes and larger drainage densities, thus allowing the prediction of baseflow ANC values ($r^2$=0.75) and $Ca^{2+}$ concentrations ($r^2$=0.77) with

widely-available spatial data. These results indicate that hydrogeomorphologic properties can explain a watershed's sensitivity to acid deposition in regions where the spatial sources of stream buffering chemistry from the bedrock mineralogy and soils appear to be fairly uniform.

## 2.2 Introduction

Strong mineral acidity in atmospheric deposition, largely resulting from the burning of fossil fuels, has acidfied surface waters and degraded aquatic ecosystems in the Northeastern U.S. (Driscoll et al., 2001; 2003). Streams become acidic if the acid neutralizing capacity (ANC), maintained by the release of base cations from mineral weathering and cation exchange, is less than the influx of acidic anions from the atmosphere and other sources. Chronically acidic streams have low ANC values during baseflow and high flow, whereas waters that are buffered during baseflow but have low ANC values during high flow are considered episodically acidified (Evan et al., 1995; Wigington et al., 1996a; 1996b).

Simple models based on discharge have been developed to predict the response of stream buffering chemistry ($Ca^{2+}$ and ANC) during episodic acidification (e.g. Davies et al., 1999; Wade et al., 1999). Kirchner et al. (1993a and 1993b) suggested that acid buffering chemistry (ANC and sum of base cations) is a logarithmic function of stream discharge and is not greatly affected by variable spatial sources of buffering. However, all these models require calibration to baseflow chemistry measurements and do not adequately explain why differences in baseflow chemistry occur (Van Sickle et al., 1997).

Predicting a watershed's ability to buffer acidity during baseflow is crucial to cost-effective management of stream chemistry and biota in the Northeastern U.S.

(Peters and Driscoll, 1987; Van Sickle et al., 1997). Regression models for predicting buffering chemistry at baseflow typically relate average stream chemistry values to geologic, land-cover, topographic, and/or soil properties (Wolock et al., 1997; Clow et al., 2000; Cooper et al., 2004; Sullivan et al., 2007). These spatial properties are used to infer the sources and flowpaths that control baseflow buffering chemistry (Peters and Driscoll, 1987; Wigington et al., 1992). Since variations in many of these subsurface properties (i.e. geology and soils) are mapped rather coarsely, these empirical models are sometimes impractical for management of smaller, more spatially uniform watersheds (Cooper et al., 2004). In these more uniform watersheds it is more likely differences in geomorphology (i.e. topography and drainage characteristics) that control the sources and flowpaths also cause variable baseflow buffering chemistry (Peters and Driscoll, 1987; Wigington et al., 1992).

The 176 $km^2$ Neversink River watershed (hereafter referred to as the Neversink) in the Catskill Mountains in New York State illustrates the difficulties of quantifying the sources and flowpaths that control stream buffering chemistry. The Neversink receives among the highest amounts of acidic deposition in North America (Murdoch and Stoddard, 1993) and streams there have shown little recovery since implementation of Title IV of the Clean Air Act Amendments in 1990 (Lawrence et al., 1999; Murdoch and Shanley, 2002; Burns et al., 2006). Despite similar land cover, geology, and soil series throughout the Neversink, sub-watersheds differ from chronically acidic, to episodically acidic, to well-buffered (Figure 2.1a,b,c). Neversink watersheds have vastly different low-flow ANC values, but become more similar at high-flow when ANC values of 0 μeq/L or less are frequently observed (Figure 2.1), when less buffered event water dominates streamflow. Despite a convergence towards similar ANC values at high flow, Figure 2.1 indicates large

differences in these values during most of the flow regime, which emphasizes to the importance of developing a conceptual framework that could indicate why such differences in baseflow ANC occur in the Neversink.

Explanations for the differences in the buffering chemistry of the Neversink sub-watersheds during baseflow (low-flows shown in Figure 2.1) include geological heterogeneities as reflected by the underlying bedrock lithology (Baldigo and Lawrence, 2000), the presence of carbonate rocks imported by glaciers from other watersheds (Stoddard and Murdoch, 1991), the distribution of groundwater springs (Burns et al., 1998a; Baldigo and Lawrence, 2000; Shaman et al., 2004), watershed area or topography (Wolock et al., 1997; Vitvar et al., 2002; Shaman et al., 2004), or gradients in acidic deposition due to elevation (Lovett et al., 1999; Lawrence, 2002). Thus far, none of these explanations has been able to adequately characterize the variable response and effects of stream acidification in the Neversink.

Another explanation for the differences in stream buffering chemistry is that variable geomorphology causes differences between watersheds. Differences in baseflow ANC in the Neversink could not be predicted, however with a distributed model of subsurface contact times (Wolock et al., 1997). In addition, residence time estimates using $^{18}O$ and $^{35}S$ indicate that stream baseflow (~300 days old) is derived from the mixing of a deeper groundwater system (groundwater springs had residence times of ~500 days) and faster, shallow flowpaths (Burns et al., 1998a). The shallow flowpaths rapidly transfer rain ('event') water through the organic horizon to the stream during runoff events (Brown et al., 1999). From these intensive field measurements in the Neversink it appears that differences in the dominant 'flowpaths' between watersheds may in part explain the wide variations in baseflow buffering chemistry.

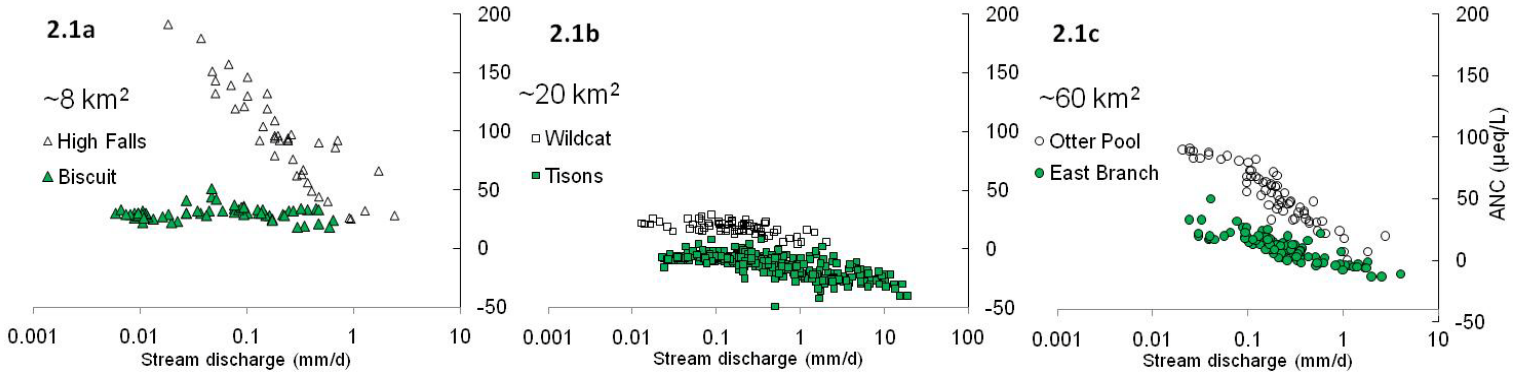


Figure 2.1: The ANC values as a function of discharge for ~8 km$^2$ watersheds (2.1a), ~20 km$^2$ watersheds (2.1b), and ~60 km$^2$ watersheds (2.1c) using data from June 1991 to October 1993.

. The units and methods used to derive these properties are explained in Table 2.1.

The goal of this research is to identify hydrologic and geomorphologic (referred to as 'hydrogeomorphologic') properties that can adequately explain the differences in $Ca^{2+}$ concentrations and ANC values among ten Neversink sub-watersheds during baseflow. Specifically we hope to 1) identify hydrogeomorphologic properties that may characterize the distribution of 'fast' (shallow) and 'slow' (deep) flowpaths, 2) determine if simple statistical relationships exist between hydrogeomorphologic properties and baseflow ANC values and $Ca^{2+}$ concentrations, and 3) understand how to apply these relationships to improve the monitoring and management of acid buffering chemistry in the Neversink.

## 2.3 Methodology

In this section we first discuss the characteristics and type of data collected at the study site. This is followed by a description of how the hydrologic and hydrogeomorphologic properties are calculated. Finally, we detail stepwise linear regression models that were used to develop relationships between hydrogeomorphologic properties and the mean growing-season ANC values and $Ca^{2+}$ concentrations.

### 2.3.1 Study Site

The Neversink River Watershed is located in the Catskill Mountains of southeastern New York State (Figure 2.2a) and is typical of many Northeastern U.S. watersheds. The Catskills received very high amounts of acidic deposition during the study period or 1991 to 1993 (Stoddard and Murdoch, 1993); sulfate loads at the National Trends Network monitoring gage in Biscuit Brook (634 m) were ~30 kg/ha in 1992 compared to ~20 kg/ha in 2002 (see Murdoch and Shanley, 2006). The Catskill Mountains were formed by the dissection of an uplifted bedrock plateau by

streams and glaciers (Rich, 1934). The bedrock mineralogy is spatially uniform with flat laying Upper Devonian-age bedrock, as much as 2000 m thick (Rich, 1934). The highly erosion resistant bedrock is 60% sandstone, with horizontal shale and siltstone bedding planes. The major surficial geological features are till, kame terraces, outwash sand and gravel, recent alluvium, and exposed rock (Figure 2.2b). The extent of till results from deglaciation processes, which left loose ablation till in the valley bottoms and lodgement till in the upland tributaries (Ozvarth 1985). The lodgement till, formed under moving glaciers, is typically less than 1.0 m in depth and highly compacted (Figure 2.2b). Thicker ablation till deposits, formed at active ice margins, create kame terraces (Figure 2.2b) and other recognizable glacial features. Glacial outwash and recent alluvium form narrow deposits of coarse sand and gravel over parts of the valley bottom (Figure 2.2b).

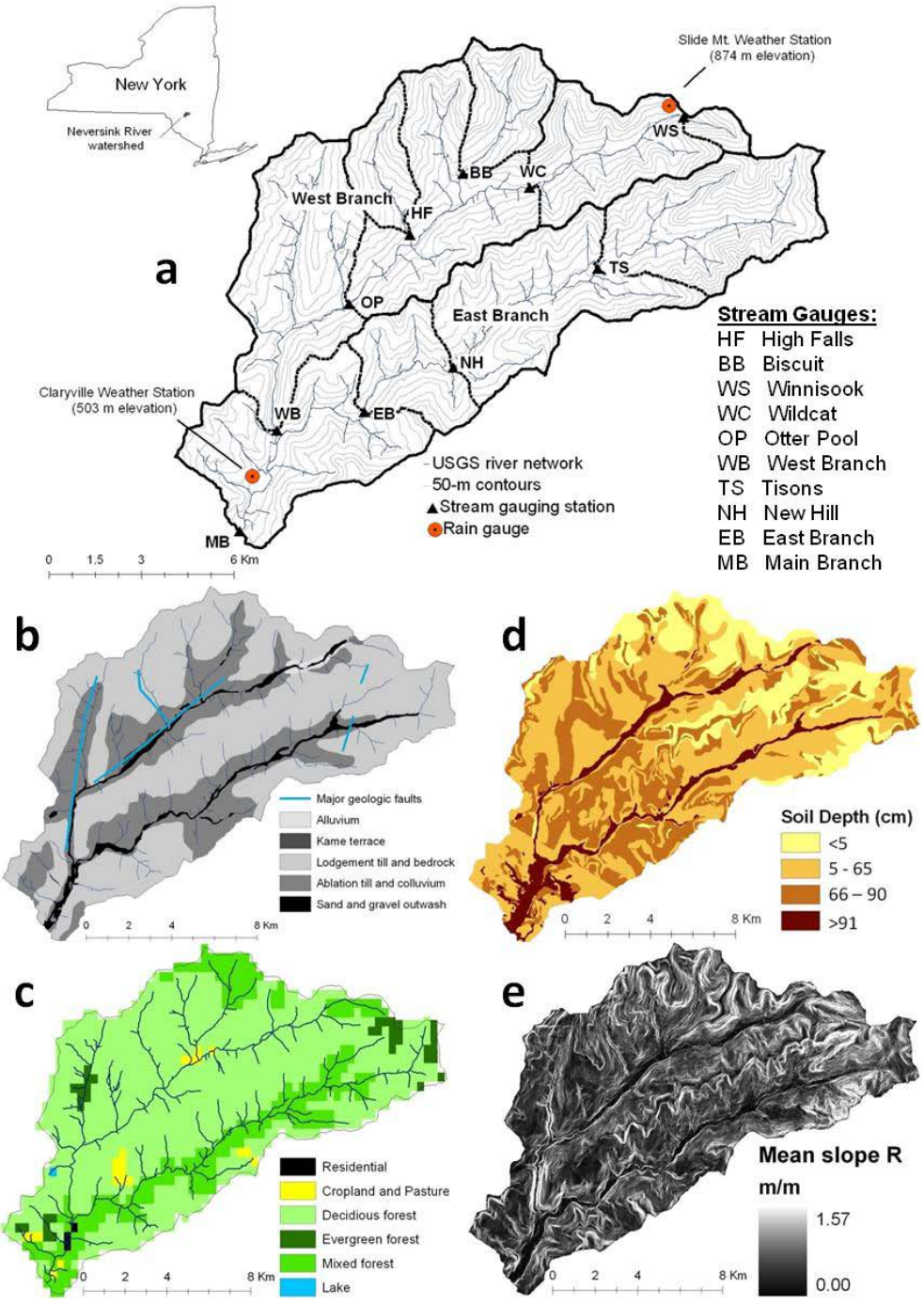


Figure 2.2: Overview of the Neversink and monitoring locations (2.2a). 2.2b shows surficial geology, 2.2c shows land cover, 2.2d shows soil depths, 2.2e is the slope.

The Neversink watershed originates at the summit of Slide Mountain (elevation 1274 m) and drains into the Neversink reservoir (elevation 408 m), a drinking water supply for New York City. The average annual precipitation at Slide Mountain was 1570 mm from 1950 to 1985, of which 20-35% falls as snow (Thaler 1996). Cold winter temperatures (mean 3.3 $^{o}$C at Slide Mountain) and spring rains typically produce peak discharge during snowmelt in April and May (Thaler 1996). The Neversink watershed has steep slopes (mean slope 0.24 m/m), quick-draining shallow till soils, and slowly weathering bedrock (Murdoch and Stoddard, 1993) and lacks major surface water storage, with only two ponds larger than 3 ha. The land cover is predominately forested (>98%) (Figure 2.2c), consisting of American beech, red maple, sugar maple, and yellow birch (Kudish 2002). The forests have returned after being harvested in the mid-19$^{th}$ century (Kudish 2002). The small residential area near the outlet occupies less than 0.25% of the watershed. Unlike some other areas in the Catskills with more suitable soils, very little land in the larger valley-bottom was cleared for agriculture or grazing (Kudish 2002). The soils are classified as Inceptisols in the Arnot-Oquaga-Lackawanna series (Soren 1961).

### 2.3.2 Data Sources

The study period is from June 1, 1991 through October 1, 1993, when the USGS collected water samples at all ten sites in the Neversink for chemical analysis. Year-round water quality samples were collected irregularly and with different frequencies among the watersheds, these year-round data were used to construct concentration-discharge relationships (six watersheds shown in Figure 2.1a,b,c). However, the statistical comparisons of stream buffering focus on a subset of data from the growing-season (June 1 through September 30) to minimize the influence of snowmelt and that generally correspond to baseflow sampling conditions.

The water samples from the growing-season were not collected simultaneously in all ten watersheds, but in general were sampled every 2 to 6 weeks. The different sampling rates meant that a total of 10 to 28 water samples were collected in each of the ten watersheds during the growing-seasons of 1991, 1992, and 1993. Standard deviation is also reported for the growing-season ANC and $Ca^{2+}$ concentrations indicate stable baseflow concentrations and relatively similar variance among watersheds. All samples were analyzed for ANC and calcium $Ca^{2+}$ (reported in μeq/L and μmol/L, respectively), using the methods described by Lawrence et al., (1995) and estimates of laboratory error given by Lincoln et al., (1996). The ANC samples were unfiltered and measured by Gran titration.

Daily precipitation was provided by the Northeast Regional Climate Center in Ithaca, N.Y. for the upper (Slide Mountain) and lower (Claryville) rain gages (Figure 2.2a). Discharge data were collected by the U.S. Geological Survey (USGS) at 15 minute intervals from ten gaging stations (Figure 2.2 a). The 15 minute data were used unless the gage was not operable (i.e. frozen in winter), in which case daily discharge was estimated via alternative methods.

Other data sources available were a 10 m by 10 m digital elevation model (DEM) and locations of gaging stations from the USGS. Surficial geological maps were produced by the New York State Museum (NYSM) and USGS (Figure 2.2b). Finer scale interpretations of sand and gravel deposits and soil depth (to restricting layer) were made via Soil Survey Geographic Database SSURGO data (Figure 2.2b,d). Bedrock geological maps also produced by the NYSM and USGS showed uniform lithology, but spatial data are not included for brevity. Digital line graphs representing stream channels were taken from the National Hydrography Dataset (NHD) available from the USGS.

### 2.3.3 Calculating Hydrogeomorphologic Properties

The ten geomorphological and three hydrological 'properties' used in this study were chosen from previous studies involving flowpath distribution (e.g. McGuire et al., 2004; Sanford et al., 2007; Tetzlaff et al., 2009). The ten properties are listed in Table 2.1 for each nested watershed: area (*A*), mean elevation (*ELEV*), mean slope (*S*), profile curvature ($Curve_{pro}$), ratio of median flowpath length to flowpath gradient (*L/G*), topographic index (*TI*), drainage density (*DD*), soil topographic index (*STI*), average hillside soil depth ($Store_{hill}$), and fraction of sand and gravel deposits ($Store_{s\&g}$). A brief description of the methods used to calculate the parameters follows and is supplemented in Table 2.1.

Table 2.1: Hydrogeomorphologic properties used in the stepwise linear regression to estimate stream buffering chemistry.

| Watershed indicator | Symbol | Units | Data sources and methods |
|---|---|---|---|
| Watershed area | $A$ | $km^2$ | GIS delineation using USGS gage locations and 10 m DEM |
| Mean elevation | *ELEV* | m | Mean elevation for all cells in a 10m DEM |
| Mean slope | $S$ | m/m | Watershed mean using all cells in a 10m DEM |
| Profile curvature | $Curve_{pro}$ | deg/mm | Profile curvature is calculated at the watershed outlet using ArcGIS toolbox and 10m DEM |
| Median flowpath length by flowpath gradient | *L/G* | m | The median of all flowpath lengths divided by the flowpath slopes from a 10-m DEM using ArcGIS toolbox |
| Topgraphic index, ln(α/tan β) | *TI* | ln(m) | Measure of lateral flow, calculated using ArcGIS toolbox using 10m DEM and following the methods of Beven (2001), where α is the contributing area per contour line and tan β is the local slope. |
| Drainage density | *DD* | $m/m^2$ | Total stream length from USGS HHD delineated channels per watershed area |
| Soil topographic index ln(α/$T_o$tan β) | *STI* | ln($dm^{-1}$) | Measure of lateral flow and surface saturation, calculated using GIS estimates from a 10m DEM and SSURGO soil survey to estimate transmissivity $T_o$, following methods of Beven (2001) |
| Hillside soil depth | $Store_{hill}$ | m | Mean depth of soil layer above impermeable material, excluding areas covered with sand and gravel deposits identified from SSURGO data |
| Fraction of area covered by sand and gravel deposits | $Store_{s\&g}$ | $m^2/m^2$ | Fraction of watershed area covered by sand and gravel deposits as measured by SSURGO data |
| Median discharge | $Q_{50}$ | mm/d | Median mean daily discharge for growing-season (6/1 to 9/30) during WY1992 and WY1993 follow Helsel and Hirsch (1993) |
| Discharge exceeded 90% of days | $Q_{90}$ | mm/d | Same as above, but mean daily 'low-flow' exceeded 90% of days. |
| Runoff ratio | *Runoff Ratio* | m/m | Mean ratio of discharge to precipitation during 20 non-snowmelt events, quickflow is separated following methods Hewlitt and Hibbert (1967) |

Both the mean elevation and mean slope are calculated as the mean of all 10 m

DEM cells within the watershed. Profile curvature reflects the change in gradient along the slope line and is calculated at the watershed outlet using the Spatial Analyst Tools within ArcGIS. The flowpath length is divided by the cell-slope for every DEM-cell using ArcGIS, and the median L/G value across the watershed is given. The drainage density is stream length (perennial streams defined by the NHD) divided by the watershed area. The *TI* and *STI* (Beven, 2001) incorporate combinations of topographic and soil features to estimate the spatial probability of runoff and were computed in ArcGIS using the Spatial Analyst Toolbox. The TI only requires the DEM, while the *STI* is calculated from a DEM and soil properties given in the SSURGO data. The average hillside soil depth is computed as the average soil depth from SSURGO maps, excluding all sand and gravel deposits (if present). Lastly, the fraction of sand and gravel deposits is given per watershed area from SSURGO measurements.

Three hydrological properties are also considered: the median of the growing-season mean daily discharges ($Q_{50}$), the growing-season mean daily low-flow exceeded 90% of the time ($Q_{90}$), and the mean runoff ratio (*Runoff Ratio*). The growing-season $Q_{50}$ and $Q_{90}$ are computed following Helsel and Hirsch (1993) for the mean daily discharge data for June 1 to September 30 in WY1992 and WY1993.

The *Runoff Ratio* is the average volume of 'quickflow' runoff to event precipitation during twenty non-snowmelt storm events. Daily precipitation total for any of the 10 watersheds were normalized using a linear relationship based on mean watershed elevation:

$$P_i = P_{Claryville} + \frac{(E_i - E_{Claryville})}{E_{SlideMt} - E_{Claryville}} \left(P_{SlideMt} - P_{Claryville}\right) \qquad \text{E}quation\ 1$$

where $P_i$ is the total daily rainfall in watershed i , $E_i$ is the mean elevation of watershed

i, $E_{Claryville}$ is the elevation at the Claryville rain gage (503 m), $E_{SlideMt}$ is the elevation at the Slide Mt. rain gage (874 m), and $P_{Claryville}$ and $P_{SlideMt}$ is the total daily rainfall at the Claryville and Slide Mt. gages, respectively.

The storms were selected for calculating the mean *Runoff Ratio* such that 1) events lasted longer than 4 days with minimum 3 days of recession and precipitation was >8 mm, 2) differences in precipitation between two rainfall gages was <100%, 3) storms were excluded if snowmelt/snowfall was likely based on the precipitation type and air temperature measured at the rain gages that could have affected the timing and volume of peak runoff. The *Runoff Ratios* were calculated from throughout the year to capture a sufficient number of non-snowmelt storms necessary for the analysis, which would not have been possible if only storms during the growing-season were used. The bulk of the runoff events (eleven) did occur during the growing-season (June to September), two in October, three in November, one in March, and three in May. The 'quickflow' separations were done according to Hewlitt and Hibbert (1967), by placing a line from the initial rise of the hydrograph with a slope of 0.8 mm $h^{-1}$ $km^{-2}$ until it intersects the recession limb.

### 2.3.4 Statistical Analysis

The nested nature of the Neversink sub-watersheds likely caused the hydrogeomorphologic properties to be correlated, which is common in these type of investigations (Buttle and Eimers, 2009; Sanford et al., 2007). In addition to the correlations, the lack of a theoretical basis for developing a physical hydrological model based on these properties, encouraged a more exploratory, statistical approach in which forward stepwise linear regression analysis (Draper and Smith, 1981) was used to predict mean baseflow stream buffering chemistry. The Pearson product-

moment correlation coefficient (reported as r-values) were determined between all the hydrogeomorphologic properties to evaluate their statistical independence using Matlab (Mathworks version R2008a) and p-values were estimated based on the student t-distribution and a 95% confidence level.

The forward stepwise regression was performed in Matlab to develop the most highly predictive model for stream buffering chemistry as a function of the 13 hydrogeomorphologic properties (Table 2.1). The method fits an initial set of properties and then compares the explanatory power of incrementally larger and smaller sets of properties. If any properties not in the regression model had a p-value less than the entrance tolerance ($p<0.05$), the term with the smallest p-value was added; and if terms in the model had p-values greater than the exit tolerance ($p>0.10$) than the term with the largest p-value was removed. The resulting model was thus the largest set of properties with $p<0.10$ (based on F-tests using a 95% confidence interval). Residual plots were also evaluated to verify the assumptions of normality and homoscedasticity in the linear predictions.

## 2.4 Results

After demonstrating distinct spatial differences in stream buffering chemistry, stepwise linear regression models were used to develop relationships between hydrogeomorphologic properties and the mean growing-season ANC and $Ca^{2+}$ concentrations. We have defined the growing-season study period (June 1 to September 30) somewhat arbitrarily, but in general this period best captures the longest period during the year in which baseflow conditions are observed in this watershed.

During the growing-seasons of 1991, 1992, and 1993 the mean ANC varied

from -20±3 to 138±21 μeq/L and $Ca^{2+}$ varied from 25±5 to 107±21 μmol/L across the ten watersheds (Table 2.2). These results are consistent with Figure 2.1, showing that low-flows vary from well-buffered to acidic across the Neversink. The relative standard error remained nearly similar, despite the range of buffering chemistry (Table 2.2). The spatial patterns in mean growing-season ANC values and $Ca^{2+}$ concentrations can be seen in Figure 2.3a and 2.3b, respectively. The East Branch is more acidic than the West Branch, but both become gradually more buffered downstream (Figure 2.3). High Falls is the most well-buffered tributary (Figure 2.3 and Table 2.2) and shows the greatest response in ANC to changes in discharge (Figure 2.1a). It should be noted that acidic deposition was still high during the study period of 1991 to 1993 due to the relatively recent enactment of the Clean Air Act Amendments of 1990 (Stoddard and Murdoch, 1993; Murdoch and Shanley, 2006).

### 2.4.1 Relationship of Stream Buffering Chemistry to Hydrogeomorphologic Properties

The 13 hydrogeomorphologic properties used in the forward stepwise regression have significant correlation (Table 2.3). This correlation is not surprising considering the nested-nature of the watersheds, but should be considered in conjunction with the subsequent stepwise regression analysis (Draper and Smith, 1981). For example, the mean slope (*S*) was strongly correlated to *TI* (Pearson product moment correlation coefficient $r=-0.92$, $p<0.01$) and *Runoff Ratio* ($r=0.75$, $p<0.05$). The fraction of sand and gravel deposits ($Store_{rip}$) were statistically correlated to *L/G* and *DD* ($r=0.78$, $p<0.05$, and $r=0.83$, $p<0.01$, respectively). These correlations are important to consider when interpreting the results from the step-wise regression.

Table 2.2: Values of summer buffering chemistry and hydrogeomorphologic properties for the ten Neversink sub-watersheds. The units and methods used to derive these properties are explained in Table 2.1.

| | West branch tributaries | | | West branch main-stem | | | East branch main-stem | | | |
|---|---|---|---|---|---|---|---|---|---|---|
| | HF High Falls | BB Biscuit | WS Winn-isook | WC Wildcat | OP Otter Pool | WB West Branch | TS Tisons | NH New Hill | EB East Branch | MB Main Branch |
| ANC [a] | 138(21) | 30 (6) | -20 (3) | 22 (3) | 81 (15) | 115 (33) | -10 (4) | 9 (5) | 19 (8) | 68 (11) |
| $Ca^{2+}$ [a] | 107(21) | 71 (9) | 25 (5) | 51 (7) | 77 (12) | 95 (14) | 27 (4) | 42 (5) | 43 (7) | 70 (10) |
| $Q_{50}$ [a,b] | 0.38 | 0.37 | 0.33 | 0.30 | 0.39 | 0.39 | 0.47 | 0.41 | 0.35 | 0.37 |
| $Q_{90}$ [a,b] | 0.11 | 0.07 | 0.08 | 0.06 | 0.12 | 0.12 | 0.15 | 0.15 | 0.10 | 0.15 |
| *Runoff Ratio* | 0.08 | 0.15 | 0.21 | 0.15 | 0.11 | 0.12 | 0.19 | 0.15 | 0.15 | 0.15 |
| *A* | 7.2 | 9.8 | 2 | 20.8 | 66.8 | 89.2 | 23.6 | 49.1 | 60.4 | 176 |
| *ELEV* | 839 | 872 | 1038 | 869 | 819 | 788 | 901 | 824 | 798 | 770 |
| *S* | 0.25 | 0.276 | 0.318 | 0.276 | 0.253 | 0.239 | 0.285 | 0.247 | 0.243 | 0.235 |
| $Curve_{pro}$ | 5.4 | 3.0 | -5.3 | 7.8 | 6.5 | 6.6 | 10.0 | 9.1 | 9.2 | 75.0 |
| *L/G* | 2.15 | 2.43 | 2.44 | 3.08 | 2.69 | 2.53 | 3.06 | 3.06 | 2.87 | 2.52 |
| *TI* | 6.76 | 6.68 | 6.49 | 6.81 | 6.84 | 6.89 | 6.64 | 6.78 | 6.82 | 6.9 |
| *DD* | 0.85 | 0.94 | 0.85 | 0.94 | 0.99 | 1.32 | 1.22 | 1.36 | 1.32 | 1.35 |
| *STI* | 5.25 | 6.86 | 5.47 | 6.52 | 5.91 | 5.65 | 6.17 | 5.84 | 5.58 | 5.47 |
| $Store_{hill}$ | 0.158 | 0.114 | 0.145 | 0.101 | 0.112 | 0.122 | 0.090 | 0.103 | 0.111 | 0.119 |
| $Store_{s\&g}$ | 0.0 | 0.6 | 0.0 | 3.0 | 3.3 | 3.0 | 4.7 | 4.4 | 4.3 | 4.0 |

[a] – summer data (6/1 to 9/30), [b] – from WY1992 and WY1993 only, () refer to 1 standard deviation in concentrations.

Figure 2.3: Spatial variability of mean summer ANC values (2.3a) and $Ca^{2+}$ concentrations (2.3b) in the ten Neversink sub-watersheds. The units and methods used to derive these properties are explained in Table 2.1.

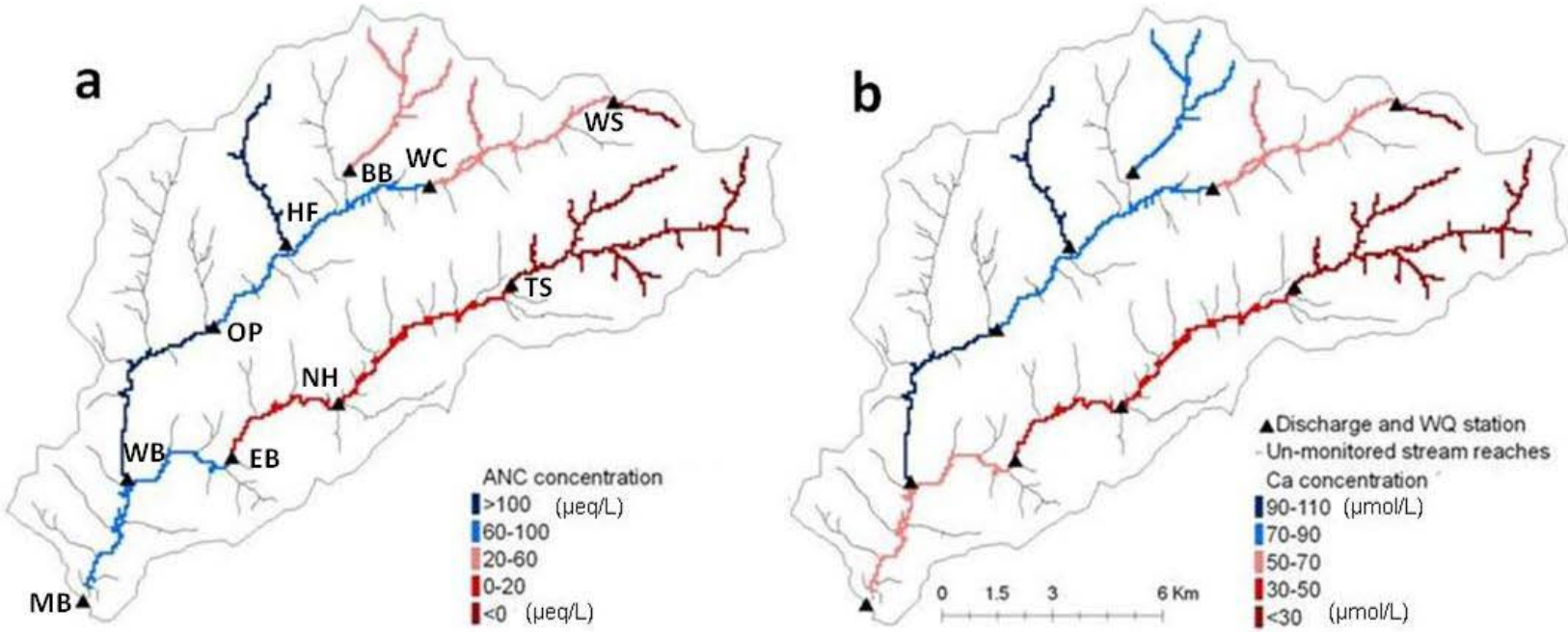
a
WS
BB
WC
HF
TS
OP
NH
WB
EB
MB
ANC concentration
>100 (μeq/L)
60-100
20-60
0-20
<0 (μeq/L)
b
▲Discharge and WQ station
Un-monitored stream reaches
Ca concentration
90-110 (μmol/L)
70-90
50-70
30-50
<30 (μmol/L)
0 1.5 3 6 Km

Table 2.3: Pearson product-moment correlation coefficient (reported as r-values) for the hydrogemorphologic properties explained in Table 2.1. Superscript * denotes p<0.05 and ** denotes p<0.01.

| | *A* | *ELEV* | *S* | $Curve_{pro}$ | *L/G* | *TI* | *DD* | *STI* | $Store_{hill}$ | $Store_{s\&g}$ | $Q_{50}$ | $Q_{90}$ |
|---|---|---|---|---|---|---|---|---|---|---|---|---|
| *ELEV* | -0.68* | 1.00 | | | | | | | | | | |
| *S* | -0.68* | 0.98** | 1.00 | | | | | | | | | |
| $Curve_{pro}$ | 0.87** | -0.51 | -0.49 | 1.00 | | | | | | | | |
| *L/G* | -0.02 | -0.07 | 0.03 | -0.06 | 1.00 | | | | | | | |
| *TI* | 0.71* | -0.95** | -0.92** | 0.51 | 0.10 | 1.00 | | | | | | |
| *DD* | 0.68* | -0.62 | -0.62 | 0.49 | 0.44 | 0.53 | 1.00 | | | | | |
| *STI* | -0.34 | 0.12 | 0.30 | -0.24 | 0.39 | -0.13 | -0.20 | 1.00 | | | | |
| $Store_{hill}$ | -0.15 | 0.24 | 0.08 | -0.10 | -0.88** | -0.22 | -0.51 | -0.62 | 1.00 | | | |
| $Store_{s\&g}$ | 0.53 | -0.54 | -0.46 | 0.39 | 0.78* | 0.51 | 0.83** | 0.05 | -0.80** | 1.00 | | |
| $Q_{50}$[a] | 0.09 | -0.22 | -0.22 | 0.05 | 0.16 | 0.02 | 0.43 | -0.05 | -0.30 | 0.40 | 1.00 | |
| $Q_{90}$[a] | 0.30 | -0.37 | -0.44 | 0.17 | 0.26 | 0.23 | 0.64 | -0.37 | -0.24 | 0.58 | 0.88** | 1.00 |
| *Ratio* | -0.21 | 0.71* | 0.75* | -0.09 | 0.38 | -0.70* | 0.03 | 0.22 | -0.30 | 0.09 | -0.07 | -0.16 |

[a] - summer data (6/1 to 9/30) from WY1992 and WY1993, * - p<0.05, ** - p<0.01

Forward stepwise linear regression analysis was used to select the hydrogeomorphologic properties that best predict the mean baseflow ANC values and $Ca^{2+}$ concentrations across all ten watersheds (Table 2.4). The regression yielded similar statistically significant relationships for the mean ANC and $Ca^{2+}$, using the properties *Runoff Ratio* and L/G (Table 2.4). Most notably, the mean *Runoff Ratio* explained more than 81% ($p<0.01$) of the variability in baseflow ANC and $Ca^{2+}$ (Table 2.4). As the mean *Runoff Ratio* increased from 8.5% to 21.1% the corresponding mean summer ANC values decreased from 138 µeq/L to -20 µeq/L (Table 2.2 and Figure 2.4a), or about 13 µeq/L for each 1.0% increase in *Runoff Ratio*. The median flowpath length over gradient *L/G* explained an additional 7% ($p=0.07$) of the variability in ANC values and 10% ($p=0.01$) of the variability in $Ca^{2+}$ concentrations, resulting in greater ANC values and $Ca^{2+}$ concentrations when the flowpath is lengthened and/or flowpath gradient becomes less steep. These results are consistent with recent studies indicating that *L/G* is positively correlated with mean residence times in some geographic settings (McGuire et al., 2004; Tetzlaff et al., 2009).

The stepwise regression results are investigated more thoroughly using the residual plots shown in Figure 2.5a for ANC values ($Ca^{2+}$ residuals are similar). The residual plot shows that mean *Runoff Ratios* predict the maximum (High Falls) and minimum (Winnisook) baseflow ANC values (notice the x-axis in Figure 2.5a is ordered with increasing ANC). Adding *L/G* to the linear regression significantly improved (>10 µeq/L closer to measured value) the prediction of New Hill, East Branch, Otter Pool, and West Branch (all >49 $km^2$) and Biscuit. These results provided an impetus for investigating the links between mean *Runoff Ratio* and other hydrogeomorphologic properties.

Table 2.4: Results of stepwise regression using the 13 hydrogeomorphologic properties, described in Table 2.1 and shown in Table 2.2, to predict mean summer buffering chemistry. The $\Delta r^2$ is the amount by which the predictor improved the variance explained by the linear regression, while $r^2$ is the overall variance in the relationship explained by the stepwise linear regression, whose significance was evaluated by the p-value.

| Mean growing-season value | Predictor | $\Delta r^2$ | $r^2$ | Slope of equation | Intercept | p-value |
|---|---|---|---|---|---|---|
| ANC | Runoff Ratio | 0.81 | 0.81 | -1157 | 347 | <0.001 |
| | L/G | 0.07 | 0.88 | -49 | 347 | 0.07 |
| $Ca^{2+}$ | Runoff Ratio | 0.81 | 0.81 | -712 | 230 | <0.001 |
| | L/G | 0.10 | 0.91 | -29 | 230 | 0.01 |

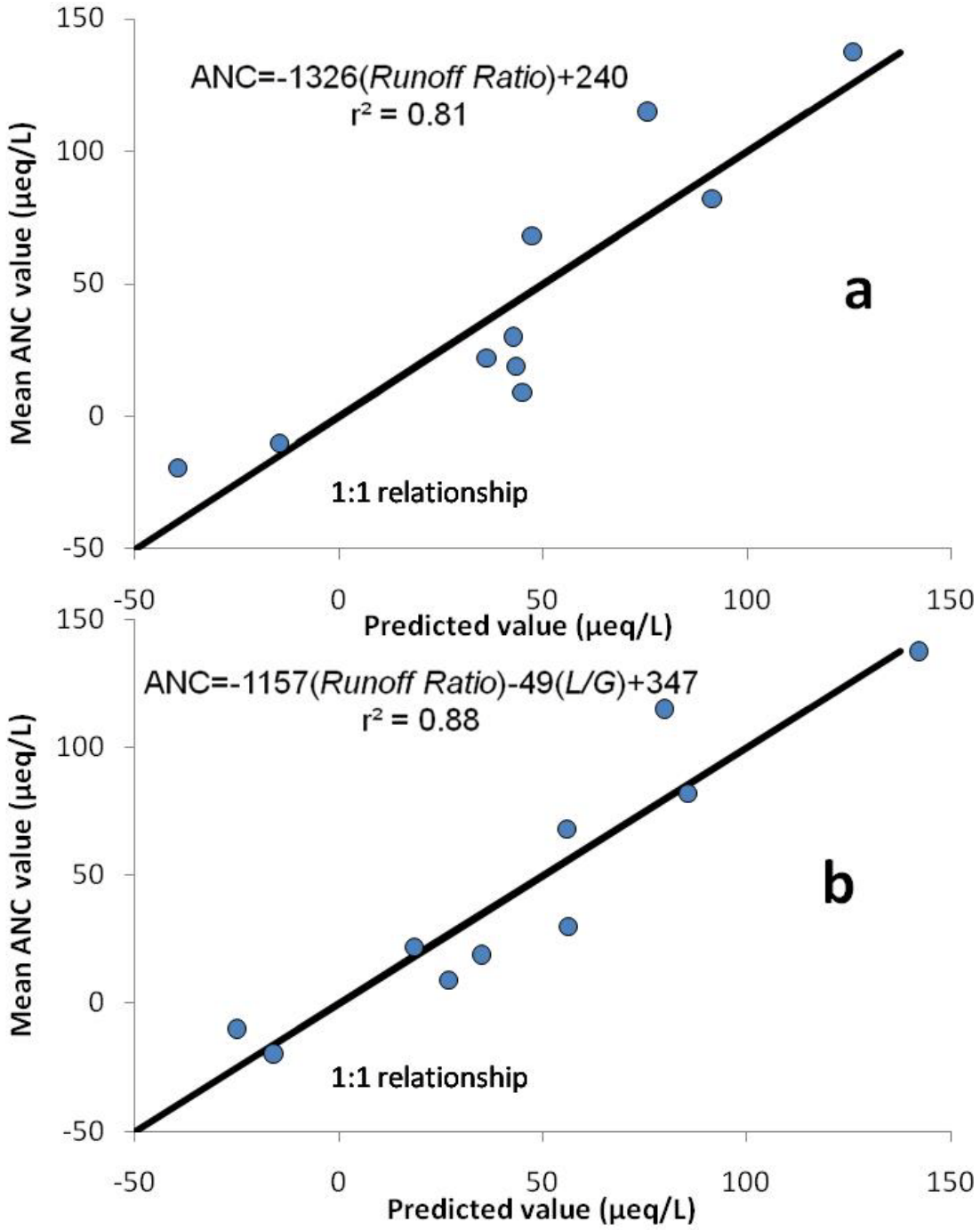


Figure 2.4: Linear relationships developed from stepwise regression for mean growing-season (June 1 to September 30) ANC values (2.4a) using *Runoff Ratio* and $Ca^{2+}$ concentrations (2.4b) using hydrogeomorphologic properties and units explained in Table 2.1 and 2.2.

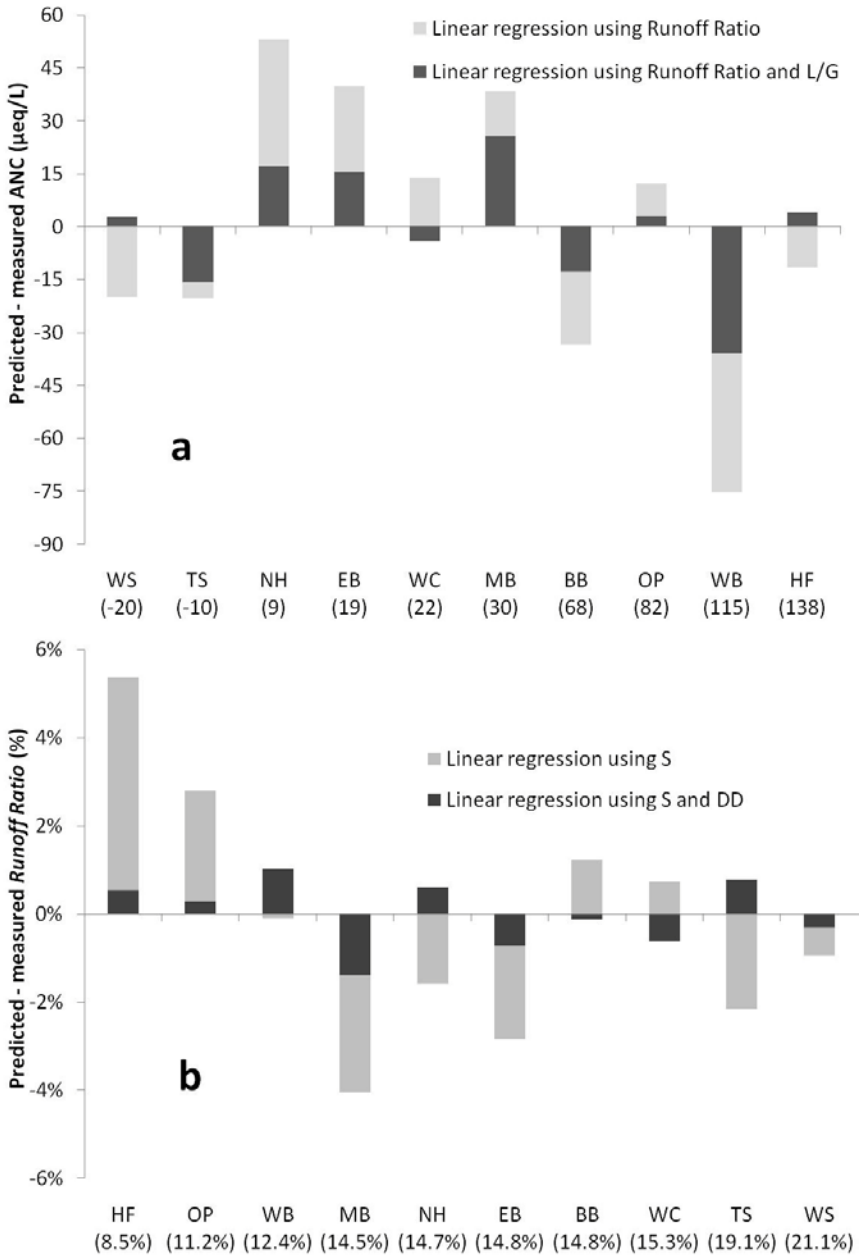


Figure 2.5: Plots of residuals between measurements and predictions from linear relationships developed from stepwise linear regression. 2.5a shows residuals between linear models using *Runoff Ratio* and *L/G* (explained in Table 2.1) to explain increasing ANC values ($Ca^{2+}$ is similar and thus not shown). 2.5b shows residuals between linear models using *S* and *DD* (explained in Table 2.1) and *Runoff Ratios*.

### 2.4.2 Predicting Stream Buffering Chemistry without Precipitation and Discharge Data

Although mean *Runoff Ratio* is a strong predictor of stream buffering chemistry, the calculation requires discharge and rainfall data, and is therefore only applicable where these measurements are available. As an alternative that could be applied at sites without such data, we employed forward stepwise linear regression to find the strongest predictors of mean *Runoff Ratio* from among the ten geomorphologic properties considered (Table 2.1 and 2.2). The new linear relationship that was developed explained greater than 95% of the variability in *Runoff Ratio* using drainage density *DD* and mean watershed slope *S* (Figure 2.6a). *Runoff Ratio* increases as each of these properties increase. Slope explained 56% of the variability in *Runoff Ratio*, but is a poor predictor of response in watersheds with low *Runoff Ratios* (Figure 2.5b). Adding *DD* explained an additional 39% of the variability in *Runoff Ratio* by reducing the prediction error for High Falls by over 50% and Otter Pool by close to 30% (Figure 2.5b). The residuals showed that neither *R* nor *DD* is a singular predictor of *Runoff Ratio,* but together these variables capture most of the variation in event runoff response.

Both *DD* and *S* are easily estimated with widely-available spatial data, making this predictive relationship potentially applicable in other Neversink sub-watersheds where discharge or chemistry measurements are lacking. This simple predictive relationship explains 75% and 77% of the variability in ANC values and $Ca^{2+}$ concentrations, respectively (Figure 2.6b). The Pearson correlation coefficients (Table 2.3) showed that S and DD are negatively correlated (r=-0.62). S is also correlated with *Runoff Ratio* (r=0.75, $p<0.05$), while DD is not correlated to *Runoff Ratio* (r=0.03). Therefore, despite their correlation, S and DD have interacting effects that control the volume of 'quickflow' (and baseflow stream chemistry) and possibly also

reflect process-based differences that will be reviewed shortly.

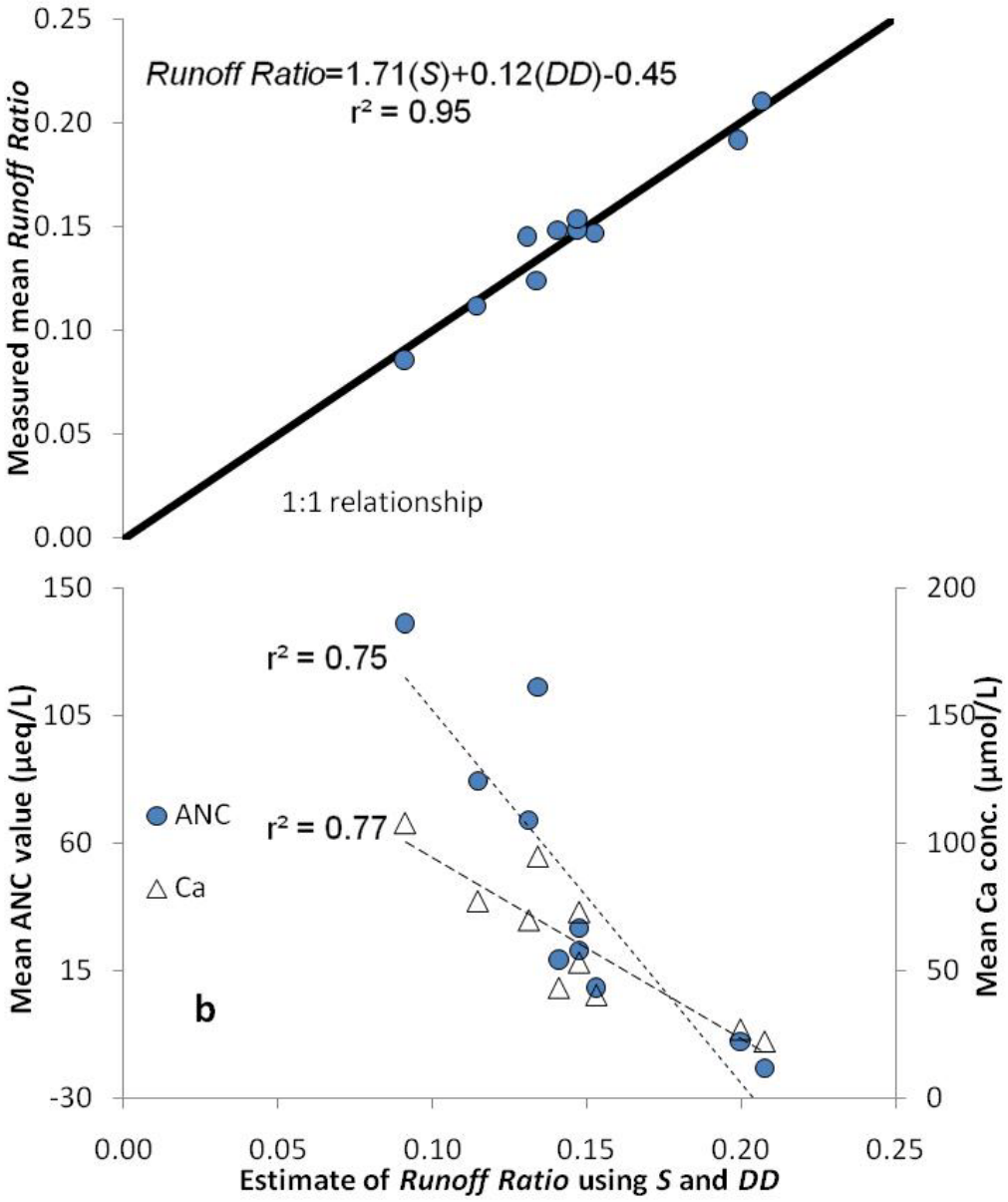


Figure 2.6: Predictions developed from mean slope S and drainage density *DD* (explained in Table 2.1). 2.6a shows that *S* and *DD* explain 95% of the variability in *Runoff Ratio* (see 2.5b for residuals). 2.6b shows the same relationship explains more than 75% of the variability in mean ANC and $Ca^{2+}$ concentrations.

## 2.5 Discussion

We demonstrated that linear relationships using hydrogeomorphologic properties could explain a significant amount of the variability in mean growing-season (June thru September) baseflow buffering chemistry (ANC values and $Ca^{2+}$ concentrations). In the following sections we attempt to explain the applicability of our simple relationship and suggest possible physical mechanisms for the connections between event runoff and baseflow chemistry.

### 2.5.1 Prediction of Baseflow Buffering Chemistry with a Geomorphologic 'Index'

The results suggested that event-scale runoff (e.g. mean *Runoff Ratio*) is a useful means for predicting the mean baseflow buffering chemistry ($r^2>0.81$ and $p<0.001$) of ten nested Neversink sub-watersheds. For every 1% increase in mean *Runoff Ratio* (1% more precipitation transferred to 'quickflow' on average) the mean baseflow ANC value decreased by 13 μeq/L (Figure 2.4a and Table 2.4). This is significant in the Neversink because mean *Runoff Ratios* varied by over two-fold, from 8.5% to 21.1% (Table 2.1). Perhaps more interestingly, this relationship showed that steeper, more efficiently drained watersheds had larger mean *Runoff Ratios* (Figure 2.6a). The potential of a geomorphologic 'index', using mean slope and drainage density, to predict baseflow buffering chemistry in the Neversink merits further discussion.

The success of a geomorphologic index in predicting stream buffering chemistry indicates there are physical (hydrologic) controls on stream chemistry in the Neversink, where there is little variability in weathering sources and land cover. Steeper watersheds have increased rapid runoff volumes and thus reduced percolation to deeper flowpaths. Similarly, watersheds with higher drainage densities should also

have greater runoff volumes and reduced flowpath lengths from the hillslopes to the nearest stream channel. What is most interesting about this relationship in Figure 2.6a is that near equal weight is given to mean slope and drainage density. As an example, the Main Branch is less steep than High Falls (Table 2.2), but the smaller drainage density in High Falls is consistent with the much smaller mean *Runoff Ratio* measured there.

The uniform soil series and consistent bedrock mineralogy (i.e. 'weatherability') within the Neversink reduces variability in spatial buffering sources, and suggests that differences in the distribution of flowpaths (and corresponding residence times) could be a more likely explanation for the differences in stream buffering chemistry. This suggests that the geomorphologic index approach used here may be less applicable in areas with more variable buffering sources (e.g. isolated carbonate sources), or where there is less topographic variation (e.g. slope). However, it should be noted that the presence of isolated carbonate mineral sources within the Neversink has previously been hypothesized as a control on stream buffering chemistry (Stoddard and Murdoch, 1991), but that such a source does not have to be invoked to explain most of the variation in buffering chemistry observed across these 10 Neversink catchments A further impediment to applying this hydrogeomorphologic approach may occur in areas without perennial stream channels, where defining an appropriate drainage density may be problematic. These limitations aside, it is difficult to truly know the applicability of this geomorphologic index to other watersheds without a better mechanistic understanding of how event runoff response alters baseflow buffering chemistry.

### 2.5.2 Connections between Baseflow Buffering Chemistry and Event Runoff Response

Although we do not have sufficient internal measurements to reliably identify the mechanisms that connect event runoff response to stream chemistry, the strength of this relationship (Table 2.4a and Figure 2.4) invites some speculation be made as to whether there are cause and effect mechanisms operating and what the basis for these mechanisms might be. There are two controls on stream buffering that are sometimes considered separately, 1) at low-flow, stream buffering chemistry reflects the subsurface residence time and the mineral weathering rate of the bedrock and soils, and 2) at high-flow, increasing discharge decreases the baseflow stream buffering chemistry (Figure 2.1) through the rapid addition of direct acidic precipitation and 'quickflow' that has not been fully neutralized in the subsurface. However, by demonstrating a strong correlation between discharge during runoff events (mean *Runoff Ratio*) and average baseflow chemistry (Figure 2.4a), we suggest that these two controls on stream buffering are related mechanistically. Although numerous mechanisms could be proposed, two alternative mechanisms are suggested here that could form the conceptual basis for additional research to explore the connections between event runoff and baseflow buffering chemistry in the Neversink: 1) mixing from different distributions of hydrological flowpaths, and 2) changes in soil base cation stores.

It is possible that watersheds have vastly different hydrological flowpaths that contribute to baseflow due to differences in geomorphology. Neversink watersheds likely maintain baseflow from multiple flowpaths, such as water that passes through the fractured bedrock, the soil matrix, and near-stream alluvial aquifers, whose relative contributions are not well quantified. If bedrock water were better buffered than soil

water for example, we could imagine that watersheds with more bedrock flowpaths would be more buffered during baseflow. Although the mixing of different hydrological flowpaths is a viable mechanism for explaining the baseflow stream buffereing chemistry, it does little to clarify why the distribution of flowpaths contributing to baseflow would be correlated to the event runoff response.

Another more nuanced mechanism appears to explain these results based on spatial variation in soil base cation stores. A simple schematic (Figure 2.7) is shown to better illustrate how the flushing of solutes by different flowpaths alters baseflow chemistry between 'flashy' and 'damped' watersheds. The 'flashy'watersheds have greater 'quickflow' runoff and often thin hillside soils (Table 2.2), which over time would cause greater flushing and loss of base cation stores (higher 'flushing frequencies'). The remaining water that does recharge deeper flowpaths in 'flashy' watersheds will thus reflect the reduced capacity to neutralize acidity in the soils of these watersheds, and will therefore have lower ANC values and $Ca^{2+}$ concentreations when the water discharges to the stream during baseflow.

A mechanism that connects event runoff response to changes in the baseflow buffering chemistry from depleted base cation stores (Figure 2.7) has been inferred from observations in the Neversink and other sites. For example, Burns et al. (1998b), working at the Panola Mountain Watershed in Georgia, showed that hillslope sections with more subsurface storm runoff (greater 'flushing frequency') also had lower base cation concentrations, which was confirmed during a 147-storm analysis by Tromp-van Meerveld and McDonnell (2006). Hydrology-driven variations in the flushing frequency of soils has also been invoked to explain varying patterns in dissolved organic carbon (Hornberger et al., 1994) and nitrate concentrations (Creed et al., 1996) in surface waters. A similar mechanism in reverse was also invoked previously in the

Neversink (e.g. Murdoch and Shanley, 2002; 2006) to explain the slower recovery of low-flow buffering chemistry in response to decreased acidic deposition, compared to a faster recovery of high-flow buffering chemistry. Measurements of groundwater spring chemistry across the Neversink from the same time period (unpublished data from D.A. Burns) showed that springs are well-buffered and have longer residence times (Burns et al., 1998a). The few acidic springs were found in the steeper, chronically-acidified watersheds (i.e. Tisons and Winnisook), which indicates that water can move through deeper flowpaths without becoming adequately buffered under certain conditions.

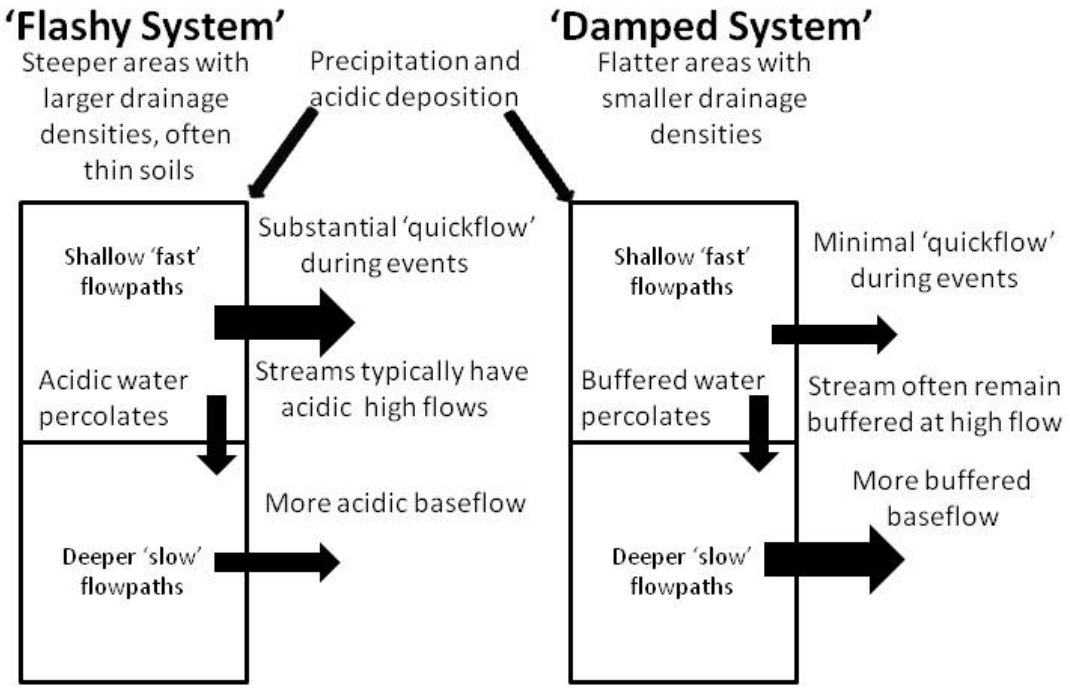


Figure 2.7: Schematic depicting differences in runoff sources between 'flashy' and 'damped' watersheds to better explain the connection between event runoff response and baseflow buffering chemistry.

### 2.5.3 Implications for the Monitoring and Management of Stream Buffering Chemistry

The results suggest that watershed geomorphology affects the distribution of flowpaths and 'quickflow' runoff and acts as an important control on the flushing and weathering of base cations across the flow regime. This confirms Burns et al.'s (2006) hypothesis that local-scale factors affect the cycling of anions and cations in the Neversink. These local-scale factors (differences in event runoff response) may confound a simple cause-effect relationship between emission trends and stream buffering chemistry (Burns et al., 2006; Driscoll et al., 2006). However, we have put forward a simple relationship (Figure 2.6a) that predicts how these local-scale factors affect stream chemistry in the Neversink using digital elevation models and hydrography to calculate *S* and *DD*. This geomorphologic index could also be used to identify tributaries in the Neversink that would be likely to be acidic, which could help minimize the need for extensive field monitoring to establish the extent of the effects of acidic deposition on aquatic biota. This approach might also be attempted in other Catskill watersheds, and in other regions to test the widespread applicability of this type of hydrogeomorphic 'index'. Past studies of spatial variation in surface water buffering chemistry have also concluded that differences in hydrologic flowpaths and subsurface residence time can be principal controls on spatial patterns in regions of relatively uniform bedrock mineralogy (Peters and Murdoch, 1985; Peters and Driscoll, 1987; Wigington, 1992).

## 2.6 Conclusions

This study has introduced a simple hydrogeomorphologic index to predict apparently complex patterns of stream buffering chemistry (acid neutralizing capacity

ANC and $Ca^{2+}$) in ten nested Neversink watersheds (2.0 $km^2$ to 176 $km^2$). In systems like the Neversink, stream acid buffering chemistry is a function of discharge because acidic event water moves through 'fast' (shallow) flowpaths that transit rapidly through the system without time to be fully neutralized by cation exchange or weathering. Thus, in the Neversink, where there is apparently little geographic difference in the 'weatherability' of the minerals, the properties that affect how rapidly event water is transported through the system have a strong control on buffering chemistry, particularly baseflow ANC values. It was therefore not surprising to find that steeper, more efficiently drained watersheds had larger 'quickflow' volumes (mean *Runoff Ratio*) and reduced buffering chemistry. From our analsysis, we speculate that more 'quickflow' correlated to lower baseflow ANC and $Ca^{2+}$ because of mixing from different flowpath distributions and/or changes in soil cation stores over time. Although, the mechanisms responsible for connecting event runoff response and baseflow chemistry are not well-understood, the proposed geomorphologic index has the potential to identify acidification 'hot-spots' with widely-avaliable spatial data. The findings from this study are consistent with a fairly simple hydrologic conceptualization of the Neversink as a system controlled by watershed geomorphology.

# REFERENCES


Baldigo, B.P. and G.B. Lawrence. 2000. Composition of fish communities in relation to stream acidification and habitat in the Neversink River, New York. Transactions of the American Fisheries Society. 129: 60-76.

Baldigo, B.P. and G.B. Lawrence. 2001. Effects of stream acidification and habitat on fish populations of a North American river. Aquatic Sciences. 63: 196-222.

Beven, K. 2001. In Rainfall-Runoff Modelling: The Primer. John Wiley and Sons: New York.

Brown, V.A., J.J. McDonnell, D.A. Burns, C. Kendall. 1999. The role of event water, rapid shallow flowpaths, and catchment size in summer stormflow. Journal of Hydrology. 217: 171-190.

Burns, D.A., P.S.Murdoch, G.B. Lawrence, and R.L. Michel. 1998a. The effect of groundwater springs on $NO_3^-$ concentrations during summer in Catskill Mountain streams. Water Resources Research. 34:1987-1996.

Burns, D.A., R.P. Hooper, J.J. McDonnell, J.E. Freer, C. Kendall, and K. Beven. 1998b. Base cation concentrations in subsurface flow from a forested hillslope: the role of flushing frequency. Water Resources Research. 34(12): 3535-3544.

Burns, D.A., M.R. McHale, C.T. Driscoll, and K.M. Roy. 2006. Response of surface water chemistry to reduced levels of acid precipitation: comparison of trends in two region of New York, USA. Hydrological Processes. 20: 1611-1627.

Buttle, J.M. and M.C. Eimers. 2009. Scaling and physiologic controls on streamflow behavior on the Precambrian Shield, south-central Ontario. Journal of Hydrology.

374: 360-372.

Clow, D. W. and J.K. Sueker. 2000. Relations between basin characteristics and stream water chemistry in alpine/subalpine basins in Rocky Mountain National Park, Colorado. Water Resources Research, 36, 49–61.

Cooper, D.M., R.C. Helliwell, M.C. Coull. 2004. Predicting acid neutralizing capacity from landscape classification: application to Galloway, south-west Scotland. Hydrological Processes. 18:455-471.

Creed, I.F., L.E. Band, N.W. Foster, I.K. Morrison, J.A. Nicholson, R.S. Semkim, and D.S. Jeffries. 1996. Water Resources Research. 32(11): 3337-3354.

Davies, T.D., M. Tranter, P.J. Wigington, K.N. Eshelman, N.E. Peters, J. Van Sickle, D.R. DeWalle, and P.S. Murdoch. 1999. Prediction of episodic acidification in North-eastern USA: an empirical/mechanistic model. Hydrological Processes. 13: 1181-1195.

Draper, N. and Smith, H. 1981. Applied Regression Analysis, 2d Edition, New York: John Wiley & Sons, Inc.

Driscoll, C.T., G.B. Lawrence, A.J. Bulger, T.J. Butler, C.S. Cronan, C. Eagar, K.F. Lambert, G.E. Likens, J.L. Stoddard, and K.C. Weathers. 2001. Acid deposition in the Northeastern United States: sources and inputs, ecosystem effects, and management strategies. Bioscience. 51(3): 180-198.

Driscoll, C.T., K.M. Driscoll, M.J. Mitchell, and D.J. Raynal. 2003. Effects of acidic deposition on forest and aquatic ecosystems in New York State. Environmental Pollution. 123(3): 327-336.

Helsel D.R. and R.M. Hirsch. 1993. Statistical Methods in Water Resources. Elsevier: NY.

Hewlett, J.D. and Hibbert, A.R. 1967. Factors affecting the response of small watersheds to precipitation in humid regions. In Forest Hydrology (eds. W.E. Sopper and H.W. Lull). Pergamon Press, Oxford. pp. 275-290

Hornberger, G.E., K.E. Bencala, and D.M. McKnight. 1994. Hydrological controls on dissolved organic carbon during snowmelt in the Snake River near Montezuma, Colorado. Biogeochemistry. 25: 147-165.

Kirchner, J.W., P.J. Dillon, B.D. LaZarte. 1993a. Prediction geochemical buffering and runoff acidification in spatially heterogeneous catchments. Water Resources Research. 29(12): 3891-3901.

Kirchner, J.W., P.J. Dillon, B.D. LaZarte. 1993b. Separating hydrological and geochemical influences on runoff acidification in spatially heterogeneous catchments. Water Resources Research. 29(12): 3903-3916.

Kudish, M. 2002. Catskill Forests. Purple Mountain Press: Fleischmanns, NY.

Lawrence, G.B., Lincoln, T.A., Horan-Ross, D.A., Olson, M.L., Waldron, L.A., 1995. Analytical Methods of the U.S. Geological Survey's New York District Water-Analysis Laboratory. U.S. Geol. Surv. Open-File Rpt., 95-416, 78 pp.

Lawrence, G.B., M.B. David, G.M. Lovett, P.S. Murdoch, D.A. Burns, J.L. Stoddard,B.P. Baldigo, J.H. Porter, and A.W. Thompson. 1999. Soil calcium status and the response of stream chemistry to changing acidic deposition rates. Ecological Applications. 9(3): 1059-1072.

Lawrence, G.B. 2002. Persistence episodic acidification of streams linked to acid rain effects on soil. Atmospheric Environment. 36:1 589-1598.

Lincoln, T. A., D. A. Horan-Ross, M. L. Olsen, and G. B. Lawrence. 1996. Quality-assurance data from routine water analyses by the U.S. Geological Survey Laboratory in Troy, New York—May 1991 through June 1993. U.S. Geological Survey, OFR 96-167, Troy, New York.

Lovett, G.M., A.W. Thompson, J.B. Anderson, and J.J. Bowser. 1999. Elevational patterns of sulfur deposition at a site in the Catskill Mountains, New York. Atmospheric Environment. 33: 617-624.

McGuire, K.J., J. J. McDonnell, M. Weiler, C. Kendall, B. L. McGlynn, J. M. Welker, and J. Seibert (2005). The role of topography on catchment-scale water residence time. Water Resources Research. 41, doi:10.10292004WR003657.

Murdoch, P.S. and J.L. Stoddard. 1993. Chemical characteristics and temporal trends in eight streams of the Catskill Mountains, New York. Water, Air, and Soil Pollution. 67(2): 367-395.

Murdoch, P.S. and J.B. Shanley. 2002. Flow-specific trends in river-water quality resulting from the effects of the Clean Air Act in three mesoscale, forested river basins in the Northeastern United States through 2002. Environmental Monitoring and Assessment. 120: 1-25.

Murdoch, P.S. and J.B. Shanley. 2006. Detection of water quality trends at high, median, and low flow in a Catskill Mountain stream, New York, through a new statistical method. Water Resources Research. 42. W08407, doi:10.1029/2004WR003892.

Ozvarth, D.L. 1985. Glacial geomorphology and the late Wisconsinain deglaciation of the western Catskill Mountains. State University of New York at Binghamton, Doctoral Dissertation. 181p.

Peters, N.E. and P.S. Murdoch. 1985. Hydrogeologic comparison of an acidic-lake basin with a neutral-lake basin in the west-central Adirondack Mountains, New York, Water, Air, and Soil Pollution. 26: 387-402.

Peters, N.E. and C.T. Driscoll. 1987. Hydrogeologic controls on surface-water chemistry in the Adirondack region of New York State. Biogeochemistry. 3:163-181.

Rich, J.L. 1934. Glacial Geology of the Catskills. New York State Bulletin, 299. University of the State of New York, Albany. 180 pp.

Sanford, S.E., I.F. Creed, C.L. Tague, F.D. Beall, and J.M. Buttle. 2007. Scale-dependence of natural variability of flow regimes in a forested landscape. Water Resources Research. 43, W08414, doi:10.1029/2006WR005299.

Shaman, J. M. Stieglitz, and D. Burns. 2004. Are big basins just the sum of small catchments?. Hydrological Processes. 18:3195-3206.

Soren, J. 1961. The ground-water resources of Sullivan County, New York: New York State Department of Conservation Bulletin GW-46, 66p.

Stoddard, J. L. 1994. Long-term changes in watershed retention of nitrogen: Its causes and aquatic consequences, in Environmental Chemistry of Lakes and Reservoirs, Am. Chem. Soc. Adv. Chem. Ser., vol. 237, edited by L. A. Baker, pp. 223– 284, Am. Chem. Soc., Washington, D. C.

Sullivan, T.J., J.R. Webb, K.U. Snyder, A.T. Herlihy, and B.J. Cosby. 2007. Spatial distribution of acid-sensitive and acid-impacted streams in relation to watershed features in the Southern Appalachian Mountains. Water, Air, and Soil Pollution. 182: 57-71.

Tetzlaff, D., J. Siebert, K.J. McGuire, H. Laudon, D.A. Burns, S.M. Dunn, and C. Soulsby. 2009. How does landscape structure influence catchment transit time across geomorphologic provinces? Hydrological Processes. 23(6): 945-953.

Thaler, J.S. 1996. In Catskill Weather. Purple Mountain Press: Fleischmanns, New York.

Van Sickle, J. P.J. Wigington, and M.R. Church. 1997. Estimation of episodic stream acidification based on monthly or annual sampling. Journal of American Water Resources Association. 33(2). 359-366.

Tromp-van Meerveld and J.J McDonnell. 2006. Threshold relations in subsurface stormflow 1. A 147 storm analysis of the Panola hillslope. Water Resources Research. 42. Doi:1029/2004WR003778.

Vitvar, T., D.A. Burns, G.B. Lawrence, J.J. McDonnell, and D.M. Wolock. 2002. Estimation of baseflow residence times in watersheds from the runoff hydrograph: method and application in the Neversink watershed. Catskill Mountain, New York. Hydrological Processes. 16: 1871-1877.

Wade, A.J., C. Neal, C. Soulsby, R.P. Smart, S.J. Langan, and M.S. Cresser. 1999. Modelling streamwater quality under varying hydrological conditions at different spatial scales. Journal of Hydrology. 217: 266-283.

Wigington, P.J. T.D. Davies, M. Tranter, and K.N. Eshleman. 1992. Comparison of episodic acidification in Canada, Europe, and the United States. Environmental Pollution. 78. 29-35.

Wigington, P.J., J.P. Baker, D.R. DeWalle, W.A. Kretser, P.S. Murdoch, H.A. Simonin, J. Van Sickle, M.K. McDowell, D.V. Peck, and W.R. Barchet. 1996a. Episodic acidification of small stream in the Northeastern United States: Episodic Response Project. Ecological Applications. 6(2): 374-388.

Wigington, P.J. and D.R. DeWalle, P.S. Murdoch, W.A. Kretser, H.A. Simonin, J. Van Sickle, and J.P. Baker. 1996b. Episodic acidification of small streams in the Northeastern United States: ionic controls of episodes. Ecological Applications. 6(2): 389-407.

Wolock, D.M., J. Fan, and G.B. Lawrence. 1997. Effects of basin size on low-flow stream chemistry and subsurface contact time in the Neversink River Watershed, New York. Hydrological Processes. 11:1273-1286.

Chapter 3

# EXPLAINING THE SPATIAL VARIABILITY OF AQUATIC BIOTA USING HYDROGEOMORPHOLOGIC PROPERTIES IN THE NEVERSINK RIVER WATERSHED, NEW YORK STATE, USA

## 3.1 Abstract

High inputs of acidic deposition continue to negatively affect populations of macroinvertebrate, periphytic diatoms, mussels, and fish despite reductions in acidic deposition in the Northeast U.S. following implementation of the Clean Air Act. Previous research from the Neversink River watershed in the Catskill Mountains, New York State developed a hydrogeomorphologic 'index' to relate areas with steep slopes and high drainage densities to lower stream baseflow acid neutralizing capacity (ANC). In this study, we applied that relationship to 28 sub-watersheds (0.3 $km^2$ to 176.0 $km^2$) to estimate inventories of aquatic biota, including various metrics of macroinvertebrate, diatom, and fish populations. The hydrogeomorphologic 'index' was strongly correlated to the macroinvertebrate-based indices. Biotic metrics involving fish and diatoms correlated less well to the hydrogeomorphologic index, perhaps because this index is based on static characteristics and these organisms are especially susceptible to episodic (short-term) changes in stream discharge and corresponding acidity that require more dynamic information to predict. Our analysis suggests that biotic and hydrologic characteristics are meaningfully correlated to each other in the Neversink watershed. From a practical perspective, perhaps easily calculated hydrogeomorphologic indices may be used to compliment, or even *in lieu*

of, expensive and time consuming biotic measurements to identify streams potentially at-risk for acidification.

## 3.2 Introduction

Strong mineral acidity in atmospheric deposition, largely resulting from the burning of fossil fuels, has contributed to biological stress and the degradation of aquatic ecosystems in the Northeastern U.S. (Driscoll et al., 2001; 2003). The decline in fossil fuel emissions since implementation of Title IV of the Clean Air Act Amendments of 1990 have reduced acidic deposition in the Northeast, but have not yet resulted in reductions in stream acidity of equal magnitude (Lawrence, 1999; Murdoch and Shanley, 2002; Burns et al., 2006). Stream acidification remains problematic in the 176 $km^2$ Neversink River watershed (hereafter referred to as the Neversink) in the Catskill Mountains of New York State because of the high rates of acidic deposition and shallow glacial soils (Stoddard and Murdoch, 1991). Acidic deposition over the past several decades has accelerated the leaching of base cations (particularly $Ca^{2+}$ and/or $Mg^{2+}$) from soils (Lawrence et al., 1999; Lawrence, 2002), delaying the recovery of acid neutralizing capacity (ANC). This delayed recovery of ANC has severe ramifications for aquatic biota in many parts of the Neversink.

Although some headwater streams have adequate ANC and provide suitable habitat for aquatic biota (Baldigo and Lawrence, 2000), most Neversink headwater streams are 'chronically' acidified (baseflow ANC<0 eq/L) or become 'episodically' acidified during runoff events. In chronically acidified Neversink sub-watersheds, native fish and macroinvertebrate communities showed little improvement between 1987 and 2003 (Burns et al., 2008) and downstream mussel species (*Alasmidonta heterodon* and *Alasmidonta varicose*) remain threatened by extinction (Baldigo et al.,

2002; 2003).

Previous studies in the Neversink have shown that ANC values are correlated to the distribution of macroinvertebrates (Ernst et al., 2008), diatoms (Burns et al., 2008), mussels (Baldigo et al., 2002; 2003), and fish populations (Baldigo and Lawrence, 2000; 2001; Van Sickle et al., 1996). Although studies of caged fish (Baldigo and Murdoch, 1997), fish surveys (Baker et al., 1996), and bioassays (van Sickle et al., 1996) showed episodic acidification caused fish mortality in the Neversink, there was little improvement in predicting mortality rates using episodic chemistry versus baseflow (long-term) chemistry (van Sickle et al., 1996). This suggests that improved explanations for the variations in baseflow ANC values in the Neversink could also explain spatial variability of aquatic biota populations.

Explanations for the differences in the buffering chemistry, i.e., ANC, of the Neversink sub-watersheds during baseflow include geological heterogeneities as reflected by the underlying bedrock lithology (Baldigo and Lawrence, 2000), the presence of carbonate rocks imported by glaciers from other watersheds (Stoddard and Murdoch, 1991), the distribution of groundwater springs (Burns et al., 1998a; Baldigo and Lawrence, 2000; Shaman et al., 2004), watershed area or topography (Wolock et al., 1997; Vitvar et al., 2002; Shaman et al., 2004), and/or gradients in acidic deposition due to elevation (Lovett et al., 1999; Lawrence et al., 2001). More recently in Chapter 2, we were able to demonstrate that variability in baseflow ANC can largely be explained by differences in the average proportions of rainfall that became ‘quickflow’ runoff (further referred to as mean *Runoff Ratio*); we used water chemistry data from 1991 to 1993, which corresponded to a period when acidic deposition was still substantial (see Murdoch and Shanley, 2006).

In general, Neversink watersheds that are steeper (higher mean slope *S*) and have more perennial stream channels per area (larger drainage density *DD*) have higher mean *Runoff Ratios*, i.e., more precipitation transferred to 'quickflow' during runoff events (Figure 3.1a), and reduced stream ANC values (Figure 3.1b). It was shown that 95% of the variability in mean *Runoff Ratio* could be explained by a simple equation (see Chapter 2) (Figure 3.1a):

$$\overline{Runoff\ Ratio} = 1.71(S) + 0.13(DD) - 0.45 \qquad \textit{Equation (1)}$$

where $\overline{Runoff\ Ratio}$ is the mean quotient of 'quickflow' to precipitation from 20 non-snowmelt runoff events, accounting for differences in precipitation between watersheds, and using the simple graphical 'quickflow' separation technique from Hewlitt and Hibbert (1967) (see section 2.3.2 for complete description). It was also shown that mean *Runoff Ratio* estimates from Equation 1 could be used to predict over 75% of the variability in mean baseflow ANC values (Figure 3.1a). The strength of this relationship suggests that baseflow ANC values are affected by hydrologic processes that are captured by easily measured 'hydrogeomorphologic' properties.

Our hypothesis is that estimates of mean *Runoff Ratio*, calculated with slope and drainage density (Equation 1), are correlated to populations of acid-sensitive aquatic biota. To test this hypothesis, we combine aquatic biota data from three previous studies, Ernst et al. (2008), Burns et al. (2008), and Baldigo and Lawrence (2000; 2001), which cumulatively included nine of the watersheds used to develop Equation 1 and 19 additional 'ungaged' watersheds where discharge was not measured. The study's goal, therefore, is to predict diatom, macroinvertebrate, and fish inventories using widely-available spatial data, specifically digital elevation models and hydrography required to calculate *S* and *DD*.

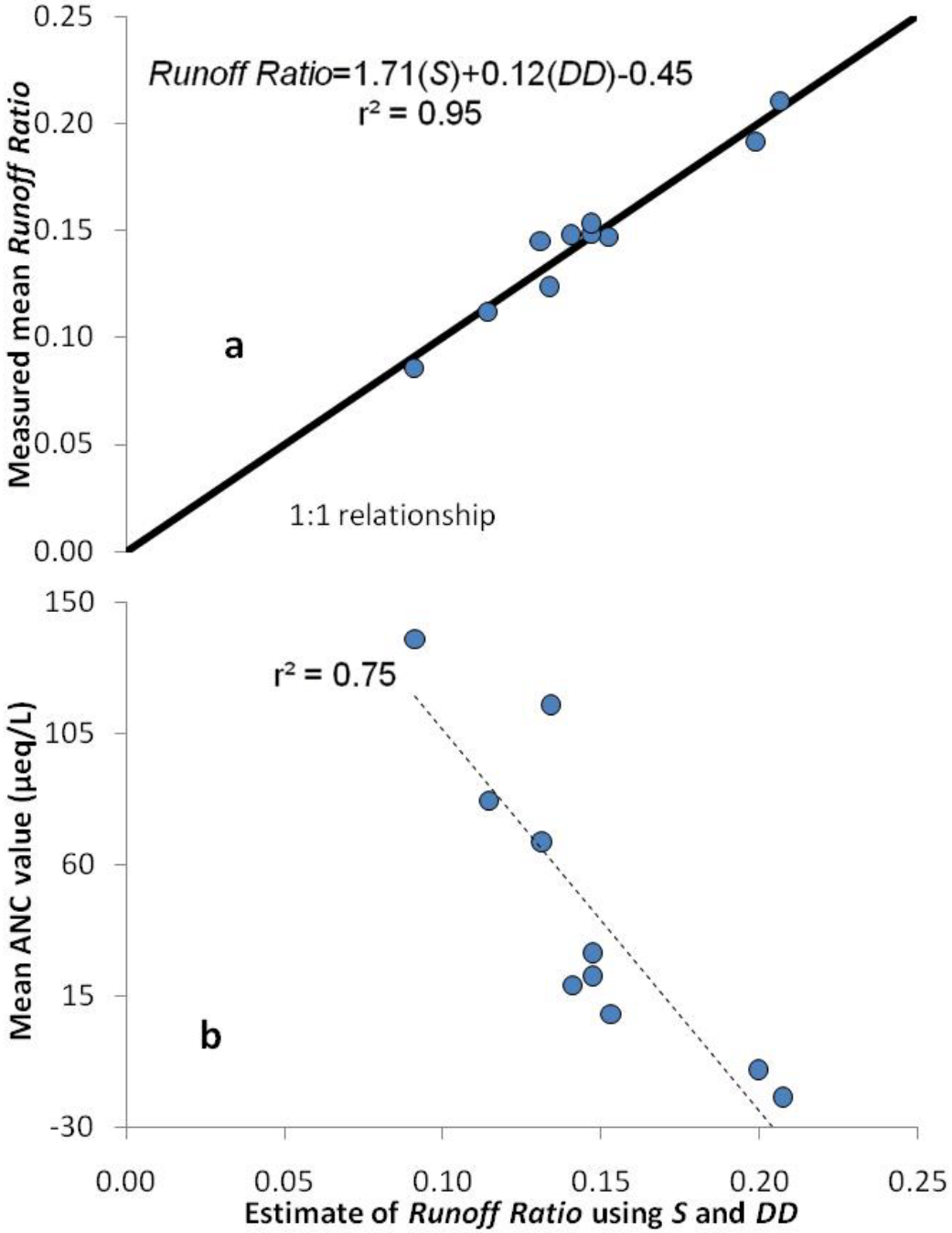


Figure 3.1: The mean *Runoff Ratio* was estimated with the mean slope (*S*) and drainage density (*DD*) using Equation 1 (values shown in Table 3.1) in 3.2a. 3.2b shows that 75% of the variability in mean growing-season ANC values can by estimated using *S* and *DD*. This is adapted from Figure 2.6.

## 3.3 Methodology

### 3.3.1 Study Site

The Neversink watershed is located in the Catskill Mountains of southeastern New York State (Figure 3.2a). The Neversink originates at the summit of Slide Mountain (elevation 1274 m) and drains into the Neversink reservoir (elevation 408 m), part of the New York City drinking water supply. The Catskills received very high amounts of acidic deposition during the study period or 1991 to 1993 (Stoddard and Murdoch, 1993); sulfate loads at the National Trends Network monitoring gage in Biscuit Brook (634 m) were ~30 kg/ha in 1992 compared to ~20 kg/ha in 2002 (see Murdoch and Shanley, 2006). The average annual precipitation at Slide Mountain was 144 cm during the study period (WY1992 and 1993). Cold winter temperatures (mean 3.3 °C at Slide Mountain) and spring rains typically produce peak discharge during snowmelt in April and May (Thaler, 1996). The Neversink has only two ponds larger than 3 ha and no major channel diversions. The land cover is predominately (>98%) old (~100-yrs) re-grown forests (Figure 3.2b), consisting of American beech (*Fagus grandifolia*), yellow birch (*Betula alleghaniensis*), sugar maple (*Acer saccharum*), red maple (*Acer rubrum*) and balsam fir (*Abies balsamea*); eastern hemlock (*Tsuga canadiensis*) dominates many riparian zones. (Kurdish, 2002). The Neversink was never substantially cleared for agriculture or grazing (Kurdish, 2002) and less than 0.25% of the watershed is low density residential. The soils are primarily well drained Inceptisols less than 1.5 m deep (Soren, 1961).

The dissection of an uplifted bedrock plateau by streams and glaciers formed the Catskill Mountains (Rich, 1934). The major surficial geological features are till, kame terraces, outwash sand and gravel, alluvium, and exposed rock. Deglaciation

left loose ablation till in the valley bottoms and more compacted lodgement till in the upland tributaries (Ozvarth, 1985). Stream habitat characteristics exhibited gradual trends from high to low-elevations and from smaller to larger watersheds (Baldigo and Lawrence, 2000). Channel width, pool-riffle ratio, percent medium gravel, and percent undercut banks were similar between the east and west branches, while channel width-depth ratio was distinctly different (Baldigo and Lawrence, 2000).

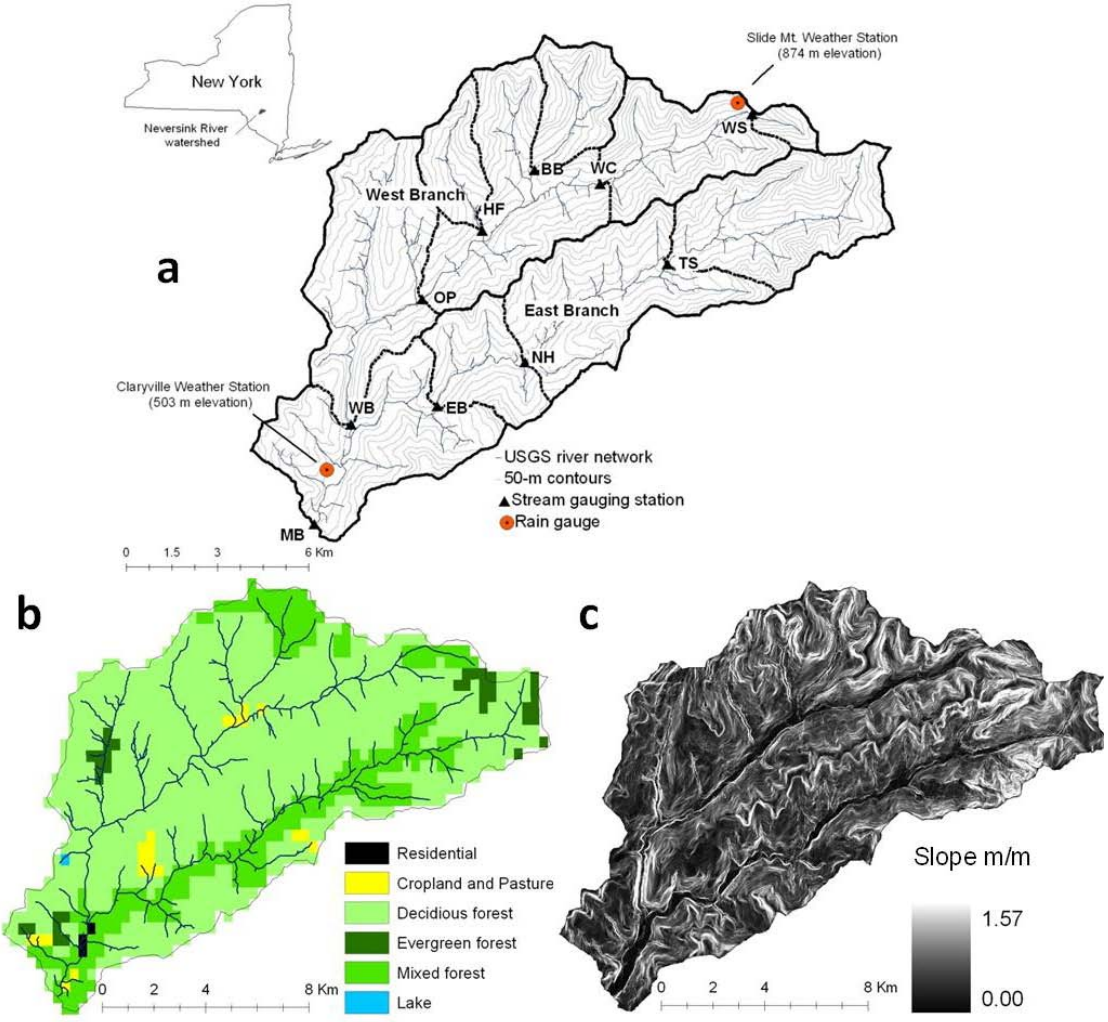


Figure 3.2: Overview of the Neversink: (a) monitoring locations used in the regression analysis to develop Equation 1 b) land cover and c) slope.

### 3.3.2 Collection of Aquatic Biota and Water Chemistry Data

The ANC values used to develop Equation 1 were from the growing-seasons (June thru September) of 1991, 1992, and 1993 and in general were sampled every 2 to 6 weeks. The different sampling rates meant that a total of 10 to 28 water samples were collected in each of the ten watersheds. The ANC values were measured by Gran titration in μeq/L via the methods described by Lawrence et al. (1995) and estimates of laboratory error were given by Lincoln et al. (1996). The additional biotic inventories used in this study by Ernst et al. (2008), Burns et al. (2008), and Baldigo and Lawrence (2000; 2001) consisted of multiple metrics of fish, macroinvertebrates, and diatom populations. The biotic inventories were collected during the growing-season, but at different times from 1987 to 2003 and in different, but overlapping watersheds (Figure 3.3).

Ernst et al. (2008) compiled data from 30 Neversink stream reaches (1991-2001), 16 of which were upstream of the reservoir and used in this study; six of these corresponded to watersheds where discharge and *Runoff Ratios* were measured (WC, BB, EB, NH, TS, MB from Chapter 2) and ten were additional 'ungaged' watersheds (WB3, WB5, WB6, WB7, WB8, B1, DC, O1, SM, NV16) (Table 3.1). Two metrics of macroinvertebrate richness (number of different species) were calculated from 100 random subsamples of 200-individuals: total macroinvertebrate richness and richness of Ephemeroptera (mayfly), Plecoptera (stonefly), Trichoptera (caddisfly), or EPT richness.

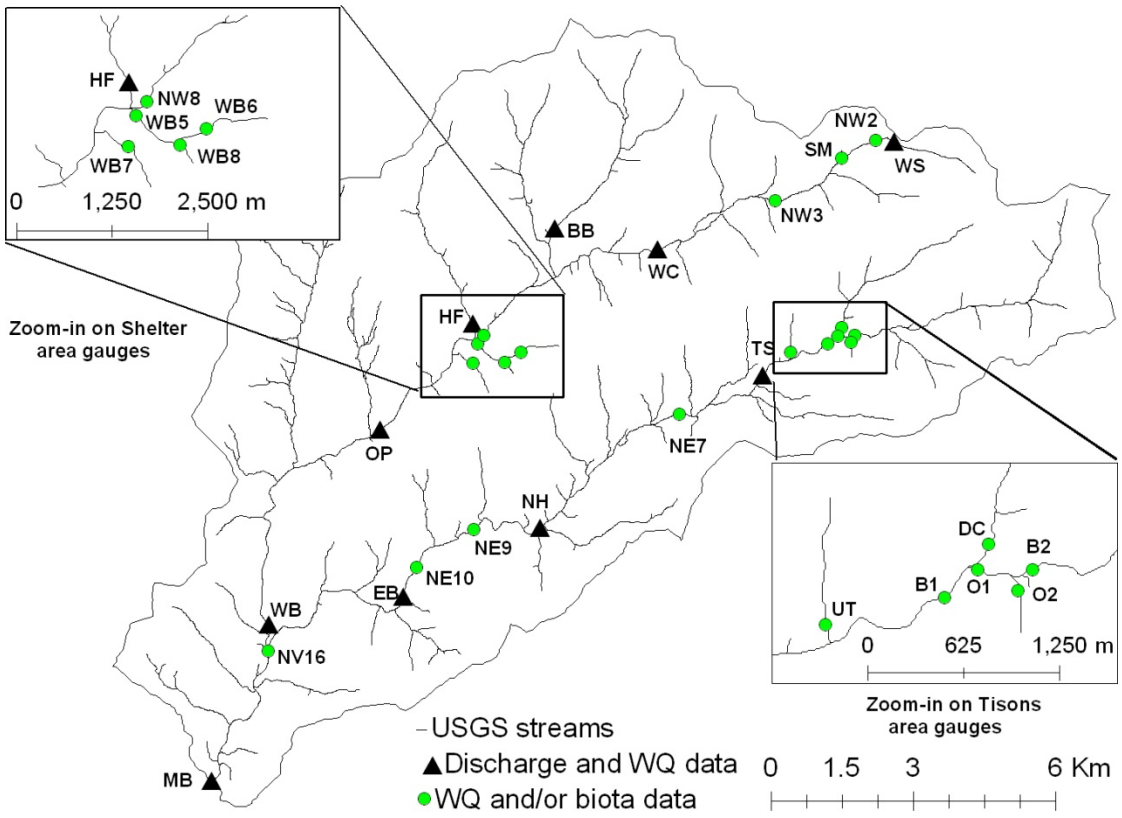


Figure 3.3: Location of the 10 watersheds with discharge and aquatic biota data (triangles also used in Figure 3.2 and 3.4) and the 18 additional 'ungaged' watersheds (circles also used in Figure 3.4) with aquatic biota data and no discharge measurements.

Table 3.1. Relevant geomorphologic properties of the ten watersheds used in the regression analysis to estimate mean *Runoff Ratio* and applied to 18 additional watersheds without discharge measurements (Figure 3.3).

| | | Watershed names and abbreviation used in other studies | Area $A$ ($km^2$) | Mean Slope $S$ (m/m) | Drainage Density $DD$ ($km/km^2$) | Estimate of mean *Runoff Ratio* using Equation 1 (measured) |
|---|---|---|---|---|---|---|
| **Used to develop Equation 1** | HF | High Falls[4] | 7.2 | 0.25 | 0.85 | 0.09 (0.08) |
| | BB | Biscuit[3,4], WB2[1], NW6[2] | 9.8 | 0.28 | 0.94 | 0.15 (0.15) |
| | WS | Winnisook[3,4], NW1[2] | 2.0 | 0.32 | 0.85 | 0.21 (0.21) |
| | WC | Wildcat[3,4], WB1[1], NW4[2] | 20.8 | 0.28 | 0.94 | 0.15 (0.15) |
| | OP | Otter Pool[3,4] | 66.8 | 0.25 | 0.99 | 0.11 (0.11) |
| | WB | West Branch[3,4], NW11[2] | 89.2 | 0.24 | 1.32 | 0.13 (0.12) |
| | TS | Tisons[3,4], EB3[1], NE5[2] | 23.6 | 0.29 | 1.22 | 0.20 (0.19) |
| | NH | New Hill[3,4], EB2[1], NE8[2] | 49.1 | 0.25 | 1.36 | 0.15 (0.15) |
| | EB | East Branch[3,4], EB1[1], NE11[2] | 60.4 | 0.24 | 1.32 | 0.14 (0.15) |
| | MB | Main Branch[3,4], NV15[1],N12[2] | 176.0 | 0.24 | 1.35 | 0.13 (0.15) |
| **Additional 'ungaged' watersheds** | WB5 | WB5[1] | 2.0 | 0.19 | 1.52 | 0.07 |
| | WB6 | WB6[1] | 1.1 | 0.20 | 0.94 | 0.01 |
| | WB7 | WB7[1] | 1.1 | 0.20 | 0.79 | 0.01 |
| | WB8 | WB8[1] | 0.4 | 0.21 | 1.31 | 0.09 |
| | NV16 | NV16[1] | 160.0 | 0.24 | 1.34 | 0.14 |
| | NE7 | NE7[2] | 32.8 | 0.27 | 1.34 | 0.19 |
| | NE9 | NE9[2] | 49.7 | 0.24 | 1.46 | 0.16 |
| | NE10 | NE10[2] | 53.1 | 0.24 | 1.46 | 0.15 |
| | NW2 | NW2[2] | 2.3 | 0.32 | 0.89 | 0.21 |
| | NW3 | NW3[2], WB3[1] | 8.2 | 0.30 | 0.99 | 0.20 |
| | NW8 | NW8[2] | 45.1 | 0.27 | 0.99 | 0.14 |
| | DC | Deer Creek[3], EB5[1] | 5.5 | 0.32 | 1.14 | 0.26 |
| | UT | Upper Tisons[3] | 0.7 | 0.27 | 1.40 | 0.20 |
| | B2 | Braid-2[3] | 15.1 | 0.28 | 1.05 | 0.17 |
| | O1 | Oasis-1[3], EB6[1] | 15.5 | 0.28 | 1.03 | 0.17 |
| | B1 | Braid-1[3], EB4[1], NE1[2] | 20.9 | 0.30 | 1.08 | 0.21 |
| | SM | Slide Mountain[3], WB4[1] | 3.2 | 0.32 | 0.67 | 0.18 |
| | O2 | Oasis-2[3] | 0.3 | 0.27 | 0.67 | 0.10 |

source: [1] Ernst et al. (2008) [2] Burns et al. (2008) [3] Baldigo and Lawrence (2001) [4] Chapter 2

Burns et al. (2008) made measurements in 2003 at 15 Neversink locations, of which eight corresponded to watersheds used to directly measure *Runoff Ratios* (TS, NH, EB, WS, BB, WC, WB, MB from Chapter 2) and seven were additional (B1, NE7, NE9, NE10, NW2, NW3, NW8) (Table 3.1). The data generated from this campaign were compared to a similar unpublished data set from 1987. Burns et al. (2008) collected macroinvertebrate data to calculate Acid Biological Assessment Profiles or the Acid BAP index (new metric developed by Burns et al. (2008)) and periphytic diatom data used to calculate Diatom Acid Tolerance Index (DATI) (Passy, 2000; Passy et al., 2006).

Baldigo and Lawrence (2000; 2001) studied the effects of stream acidity on fish populations in 16 Neversink reaches (1991-1994), nine of which had measured *Runoff Ratios* (BB, WS, WC, OP, WB, TS, NH, EB, MB from Chapter 2) and seven were additional watersheds (DC, UT, B2, O1, B1, SM, O2) (Table 3.1). Fish data were summarized as total density (number of fish/$m^2$) and species richness, i.e., total number of fish species found, which included brook trout, brown trout, Atlantic salmon, blacknose dace, longnose dace, and slimy sculpin. Total fish biomass ($g/m^2$) was not included because it lacked correlation to ANC values (Baldigo and Lawrence, 2001).

### 3.3.3 Statistical Analysis

The measurements of mean *Runoff Ratios* were collected from 20 storms from 1991 to 1993, where runoff was estimated as 'quickflow' following Hewlitt and Hibbert (1967) (see Chapter 2 for complete description). Watershed mean *Runoff Ratios* were calculated using mean slope and drainage density with Equation 1 and are shown in Table 3.1. The mean slope (S) was calculated as mean slope in all 10 m

DEM cells within the watershed using ArcGIS. Digital line graphs representing stream channels were taken from the National Hydrography Dataset (NHD) and drainage density was calculated as the length of stream channel per area for each watershed.

The estimate of mean *Runoff Ratio* from Equation 1 was then correlated to macroinvertebrate, periphytic diatom, and fish populations, from three previous studies: Ernst et al. (2008), Burns et al. (2008), and Baldigo and Lawrence (2000; 2001). The Pearson product-moment correlation coefficient (reported as r-values) were determined between the estimate *Runoff Ratios* and the various biotic indices using Matlab (Mathworks version R2008a) and p-values were estimated based on the student t-distribution and a 95% confidence level. It is particularly important to compare p-values, instead of r-values, in this study because the biotic indices are calculated from varying sample sizes.

## 3.4 Results

The goal of this study was to apply the relationships between hydrogeomorphologic properties, specifically watershed slope (*S*) and drainage density (*DD*) (via equation 1), to investigate potential predictive relationships for inventories of aquatic biota in Neversink watersheds. This goal was motivated by previous work showing a relationship between aquatic biota and ANC (e.g. Baldigo et al., 2000; Bladigo and Lawrence, 2000; Ernst et al., 2008; Burns et al., 2008) and between estimates of mean *Runoff Ratio* and ANC in watersheds with measured discharge (Figure 3.1b). Initially, we evaluate the estimated mean *Runoff Ratios* in all watersheds where biotic inventories were available, before focusing on 'ungaged' watersheds that were not used to develop Equation 1.

Considering the whole population of watersheds, mean *Runoff Ratios* estimates were particularly well correlated to macroinvertebrate inventories (Figure 3.5a,b,c,d). The correlations to total macroinvertebrate richness, EPT richness, and Acid BAP index are significant ($|r|>0.74$, $p<0.01$) in all cases. The estimates of *Runoff Ratio* correlated particularly strongly to the Acid BAP Index (Figure 3.5c,d) developed by Burns et al. (2008) ($r=-0.93$ and $-0.89$, $p<0.01$ and $p<0.01$, for measurements in 1987 and 2003, respectively; Figure 3.5c,d). Correlation to the less acid-focused macroinvertebrate indices, total and EPT richness (Figure 3.5a,b), were slightly weaker, although still strong($r=-0.79$ and $-0.76$, $p<0.01$ and $p<0.01$, respectively). The estimates of *Runoff Ratio* were significantly correlated ($p<0.01$) to these macroinvertebrate indices, despite sampling dates that varied from 1987 to 2003.

The correlations of fish indices to the estimated mean *Runoff Ratios* (Figure 3.5e,f) were somewhat weaker compared to macroinvertebrate indices (Figure 3.5a,b,c,d). The correlations to total fish density and fish species richness were$=-0.76$ and $r=-0.72$, $p<0.01$ and $p=0.01$, respectively.

The acid tolerance of diatoms, measured using the DATI, was the most weakly correlated to the *Runoff Ratio* estimates ($r=0.57$, $p=0.04$) (data not shown). However, the overall strong and significant correlation of the *Runoff Ratio* estimates ($|r|>0.57$, $p<0.05$) from the entire population of watersheds to all the biotic indices is encouraging.

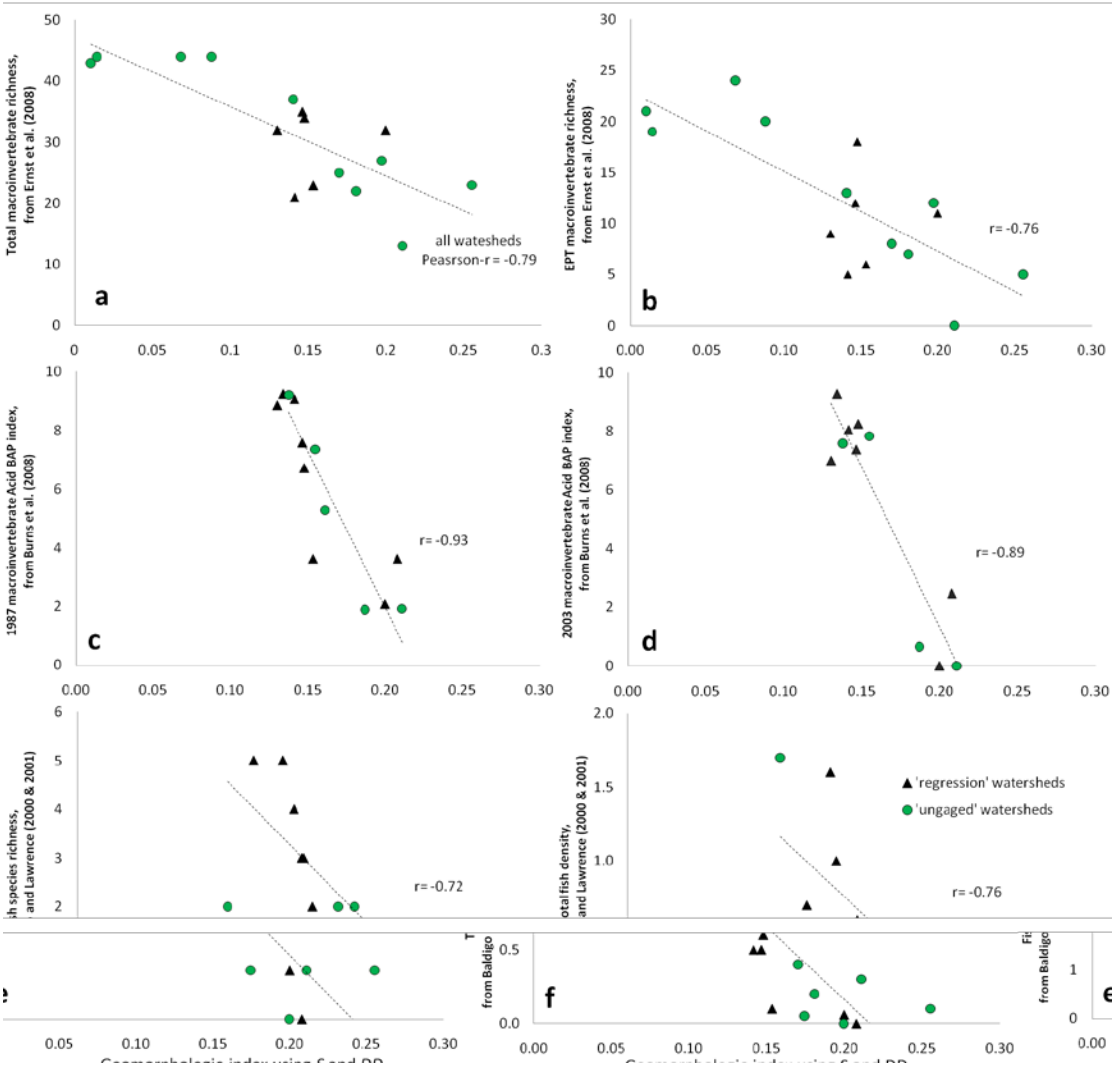


Figure 3.4: Relationships between: (a) total macroinvertebrate richness versus estimated *Runoff Ratio*; (b) EPT richness versus estimated *Runoff Ratios*; (c) Acid BAP index in 1987 versus estimated *Runoff Ratio*; (d) Acid BAP index in 2003 versus estimated *Runoff Ratio*; (e) fish species richness versus estimated *Runoff Ratio*; (f) total fish density versus estimated *Runoff Ratio*. Triangles correspond to the watersheds used to develop Equation 1, circles correspond to additional watersheds (Table 3.1) with r-values given for correlation to all watersheds.

The effectiveness of the *Runoff Ratio* estimates for predicting biotic indices varied in 'ungaged' watersheds compared to the 'regression' watersheds used to develop Equation 1 (Figure 3.3 and Table 3.1). Interestingly, some macroinvertebrate indices were more strongly correlated to *Runoff Ratio* estimates in 'ungaged' versus 'regression' watersheds, including total richness ($r=-0.83$, $p=0.04$ versus $r=0.14$, $p=0.80$) and EPT richness ($r=-0.87$, $p=0.02$ versus $r=0.13$, $p=0.81$) (Figure 3.5a,b). This is clearly because there were fewer 'regression' watersheds sampled and they covered a smaller range of ANC values than the 'ungaged' watersheds. As an example, the low correlation between macroinvertebrate richness data from Ernst et al. (2008) ($|r|>0.13$, $p<0.81$) was likely because 'regression' and 'ungaged' watersheds were sampled with different frequencies ($n=6$ and $n=10$, respectively) and at different times between 1991 and 2001.

Other biotic indices had similar correlation between 'ungaged' and 'regression' watersheds, including the 2003 Acid BAP index ($r=-0.94$, $p<0.01$ versus $r=-0.85$, $p<0.01$) and total fish density ($r=-0.81$, $p=0.03$ versus $r=-0.72$, $p=0.03$) (Figure 3.5d and 3.5f, respectively). In some cases however, *Runoff Ratio* estimates were less predictive in 'ungaged' versus 'regression' watersheds, including the 1987 Acid BAP index ($r=-0.92$, $p<0.01$ versus $r=-0.94$, $p=0.06$; Figure 3.5c), DATI ($r=0.56$, $p=0.15$ versus $r=0.53$, $p=0.36$; data not shown), and fish species richness ($r=-0.92$, $p<0.01$ versus $r=-0.55$, $p=0.20$; Figure 3.5e). Despite the inconsistency in the strength of predicting aquatic biota in 'ungaged' watersheds, the overall effectiveness of *Runoff Ratio* estimates in predicting various biotic inventories (Figure 3.5) suggests that its effectiveness was not limited to the narrow set of watersheds from which Equation 1 was developed.

## 3.5 Discussion

The reduced prediction of fish (slightly) and diatom (more substantial) inventories compared to the macroinvertebrate indices used here suggests that aquatic biota that are sensitive to instantaneous sampling conditions (e.g. changes in streamflow) were more difficult to predict with the hydrogeomorphologic index (Equation 1). This is consistent with observations of fish by Baldigo and Lawrence (2001) who suggested that well-buffered headwater streams (e.g. O1 and O2) are an 'oasis' from acidic event water that reduces fish density and species richness. It is also consistent with observations of Burns et al. (2008) who speculated that DATI values were reduced in August 2003 versus August 1987 because stream discharge was sharply higher during the later sampling date (data not shown here). Although the index still did adequately well in predicting fish inventories ($|r|>0.72$ $p=0.01$) and even diatoms ($|r|=0.57$ $p=0.04$), it appears better suited to predicting macroinvertebrate inventories ($|r|>0.74$, $p<0.01$) because of their reduced sensitivity to episodic changes in stream discharge and acidity.

The proposed hydrogeomorphologic index captured the more buffered stream chemistry (high ANC) and reduced biota populations in some small watersheds (>10 $km^2$) that were less steep and had fewer stream channels (Table 3.1). For example, WB6 and WB7 are less steep (0.20 m/m) and HF and O2 have smaller drainage densities (<0.85 $km/km^2$). The index was less effective, however, at indicating that small tributaries alter downstream stream chemistry. For example, the addition of O2 (*Runoff Ratio* estimate = 0.10) below B2 (*Runoff Ratio* estimate = 0.17) does not correspond to the better buffered section of O1 (*Runoff Ratio* estimate = 0.17) (see Figure 3.3 and Table 3.1). The hydrogeomorphologic index (Equation 1) would be less applicable in areas with more isolated, small buffering sources or where

topographical differences (e.g. slope) are more subtle. Additionally, defining the perennial stream channels to derive drainage density may be problematic in some areas.

The relationships between the proposed geomorphologic index and inventories of aquatic biota are strongly linked to the reliability of Equation 1 to estimate the mean *Runoff Ratio* (Figure 3.2a). Measurements of mean *Runoff Ratio* are somewhat stochastically controlled by weather and runoff conditions. Measurements taken from 20 storms during 1991 to 1993 may not reflect any repeatable runoff response, but do provide a strong measure of the relative hydrological differences between the watersheds. The hydrogeomorphologic index based on average slope (*S*) and drainage density (*DD*) is thus a 'static' indicator independent of rainfall and antecedent conditions. It is possible that some dynamic characteristics of mean *Runoff Ratio* are not included in our simple regression equation (Figure 3.1a), which may have reduced the accuracy of our predictions.

These limitations in our 'static' hydrogeomorphologic index aside, there is clear potential for improving watershed monitoring and management in areas with similar geomorphological controls on hydrology. Hydrogeomorphologic-based indices have the potential to focus sampling locations for aquatic biota without the need for field monitoring. Knowledge about the spatial distribution of aquatic biota could also be used for developing comprehensive biotic inventories or focusing mitigation strategies to areas at-risk for stream acidification. Although this study is unlikely to apply in watersheds with contrasting topography or isolated buffering sources, it indicates that under some conditions aquatic biota can be predicted using simple, widely-available spatial data.

## 3.6 Conclusions

High inputs of acidic deposition have reduced soil base-cation stores and stream acid neutralizing capacity (ANC) in parts of the Neversink watershed. As a result, stream acidity continues to negatively affect a variety of aquatic biota populations in many Neversink streams. In this study, an estimate of the mean *Runoff Ratio* was calculated for 28 Neversink sub-watersheds (0.3 to 176.0 $km^2$) using a hydrogeomorphologic index based on mean slope and drainage density. The hydrogeomorphologic index was then correlated to macroinvertebrate, diatoms, and fish inventories collected in previous studies. The geomorphologic index was particularly effective in predicting macroinvertebrate populations ($|r|>0.74$, $p<0.01$). However, aquatic biota that are especially susceptible to rapid, episodic changes in stream acidity (e.g. fish and diatoms) were more difficult to predict ($|r|>0.57$, $p<0.05$) with our 'static' hydrogeomorphologic index. The hydrogeomorphologic index also correlated to biotic inventories from 'ungaged' watersheds that did not have discharge data. Despite some limitations, the proposed hydrogeomorphologic index could offer a cost-effective alternative to identify where aquatic biota will be at risk from surface water acidification.

# REFERENCES

Baker, J.P., J. Van Sickle, C.J. Cagen, D.R. DeWalle, W.E. Sharpe, R.F. Carline, B.P. Baldigo, P.S. Murdoch, D.W. Bath, W.A. Krester, H.A. Simonin, and P.J. Wigington. 1996. Episodic acidification of small stream in the Northeastern United States: effects on fish populations. Ecological Applications. 6(2): 422-437.

Baldigo, B.P. and P.S. Murdoch. 1997. Effect of stream acidification and inorganic aluminum on mortality of brook trout (Salvelinus fontinalis) in the Catskill Mountains, New York. Canadian Journal of Fisheries and Aquatic Sciences. 54: 603-615.

Baldigo, B.P. and G.B. Lawrence. 2000. Composition of fish communities in relation to stream acidification and habitat in the Neversink River, New York. Transactions of the American Fisheries Society. 129: 60-76.

Baldigo, B.P. and G.B. Lawrence. 2001. Effects of stream acidification and habitat on fish populations of a North American river. Aquatic Sciences. 63: 196-222.

Baldigo, B.P., Schuler, G.E., and Riva-Murray, K.R., 2002, Mussel community composition in relation to macrohabitat, water quality, and impoundments in the Neversink River, New York: U.S. Geological Survey Open-File Report 2002–104, 26 pp.

Baldigo, B.P., Riva-Murray, K.R., and Schuler, G.E., 2003, Effects of environmental and spatial features on mussel populations and communities in a North American river: Walkerana, v. 14, no. 31, p. 1–32.

Burns, D.A., M.R. McHale, C.T. Driscoll, and K.M. Roy. 2006. Response of surface

water chemistry to reduced levels of acid precipitation: comparison of trends in two region of New York, USA. Hydrological Processes. 20: 1611-1627.

Burns, D.A., K. Riva-Murray, R.W. Bode, S. Passy. 2008. Changes in stream chemistry and biology in response to reduces levels of acid deposition during 1987-2003 in the Neversink River Basin, Catskill Mountains. Ecological Features. 8(3): 191-203.

Driscoll, C.T., G.B. Lawrence, A.J. Bulger, T.J. Butler, C.S. Cronan, C. Eagar, K.F. Lambert, G.E. Likens, J.L. Stoddard, and K.C. Weathers. 2001. Acid deposition in the Northeastern United States: sources and inputs, ecosystem effects, and management strategies. Bioscience. 51(3): 180-198.

Driscoll, C.T., K.M. Driscoll, M.J. Mitchell, and D.J. Raynal. 2003. Effects of acidic deposition on forest and aquatic ecosystems in New York State. Environmental Pollution. 123(3): 327-336.

Ernst, A.G., B.P. Baldigo, G.E. Schuler, C.D. Apse, J.L. Carter, and G.T. Lester. 2008, Effects of habitat characteristics and water quality on macroinvertebrate communities along the Neversink River in southeastern New York, 1991-2001. USGS Scientific Investigation Report, 2008-5024, 15p.

Hewlett, J.D. and Hibbert, A.R. 1967. Factors affecting the response of small watersheds to precipitation in humid regions. In *Forest Hydrology* (eds. W.E. Sopper and H.W. Lull). Pergamon Press, Oxford. pp. 275-290

Kurdish, M. 2002. Catskill Forests. Purple Mountain Press: Fleischmanns, NY.

Lawrence, G.B., Lincoln, T.A., Horan-Ross, D.A., Olson, M.L., Waldron, L.A., 1995.

Analytical Methods of the U.S. Geological Survey's New York District Water-Analysis Laboratory. U.S. Geol. Surv. Open-File Rpt., 95-416, 78 pp.

Lawrence, G.B., M.B. David, G.M. Lovett, P.S. Murdoch, D.A. Burns, J.L. Stoddard,B.P. Baldigo, J.H. Porter, and A.W. Thompson. 1999. Soil calcium status and the response of stream chemistry to changing acidic deposition rates. Ecological Applications. 9(3): 1059-1072.

Lawrence, G.B., D.A. Burns, B.P. Baldigo, P.S. Murdoch, and G.M. Lovett. 2001. Controls on stream chemistry and fish populations in the Neversink Watershed Catskill Mountains, New York. USGS WRIR 00-4040.

Lawrence, G.B. 2002. Persistence episodic acidification of streams linked to acid rain effects on soil. Atmospheric Environment. 36:1 589-1598.

Lincoln, T. A., D. A. Horan-Ross, M. L. Olsen, and G. B. Lawrence. 1996. Quality-assurance data from routine water analyses by the U.S. Geological Survey Laboratory in Troy, New York—May 1991 through June 1993. U.S. Geological Survey, OFR 96-167, Troy, New York.

Lovett, G.M., A.W. Thompson, J.B. Anderson, and J.J. Bowser. 1999. Elevational patterns of sulfur deposition at a site in the Catskill Mountains, New York. Atmospheric Environment. 33: 617-624.

Murdoch, P.S. and J.B. Shanley. 2002. Flow-specific trends in river-water quality resulting from the effects of the Clean Air Act in three mesoscale, forested river basins in the Northeastern United States through 2002. Environmental Monitoring and Assessment. 120: 1-25.

Murdoch, P.S. and J.L. Stoddard. 1993. Chemical characteristics and temporal trends in eight streams of the Catskill Mountains, New York. Water, Air, and Soil Pollution. 67(2): 367-395.

Ozvarth, D.L. 1985. Glacial geomorphology and the late Wisconsinain deglaciation of the western Catskill Mountains. State University of New York at Binghamton, Doctoral Dissertation. 181p.

Passy, S.I. 2000. Stream biomonitoring in New York using periphytic diatoms. NY State Department of Environmental Conservation. Technical Reaport. 17pp.

Passy, S.I., I. Ciugulea, G.B. Lawrence. 2006. Diatom diversity in chronically versus episodically acidified Adirondack streams. Internat. Rev. Hydrobiol. 91(6): 594-608.

Rich, J.L. 1934. Glacial Geology of the Catskills. New York State Bulletin, 299. University of the State of New York, Albany. 180 pp.

Shaman, J. M. Stieglitz, and D. Burns. 2004. Are big basins just the sum of small catchments?. Hydrological Processes. 18:3195-3206.

Soren, J. 1961. The ground-water resources of Sullivan County, New York: New York State Department of Conservation Bulletin GW-46, 66p.

Thaler, J.S. 1996. In Catskill Weather. Purple Mountain Press: Fleischmanns, New York.

Van Sickle, J., J.P. Baker, H.A. Simonin, B.P. Baldigo, W.A. Kretser, and W.E. Sharpe. 1996. Episodic acidification of small stream in the Northeastern United Sates: fish mortality in field bioassays. Ecological Applications. 6(2): 408-421.

Vitvar, T., D.A. Burns, G.B. Lawrence, J.J. McDonnell, and D.M. Wolock. 2002. Estimation of baseflow residence times in watersheds from the runoff hydrograph: method and application in the Neversink watershed Catskill Mountain, New York. Hydrological Processes. 16: 1871-1877.

Wolock, D.M., J. Fan, and G.B. Lawrence. 1997. Effects of basin size on low-flow stream chemistry and subsurface contact time in the Neversink River Watershed, New York. Hydrological Processes. 11:1273-1286.

Chapter 4

# EFFECTS OF PREFERENTIAL HYDROLOGICAL PATHWAYS IN A GLACIATED WATERSHED IN THE NORTHEASTERN USA

## 4.1 Abstract

Despite observational evidence of preferential flowpaths in watersheds in the Northeastern U.S., their effects on the spatial sources of runoff remain unclear. An intense field survey was undertaken during the 2007 growing-season to determine the sources of stream runoff to a 2.51 $km^2$ watershed in the Catskill Mountains, New York State, where preferential pathways are caused by groundwater springs and soil piping. A two-component hydrograph separation using $\delta^{18}O$ shows that the contribution from event water (new rain water) ranged from 14% to 37% of the runoff volume and 18% to 49% of the peak streamflow for nine rainfall events. Further, end-member mixing analysis (EMMA) using $\delta^{18}O$, Si, and DOC shows that groundwater is the dominant runoff source, but saturated areas account for between 2% to 24% of the total volume 4% to 59% of discharge at peak streamflow. Field surveys of saturated areas suggest that near-stream areas are insufficient to generate the observed tracer concentrations in rainfall events >8 mm, and require connection of upslope areas to explain the hydrograph separations. These results are corroborated by the timing of the transient groundwater and overland flow response that confirm hill side preferential flowpaths rapidly transport water to near-stream saturation areas. Conventional methods for estimating variable saturated areas (VSA) using surface topography and soil transmissivity over predict VSA in the valley-bottom and do not capture the concentrated VSA on the hill sides. Overall these results are consistent with recent

findings from other landscapes with co-evolved glacial soils, where the lateral re-distribution in hill side areas can reduce the influence of the topography and drainage network spatial sources of stream runoff.

## 4.2 Introduction

The spatiotemporal characterization of hydrological pathways resulting from complex subsurface heterogeneity is fundamental to modeling catchment hydrology and water quality (Lin 2006; Beven 2002). Models based on most conventional theories (such as Darcy's Law, advection-dispersion equation, and the conservation of mass) imply that water and solutes move within a small deviation of an average velocity. To account for both the 'long' and 'short' term memory found in real hydrologic systems (Kirchner 2000) using these conventional theories would require the explicit mapping of all the heterogeneous subsurface properties, an impossible task in even small research watersheds (Beven 2002; McDonnell et al. 2007). Most models instead rely on calibration to account for a lack of knowledge about spatial heterogeneities (McDonnell et al. 2007). However, there is concern that models calibrated to the outlet response may not be capturing the internal processes of the watershed that are critical for soil and water management. McDonnell et al. (2007) therefore suggests that simple explanations for the emergence, maintenance, and interconnections of landscape heterogeneities would have widespread implications for improving modeling. Although their work points a way forward, simple and generalizable explanations capable of predictions in ungauged basins remain elusive because of the incredible variety in measured watershed responses (Troch et al. 2008).

Some principles are emerging for predicting dominant runoff processes in ungauged watersheds by comparing watersheds from different landscape units (e.g. McGlynn et al. 2004), across spatial scales (e.g. McGuire et al. 2005; Hrachowitz et

al. 2009), and from differing geomorphologic provinces (Tetzlaff et al. 2009). It is general accepted that in steep terrain, gravitationally driven subsurface flowpaths dominate and topography is more important than catchment size in determining the average hydrologic response (Tetzlaff et al. 2009, McGuire et al. 2005). The drainage network (topology) is also an important hydrologic control in watersheds where landscape features adjacent to the stream are important sources of runoff (Buttle 2006; McGlynn et al. 2004) and at larger spatial scales when in-stream transit is significant. However, Buttle (2006) proposes that a third control, in addition to topography and topology, is necessary for watersheds with heterogeneous subsurface properties.

When parts of the landscape partition water differently between lateral and vertical movement (typology) the effects of subsurface properties become increasingly important. For example, the typology of the Cairngorms Mountains, Scotland is radically different between the highly-responsive peat soils, where water is transported laterally by overland flow, and more free draining podzolic soils, where vertical flow dominates (Soulsby et al. 2006; Soulsby and Tetzlaff 2008; Hrachowitz et al. 2009). As a consequence, Soulsby and Tetzlaff (2006) could show that even at a basin scale of 230 $km^2$, differences in typology at the hillslope-scale reduce the influence the drainage network (topology) and topography. The work in the Cairngorms and in other areas (Laudon et al. 2007; Broxton et al. 2009) demonstrates that differences in typography can alter the flowpaths and source areas in landscapes with co-evolved soils.

The landscape in the glaciated Northeastern U.S. is composed of hill sides and uplands with shallow, highly permeable soils and valley bottoms with deeper soils that are more poorly drained. Clear differences in typography occur between variable saturation areas (VSA) that are dominated by lateral runoff versus deep drift and

alluvial deposits that are more freely draining. Saturation-excess runoff from VSA is the dominant runoff mechanism (Betson 1964; Dunne and Black 1970; Dunne et al. 1975) and high infiltration rates make infiltration-excess runoff unlikely during storms (Walter et al. 2002). The spatial distribution of VSA is in part driven by topography, causing saturation in flatter areas, at breaks in slope, or when upslope contributing areas are large (Beven and Kirkby 1979). The classical conceptualization of VSA dynamics predicts that VSA will develop in the areas adjacent to the stream channel (Dunne et al. 1975; Engman 1974), making the drainage network (topology) important when subsurface differences is small. Not surprisingly, the models derived from these 40 year-old conceptualizations have focused on topographic controls on VSA and may be neglecting the subsurface heterogeneity in these complex glacial landscapes.

Conventional VSA models are routinely used to calibrated with watershed discharge to predict runoff source areas for management decisions (Mehta et al. 2004), but a lack of field-scale validation means that we may not be 'getting the right answers for the right reasons'. Steenhuis et al. (1995) convincingly showed that in watersheds dominated by VSA hydrology, discharge could be predicted by just part of the watershed soils being at field capacity (the VSA extent) prior to runoff. The disadvantage of this approach is that it does not explain the distribution of storages, thus techniques have been developed to predict VSA locations based on the Topographic Index (Beven and Kirkby, 1979) and the Soil Topographic Index (Beven, 1986), which use local slope, upslope area, and soil transmissivity (see Methodology section). These saturation maps can be parameterized into distributed models to predict the spatiotemporal sources of runoff during rainfall events and across antecedent conditions (Mehta et al 2004; Lyon et al. 2004; Dahlke et al. 2009). Unfortunately, when these models are calibrated to the outlet discharge the effective

lateral hydraulic conductivity must be increased up to ten-fold from the soil survey properties (Mehta et al. 2004). A lack of consideration for the distribution and dynamics of preferential flowpaths, and their impacts on landscape typology, within distributed VSA models could have important ramifications on soil and water management.

The potential control of preferential flowpaths on the extent VSA is limited by the lack of field-scale validation. Several previous researchers observed that water was supplied to near-stream saturation areas from subsurface macropores (Waddington et al. 1993; Buttle and Peters 1997) and overland flow from upslope springs (Engman 1974; Inamdar and Mitchell 2007). Dunne et al. (1975) and Dunne and Black (1970) showed that during wet conditions in Sleepers River, Vermont the saturated areas and overland flow were controlled by the location of groundwater seeps. Subsurface preferential flowpaths also connect perched water tables on restrictive layers (Lin 2006; Lin and Zhou 2008) or along the bedrock (Tromp van Meerveld and McDonnell 2006), which can be connected to the stream or near-stream VSA in larger events. Overall, these preferential flowpaths act to change the typography across the landscape by increasing lateral flow and thereby reducing the influence of surface topography and topology on runoff sources. The inclusion of preferential flowpaths in VSA models therefore has the potential improve runoff predictions and management decisions.

The goal of this study is to determine the importance of hill side preferential flowpaths to the spatial distribution of runoff sources during rainfall events. The study is carried out in a tributary to Town Brook watershed (2.51 $km^2$) in the Catskill Mountains, New York State where several preferential flowpaths have been located and monitored, including soil pipes and groundwater springs. Intensive field mapping

was used to document the saturated areas in the landscape and their hydrologic connectivity. The contributions of the saturated areas to stream runoff are investigated using a combination of hydrometric, chemical, and isotopic measurements during nine storm events. The study is intended to define basic watershed function and verify that conventional distributed models can capture the complex flowpaths present in the glaciated, mixed-use watersheds in the Northeastern U.S.

## 4.3 Methodology

### 4.3.1 Study Site

The 60 ha study hillslope is part of a 2.51 km2 study watershed in the southwest corner of the 36.5 km2 Town Brook watershed in the Catskill Mountain region of New York State (Figure 4.1). The study watershed was cleared for grazing in the early 18$^{th}$ century, but has returned to 75% forest, dominated by hardwoods like American beech (fagus grandifolia), red maple (acer rubrum), sugar maple (acer saccharum), and yellow birch (betula alleganiensis) (Kurdish 2002), and 25% shrub and brush (Figure 4.1). The watershed ranges in elevation from 585 m to 935 m, with slopes from 0° to 40°. The climate is characteristically humid, with an average annual temperature of 8° C and average annual precipitation of about 900 mm.

The Catskill Mountains have characteristic glacial features typical of watersheds in the Northeastern U.S. The geology is sandstones (60%) and interbedded siltstones and shales (40%) that produce contact springs on the hill sides (Rich 1934; Reynolds 2000). The soil development has been highly influenced by glacial features, with deep drift features in the valley-bottoms and shallow, undeveloped till soils on the hillslopes. The effective soil depths are reduced by a compacted restrictive layer, referred to as a ‘fragipan’, at depths between 30 and 70

cm across most of the hillslope (USDA 2007). The effective conductivity of the fragipan is roughly 0.5 cm/hr, or an order of magnitude less than the well-drained surface material that drains at 15 cm/hr. Dahlke et al (2009) used seismic refraction to estimate a glacial till thickness of up to 4 m in near stream areas.

The catena at the study hillslope is derived from glacial till composed from reddish sandstone, siltstone, and shale. The soils are all silt loam with high (>10%) amount of rock fragments, the study watershed is composed of about 35% Willowmoc soils, 30% Lackawanna soils, 10% Onteora soils, and 25% soils of minor extent (USDA 2007). The Lackawanna soils are on the hillsides and convex hilltops with a moderately draining layer above the dense fragipan (Figure 4.1). The Willowmoc soils are located slightly down the hill sides and also have moderately draining surface layers. The Onteora soil series is in the flat area adjacent to the stream have much lower transmissivity. Soil maps are developed from Soil Survey Geographic (SSURGO) data along with associated attribute tables (Map Unit Identification Records), which are used to extract soil properties.

Figure 4.1: Measurements locations at Town Brook watershed, a mixed land-use watershed in the Catskill Mountains. Watershed analysis is completed in the study watershed in the southeast corner of Town Brook. Hillslope measurements are made at four well locations, four weirs, a rain gauge, and two saturated areas during nine storm events. Soils are composed of several classification series across the hillslope.

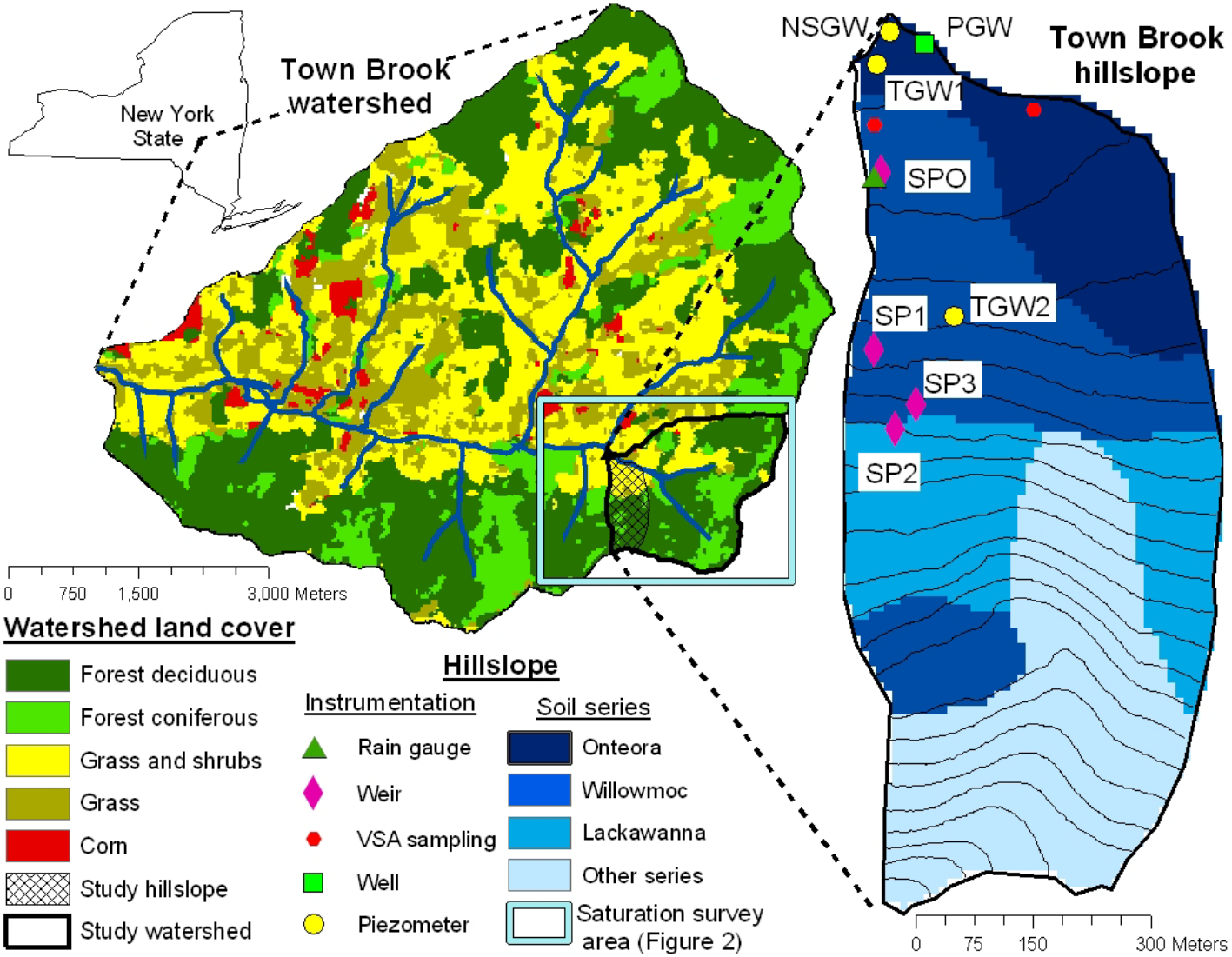
New York State
Town Brook watershed
0 750 1,500 3,000 Meters
Watershed land cover
Forest deciduous
Forest coniferous
Grass and shrubs
Grass
Corn
Study hillslope
Study watershed
Hillslope
Instrumentation
Rain gauge
Weir
VSA sampling
Well
Piezometer
Soil series
Onteora
Willowmoc
Lackawanna
Other series
Saturation survey area (Figure 2)
NSGW
PGW
Town Brook hillslope
TGW1
SPO
SP1
TGW2
SP3
SP2
0 75 150 300 Meters

### 4.3.2 Field Collection

Water chemistry and quantity measurements were made at a variety of locations during the growing season of 2007. Water table heights were measured at four locations (Figure 4.1) using WT-HR 500 and 1000 capacitance probes from TruTrack, Inc. inside 2.5-cm PVC tubes and screened to various depths. The measurements were made at different positions along the hillslope to capture the transient groundwater response above the fragipan layer and the deeper permanent groundwater response. The permanent groundwater (henceforth referred to as PGW) measurement was made about 1.0 m from the stream using a well that was screened from 0.2 m to 0.6 m from the surface at a location without a fragipan layer. The remaining three piezometers measured the transient groundwater directly above the fragipan at various depths and locations; in the near-stream to a depth of 50 cm, (NSGW), 55 cm in the low-angle valley bottom (TGW1), and 40 cm on the steeper hill side (TGW2). Water table depths were measured at 15 minute intervals during the rainfall events.

Overland flow discharge measurements were also made at four locations (Figure 4.1). In the areas where continuous baseflow was maintained, spring 1 (SP1) and the soil pipe outlet (SPO), H-flumes were installed. At the other two more transient overland flow locations, spring 2 (SP2) and spring 3 (SP3), Parshall flumes were installed. Overland flow was too diffuse just below the spring outlet to install the flumes, thus installation was approximately 5 m to 10 m below the outlet, leaving a small saturated area above some of the flumes (explained more in the Results section). Stage-discharge relationships were developed for the flumes across a range of discharges. Discharge data was collected every 15 minutes using Druck water level pressure transducers connected to Telog data recorders.

The extent of saturated areas was measured using a global positioning system (GPS) unit and intensive field surveys. The soil was determined to be saturated using the 'boot-print' technique by making a small depression in the soil (1 to 2 cm) and observing if it re-filled with water. The GPS had an accuracy of 3 m or better during the surveys and was subsequently uploaded into a geographic information systems (GIS) program to calculate the spatial coverage. Errors in these estimates could result from small (< 5 $m^2$) saturation areas that were missed or not well-represented by the GPS measurements. As a result more detailed surveys with measuring tapes were made at the small saturation areas above the weirs of SP1, SP2, and SP3 across a range of conditions. The extent of saturated area caused above SP2 varied from ~0 to ~16 $m^2$ and ~2 to ~19 $m^2$ at SP3. The continuous baseflow discharge at SP1 creates a larger saturation area of ~5 $m^2$ to ~24 $m^2$. The soil pipe also maintains discharge during the driest summer periods, dye tracing revealed that water is transported at least 80 m and at velocities of up to 0.70 m/s in the soil pipe.

The topographic index (TI) (Beven and Kirkby 1979) and soil topographic index (STI) (Beven, 1986) are employed to capture the overall dynamics of saturated extent based on topography and soils. The TI is calculated based on the Digital Elevation Model (DEM):

$$TI = \frac{\alpha}{tan\beta} \qquad (1)$$

where $a$ is the upslope contributing area ($m^2$) and $\beta$ is the local surface topographic slope (radians). Large TI values mean that areas receive more upslope water and/or are less steep. The STI is calculated from a DEM and soil properties given in the SSURGO soil survey data:

$$STI = \frac{\alpha}{DK_s tan\beta} \qquad (2)$$

where $D$ is the local soil depth (m) and $K_s$ the saturated hydraulic conductivity ($md^{-1}$). Large *STI* values indicate locations that are more prone to saturation than small $\lambda$.

Water chemistry was also monitored at a variety of locations across the watershed. Grab samples were collected from the stream at up to 15 minute intervals using an ISCO automatic water sampler mounted 5 cm above the channel bed. Rain water was collected 0.5 from the ground surface near the tipping bucket and at a forested location below the canopy. Rain water was collected in 2 mm increments and mixed between the two 30-cm funnel collectors proportionate to the volume collected. Soil water was collected using free draining lysimeters that were made from 5 cm PVC and gravity fed to a collection vessel that was pumped after the storm events. The lysimeters were installed at depths of 15 and 40 cm adjacent to the NSGW location (Figure 4.1). The volume of water collected from each lysimeter was considered indicative of the amount of flow through the soil horizon, which was minimal in the largest events and did not occur in five of the nine events. Saturation area sampling was mixed from two locations (Figure 4.1) and was sampled at the surface to minimize the amount of particulate organic matter collected. Near-stream groundwater samples were collected prior to and during each event from the observation well located 1 m from the stream (Figure 4.1). Spring water is sampled during baseflow from the weirs located 5 to 10 m from the spring outlet.

### 4.3.3 Laboratory Analysis

All samples were refrigerated until they were analyzed. Major ions and dissolved organic carbon (DOC) were analyzed in the Soil and Water Laboratory in the Biological Environmental Engineering Department at Cornell University. The water samples were passed through a 0.45 µm nitrocellulose filter before being

analyzed. The cation Si was analyzed with ThermoJarrel Ash with customized axial view torch inductively coupled plasma (ICP) spectrometer and reported to with a 15% error. The anions Cl were analyzed with the Dionex ICS-2000 with anion column and reported to within a 10% error. The DOC was measured with the OIAnalytical 1010 wet oxidation TOC/DOC analyzer with an error within 10% and a coefficient of variation of 10%.

The $\delta^{18}O$ samples were stored in glass vials with polyseal caps to prevent evaporation prior to transport to the Laboratory of Isotope Geochemistry at the University of Arizona. The samples were analyzed for $\delta^{18}O$ at the University of Arizona using a DLT-100 Liquid Water Isotope Analyzer. Standards were analyzed immediately preceding the analysis of every sample to ensure adequate results. The analysis procedure is outlined in Lyon et al. (2009). The analyzer has a reported measurement error of 0.1‰ and 0.8‰ for $\delta^{18}O$ and $\delta^{2}H$ measurements, respectively (Lis et al., 2008), and in-house error estimates of 0.11‰ and 0.4‰.

### 4.3.4 Hydrograph Separation Techniques

Three hydrograph separation techniques were applied in this study: 1) graphical techniques, 2) two-component isotopic separation (Sklash and Farvolden 1979), and 3) end-member mixing analysis (Christopherson and Hooper 1992). The hydrograph was separated into quickflow and delayed flow for each of nine storm events, as described by Hewlett and Hibbert (1967). A separation line was projected from the initial rise of the hydrograph at a slope of 0.5 $s^{-1}km^{-2}h^{-1}$. This method was used to estimate the runoff ratio, by dividing the quickflow by the rainfall amount for each event.

The two-component technique (Sklash and Farvolden 1979) is a mass balance approach that separates the hydrograph into pre-event water (baseflow and water stored within the watershed prior to rainfall) and event water (rain water) based on the stable isotope ratios:

$$Q_t C_t = Q_p C_p + Q_e C_e \qquad (3)$$

where Q is discharge, C is $\delta^{18}$O composition, and the subscripts t, p, and e refer to total, pre-event, and event water, respectively. The contributions of event and pre-vent water were estimated for each stream sample. The event water was estimated based on median $\delta^{18}$O of the rain samples collected at 2 mm increments. The pre-event water is the baseflow chemistry within 24 hr of the beginning of the rain event. The uncertainty of each computed mixing fraction was evaluated using the technique described by Genereux (1998).

$$W_{fp} = \sqrt{\left[\frac{C_e - C_s}{(C_e - C_p)^2} W_{Cp}\right]^2 + \left[\frac{C_s - C_p}{(C_e - C_p)^2} W_{Ce}\right]^2 + \left[\frac{1}{(C_p - C_e)} W_{Ce}\right]^2} \qquad (4)$$

An EMMA model was used to estimate the runoff source areas following the steps outlined by Christopherson and Hooper (1992). First, linear plots of pairwise combination of solutes (mixing diagrams) are used to find conservative tracers across all nine events. Second, the selected tracers are standardized into a correlation matrix such that solutes with greater variation do not exert more influence. Third, a principal component analysis is completed for all combination of three, four, and five solutes ($\delta^{18}$O, Si, DOC, Cl, and Ca). The model selected accounted for the greatest variability across all nine events with two principal components, implying three end-members are necessary and using the three solutes $\delta^{18}$O, Si, and DOC. The concentrations of the end-members are then projected in the U-space defined by the stream PCA. The goodness-of-fit for the predicted tracer concentrations are compared through least-

squares linear regression. The EMMA model was used then used to estimate the contributions from each of the three end members by solving the mass balance:

$$Q_{st} = Q_{of} + Q_{tf} + Q_{gw} \quad (5)$$

$$U1_{st} Q_{st} = U1_{of} Q_{of} + U1_{tf} Q_{tf} + U1_{tf} Q_{gw} \quad (6)$$

$$U2_{st} Q_{st} = U2_{of} Q_{of} + U2_{tf} Q_{tf} + U2_{tf} Q_{gw} \quad (7)$$

where Q is discharge, U1 and U2 are the first and second components of PCA, and three end-members of, tf, and gw, corresponding to overland flow, throughfall (rainfall), and groundwater, respectively.

The chemistry of each end-member is estimated as the median of samples taken before, during, and after the event. The temporal variability of the solute concentrations, particularly near stream groundwater and spring water, was small during the events. The short duration high intensity rain storms also had minimal temporal variability in chemistry, although concentrations changed over the course of the study period. The water chemistry in the saturated areas also did not change appreciably during the storm events, but did show some dilution of Si and DOC, and enrichment of $\delta^{18}$O. Varying tracer concentrations is recommended when temporal variability is large, although in this study more consistent results from all nine events were found when the median concentrations are taken. The assumption of static end-members is unlikely across all events, but provides an effective means for comparing a range of rainfall events.

The uncertainty for each principal component is estimated using the method described by Burns et al. (2001) based on the analytical uncertainty of each solute:

$$W_{ui} = [(V_{ia} W_a)^2 + (V_{ib} W_b)^2 + \cdots]^{0.5} \quad (8)$$

Where $W_{ui}$ is the uncertainty value for principal component I, $V_{ia}$ and $V_{ib}$ are eigenvectors for solutes a and b for principal component i, and $W_e$ and $W_{eb}$ are the analytical uncertainties. The uncertainty value for each component is then used to create two new sets (high estimate and low estimate) of values for U1 and U2. These new values of U1 and U2 are then used in Equations 3 through 5 to calculate an uncertainty range for each event.

## 4.4 Results

In this section, the geochemical, isotopic, and hydrometric measurements are described for nine rainfall events. Additionally, six field surveys are used to map the saturated areas.

### 4.4.1 Mapping of Surface Saturation Patterns

Hill side and near-stream saturated areas are evident from simple field surveys. Six surveys were collected immediately prior to, during, and after the 2007 growing season (Figure 4.2) using a handheld GPS receiver. The saturation extent decreases after snowmelt through the summer (4.2a through 4.2d), until the watershed 'wets-up' after the 9/12/07 survey (4.2e), characteristic of early Fall events. As the soil profile dries, the estimate of saturation extent drops from 9.90% after snowmelt to 1.70% of the surveyed area during the summer low-flow. The location of saturation also shifts from near-stream areas after snowmelt to more finger-like patterns originating from point-sources (Figure 4.2). The consistent hill side saturation patterns are fixed by groundwater springs (Figure 4.2), which maintain down slope saturation through the driest periods.

The size of saturated areas varies little over the dry summer conditions, changing from 1.7% to 4.3%, but responding rapidly to rainfall events. For example, the survey on 9/5/07 was made during summer low flow conditions, but prior to the rainfall events on 9/8, 9/9, and 9/11/07 (Figure 4.2). The survey on 9/12/07 is made within 3 hours of peak stream runoff from a 13 mm rainfall event. Comparing the 9/5 and 9/12/07 surveys shows that the spatial extent of saturated areas increases over two-fold from 29 mm of rainfall over three days. The hill side saturated areas extend down slope and become temporarily connected to the stream in the 9/12/07 survey. After the system 'wets up' during the 9/12/07 event, the extent of saturated areas does not decrease appreciably again before the 10/5/07 survey, but in the later survey lacks the overland connections to the stream (Figure 4.2e versus 4.2f). These simple surveys provide qualitative evidence of the spatial and temporal dynamics of overland flow pathways and are used to validate the measurements made during the rainfall events.

Figure 4.2: Maps of surface saturated areas made using field surveys. Six field surveys using the 'bootprint' method of saturation and GPS system (to accuracy of 3 meters). 4.2a also shows the hillshade (topography), 4.2b shows the topographic index, 4.2c shows the soil topographic index, and 4.2f shows the USGS delineated stream channels.

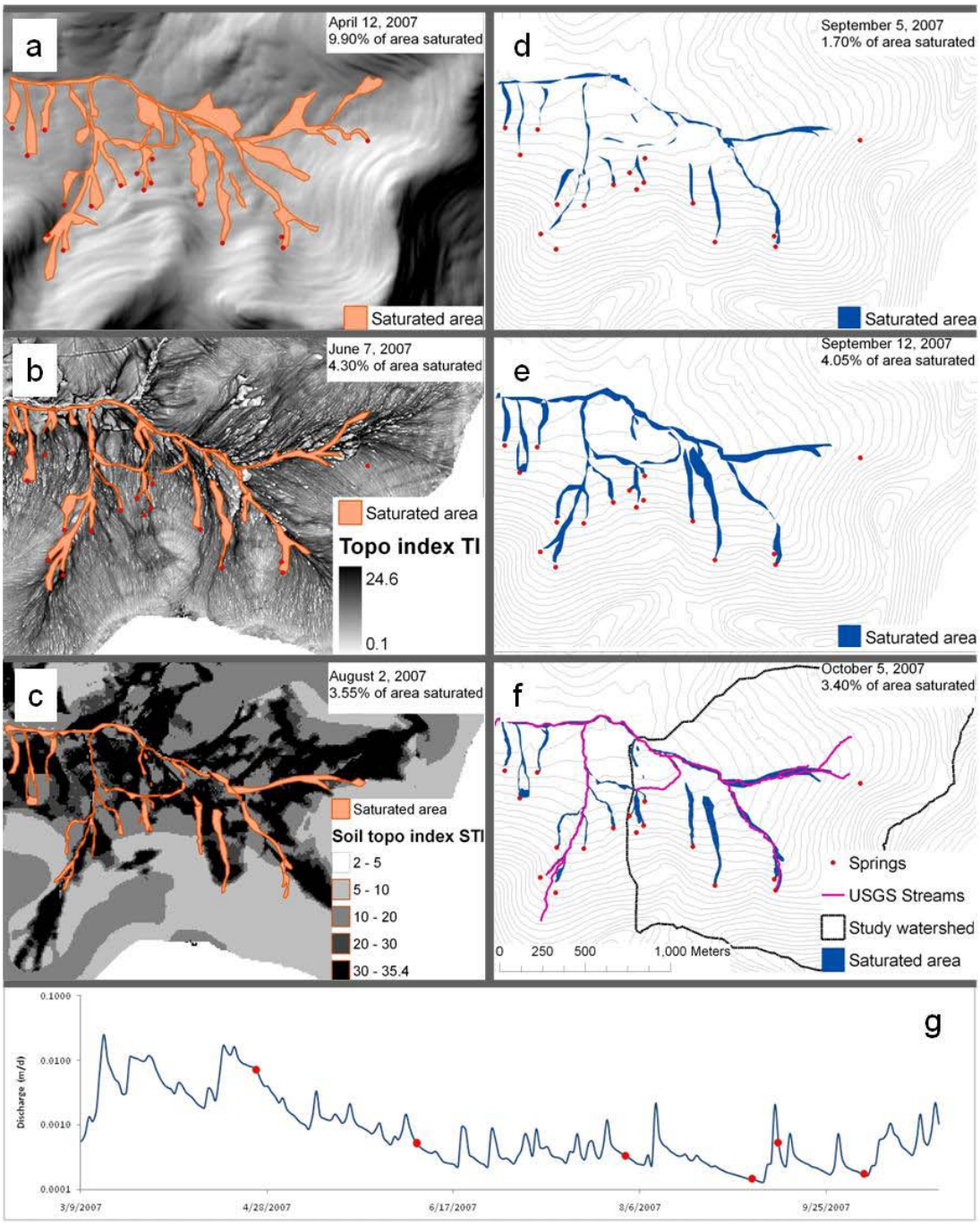
a
April 12, 2007
9.90% of area saturated
Saturated area
d
September 5, 2007
1.70% of area saturated
Saturated area
b
June 7, 2007
4.30% of area saturated
Saturated area
Topo index TI
24.6
0.1
e
September 12, 2007
4.05% of area saturated
Saturated area
c
August 2, 2007
3.55% of area saturated
Saturated area
Soil topo index STI
2 - 5
5 - 10
10 - 20
20 - 30
30 - 35.4
f
October 5, 2007
3.40% of area saturated
Springs
USGS Streams
Study watershed
Saturated area
0 250 500 1,000 Meters
g
Discharge (m/d)
0.1000
0.0100
0.0010
0.0001
3/9/2007
4/28/2007
6/17/2007
8/6/2007
9/25/2007

### 4.4.2 Analysis of Nine Storm Events

Nine rain events were monitored over a 5 month period from 7/4/2007 to 10/19/2007. The rain events ranged from 2.4 mm to 12.6 mm and occurred over a variety of antecedent rainfall conditions (Table 4.1). The average rainfall rate varied from 0.31 to 5.78 mm/hr and the rainfall events lasted from 0.8 to 15.2 hours. The maximum 15 minute rainfall rate (84 cm/d) did not exceed the estimate of saturated conductivity of 110 cm/d. The 7-day antecedent rainfall varies from 0.0 to 8.7 mm and 21-day varies from 0.5 to 28.1 mm.

The differences in rainfall and antecedent rainfall conditions produced a correspondingly large range of runoff conditions in the stream and hill side weirs. The length of the stream runoff events ranged from 16 to 72 hours and had average 3-day antecedent runoff of 0.046 to 0.227 mm/d (Table 4.2). The peak stream discharge varied from 0.63 mm/d to 9.69 mm/d (Table 4.2) and was lagged from the rainfall by between 1.0 and 5.3 hours. Overland flow occurred during every event at the spring 1 weir (SP1) and the weir at outlet of the soil pipe (SPO), the same locations that maintained constant baseflow through the summer. The more transient springs 2 and 3 (SP2 and SP3) produced overland runoff in five of the nine events, presumably when small saturated areas formed above the weir. The mean discharge from the SPO was between 0.118 and 0.668 L/s, which is about ten times the discharge from the SP1 during the nine events.

Table 4.1: Rainfall information for nine storm events. Storms ranged from in volume and antecedent rainfall conditions.

| Event date | 7/4/07 | 7/23/07 | 9/8/07 | 9/9/07 | 9/11/07 | 9/27/07 | 10/9/07 | 10/10/07 | 10/19/07 |
|---|---|---|---|---|---|---|---|---|---|
| Length or rainfall (hrs) | 1.33 | 0.83 | 3.80 | 10.50 | 14.50 | 15.20 | 10.17 | 5.50 | 7.83 |
| Total rainfall (mm) | 7.67 | 4.70 | 3.41 | 4.92 | 12.61 | 10.82 | 2.78 | 2.39 | 8.50 |
| 7 day antecedent rain (mm) | 2.16 | 8.69 | 0.00 | 0.54 | 7.08 | 3.74 | 1.21 | 1.49 | 2.53 |
| 21 day antecedent rain (mm) | 15.40 | 22.67 | 0.54 | 3.98 | 12.98 | 28.12 | 12.10 | 12.38 | 20.32 |
| Max 15 min. rainfall (mm/hr) | 34.81 | 12.14 | 7.89 | 6.21 | 18.62 | 10.21 | 6.62 | 2.40 | 5.42 |
| Average 15 min. rainfall (mm/hr) | 5.78 | 5.61 | 0.89 | 0.47 | 0.87 | 0.31 | 0.67 | 0.47 | 1.09 |

Table 4.2: Runoff information for nine storm events. Runoff event information is given for the stream and for four weir locations (with standard deviation in parenthesis).

| Event date | 7/4/07 | 7/23/07 | 9/8/07 | 9/9/07 | 9/11/07 | 9/27/07 | 10/9/07 | 10/10/07 | 10/19/07 |
|---|---|---|---|---|---|---|---|---|---|
| Length of runoff event (hrs) | 46.8 | 33.4 | 16.2 | 26.8 | 89.3 | 36.1 | 21.8 | 28.8 | 76.3 |
| 3 day antecedent average runoff (mm/d) | 0.050 | 0.118 | 0.046 | 0.052 | 0.065 | 0.073 | 0.132 | 0.147 | 0.227 |
| Runoff volume (mm) | 0.038 | 0.075 | 0.051 | 0.116 | 0.479 | 0.345 | 0.063 | 0.134 | 0.706 |
| Time to peak (hr) | 1.5 | 2.2 | 5.3 | 1.8 | 1.0 | 2.5 | 2.5 | 2.3 | 1.3 |
| Peak runoff (mm/d) | 2.15 | 0.63 | 0.90 | 1.49 | 4.66 | 3.65 | 2.41 | 2.46 | 9.69 |
| Mean soil pipe discharge (standard deviation) L/s | 0.143 (0.012) | 0.206 (0.043) | 0.118 (0.005) | 0.125 (0.004) | 0.143 (0.045) | 0.668 (0.171) | 0.534 (0.028) | 0.582 (0.022) | 0.279 (0.094) |
| Mean spring 1 discharge (standard deviation) L/s | 0.161 (0.007) | 0.159 (0.004) | 0.053 (0.008) | 0.051 (0.007) | 0.067 (0.017) | 0.074 (0.003) | 0.069 (0.005) | 0.073 (0.007) | 0.076 (0.009) |
| Mean spring 2 discharge (standard deviation) L/s | 0 | 0 | 0 | 0 | 0.022 (0.017) | 0.041 (0.003) | 0.043 (0.004) | 0 | 0.066 (0.002) |
| Mean spring 3 discharge (standard deviation) L/s | 0 | 0 | 0 | 0 | 0.019 (0.033) | 0.114 (0.03) | 0.012 (0.007) | 0 | 0.018 (0.033) |

Water table heights were also measued at four locations along the hillslope, a riparian well (PGW), a near-stream transient piezometer (NSGW), and two upslope piezometers (TGW1 and TWG2). The water table heights respond to the nine rainfall events at all locations, but the rate of groundwater rise (rise rate) varies significantly between events from 4.4 to 55.6 cm/hr at the PGW (Table 4.3). A water table was only maintained throughout the study period at the PGW, while the other piezometers keep a transient water table only during rainfall events (Figure 4.3). The transient response of a perched water table is caused by an impermeable 'fragipan' layer at a depth of 30 to 70 cm (NRCS). The PGW responds slower and declines more gradually than the transient groundwater during the storm events (Table 4.3 and Figure 4.3).

The hydrographs shown in Figure 4.3 are indicative of the range of rainfall events measured and are used as examples throughout this section. The events begin with a small event with dry antecedent conditions on 9/8/2007 (4 mm rainfall in last 21 days), followed by larger events with wetter conditions on 9/11/07 (13 mm rainfall in last 21 days), and into the Fall much wetter conditions on 10/19/07 (20 mm rainfall in last 21 days). Over this time the mean PGW height increases from 42 cm from the surface during the 9/8/07 event, to 14 cm during the 9/11/07 event, and 11 cm during the 10/19/07 event. Correspondingly, the runoff coefficients show a large range from 0.14% during the 9/8/2007 with the driest antecedent conditions, 1.60% as the system 'wets up' during 9/11/07, and up to 8.30% during the 10/19/2007 event with the most antecedent rainfall. The nine rainfall events thus represent a variety of conditions from which to assess common source areas and flowpaths in the study watershed.

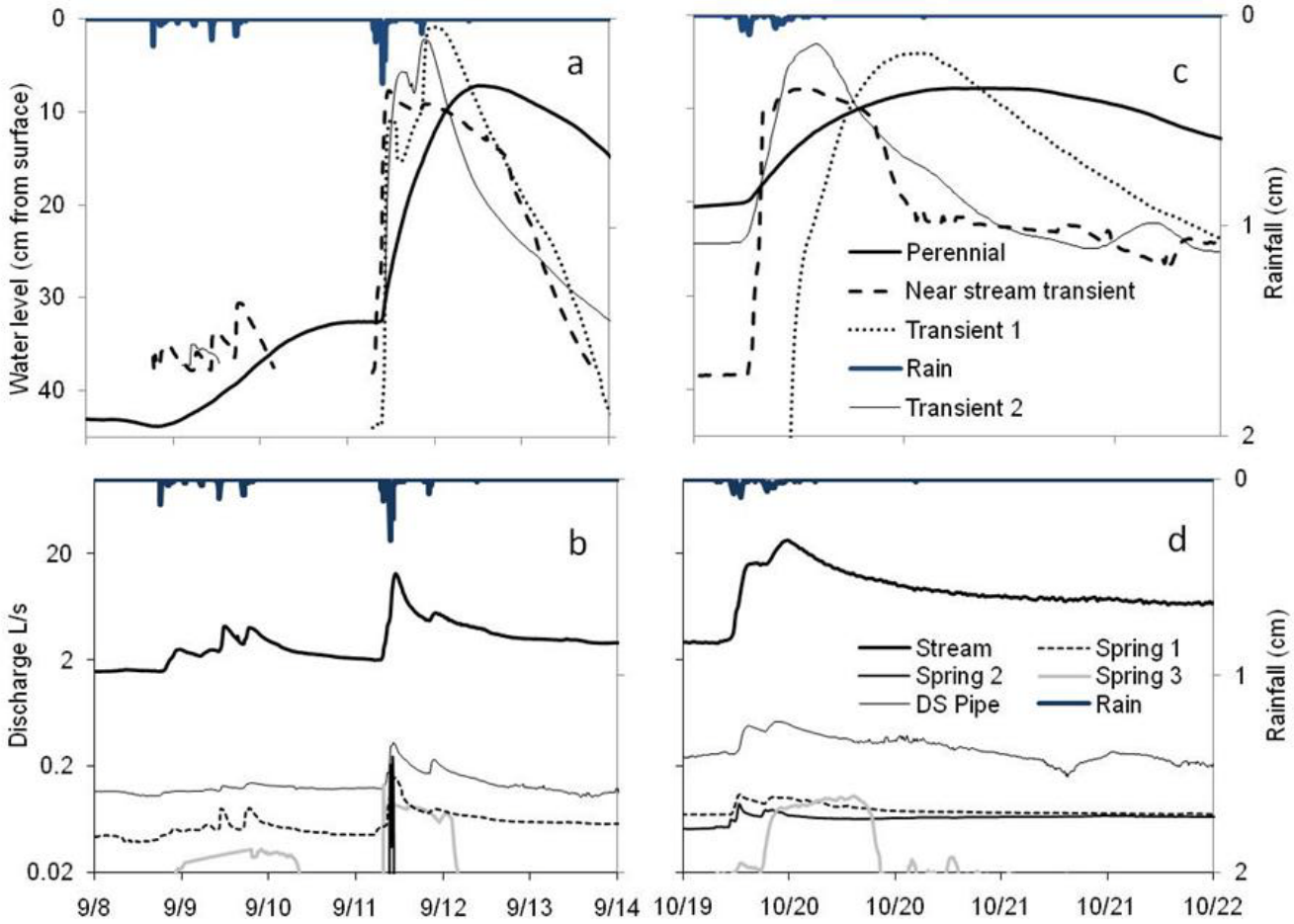


Figure 4.3: Groundwater level information for nine storm events. Level is measured as distance from the surface. Rise rate refers to rate of groundwater at the initiation of runoff. Piezometer locations are shown in Figure 4.1.

#### 4.4.2.1 Groundwater Table-Stream Runoff Relationships

The groundwater table-stream runoff relationship shows significant variability depending on the antecedent conditions and rainfall. The PGW heights showed consistent counter-clockwise hysteresis versus stream discharge (Figure 4.4), indicating the PGW lagged behind the stream response during the rising limb of the hydrograph (Figure 4.3). The PGW lags the stream response during both the 9/11/07 and 10/19/07 events, despite wetter antecedent conditions (Table 4.1) and a 20 cm difference in the pre-storm PGW height during the 10/19/07 event. The NSGW heights also have a counter-clockwise hysteresis during the 9/12/07 and 10/19/07 events, but peak at the same time as the stream (Figure 4.1). During both storms, the NSGW height begins around 40 cm from the surface, rises rapidly, and then reaches a maximum of about 10 cm where it remains for 3 to 5 hours. A 5 to 15 cm shallow layer with high organic content has highly conductive soils that likely cause the water near the stream to move laterally at shallow depths (Lyon et al. 2006a; 2006b) and effectively act as overland flow. Thus, while the NSGW heights remain close to 10 cm for much of the event, the upslope saturation areas are connected via overland flow, which is consistent field observations in this area during larger some events (4.2b and 4.2e).

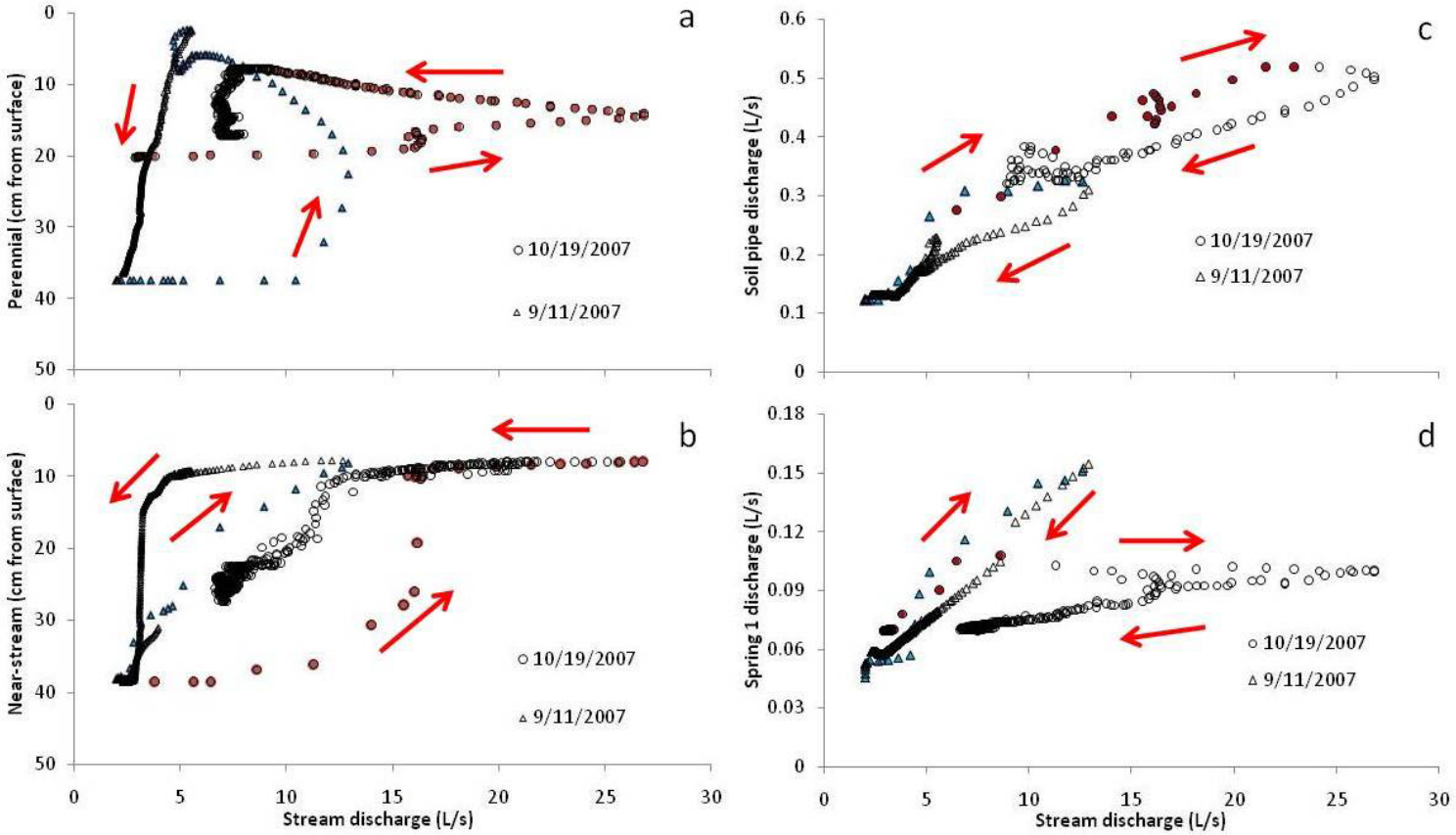


Figure 4.4: Temporal relationships during the 9/11/07 and 10/19/07 events between the stream and PGW (4.4a), NSGW (4.4b), SPO (4.4c), and SP1 (4.4d). Comparisons are made every 15 minutes and arrows indicate direction of hysteresis. Filled symbols represent measurements during the rising limb of the hydrograph.

The overland flow measurements made at SP1 and the SPO show both overland flow locations have a small clock-wise hysteresis loop, indicating that they respond faster than the watershed outlet (Figure 4.4c, d). The rapid response of the SP1 discharge is due to a small saturated area below the spring head, whose size depends on the antecedent conditions (see Methods section). The SP1 discharge is more than 50% greater during the 9/11/07 storm (Figure 4.4d), despite wetter antecedent conditions during the 10/19/07 event (Table 4.1 and 4.2). The differences instead likely reflect the greater rainfall intensity during the 9/11/07 event which produces increasing amounts of overland flow, versus more constant rainfall during the 10/19/07 event (Figure 4.3a and c). Conversely, the soil pipe response increases in a similar linear way during both events, supplying nearly twice as much runoff in the 10/19/07 event than the 9/11/07 event (Figure 4.4c). The sources to the soil pipe are not clear because there are no distinguishable upslope saturated areas and the nearby TGW1 response is lagged.

#### 4.4.2.2 Tracer Response

The rainfall caused consistent deflection in $\delta^{18}O$ in the stream water during the storm events (Figure 4.5). The $\delta^{18}O$ response reflects the addition of isotopically enriched event water during the rainfall events, the mean rain $\delta^{18}O$ is -4.92±0.87‰ over the nine events versus an average stream baseflow concentration of -10.61±0.57‰ (Table 4.4). The baseflow (prevent) $\delta^{18}O$ is a mixture of enriched near-stream groundwater (mean -9.73‰) and depleted groundwater springs (mean -10.91‰) that discharge directly into the stream from zero-order tributaries (see spring location in Figure 4.2). The stream concentrations range from -10.85‰ to -8.55‰ and are positively correlated to stream discharge ($r^2 = 0.69$) over the nine events.

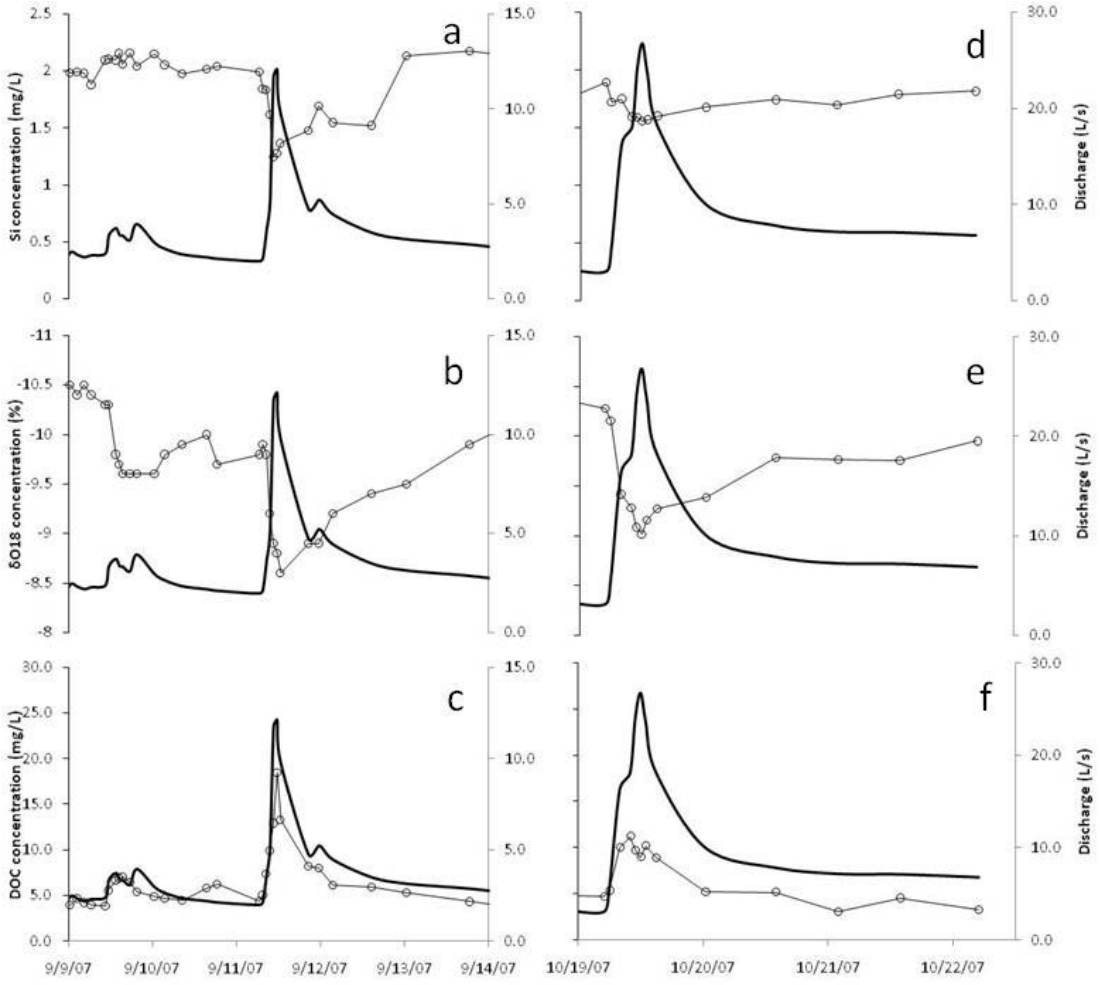


Figure 4.5: Chemograph and hydrograph for the 9/8/07, 9/9/07, and 9/11/07 storms (4.5a,b,c) and the 10/19/07 storm (4.5d e,f). The Si and $\delta^{18}O$ concentrations show consistent dilution during storm events, versus a flushing of DOC.

The stream Si concentration decrease during the rainfall events ($r^2$=0.50) and DOC concentrations increase more linearly ($r^2$=0.72) (Figure 4.5). The variability in the Si concentration is relatively small during the events, 1.32 mg/L to 2.0 mg/L, with minimums during peaks flows consistent with dilution-type effects (rain Si concentrations are 0.06 mg/L). Conversely, DOC concentration are maximum at peak discharge ('flushing' effects) and have more variability, with baseflow concentrations

around 5 mg/L to peak flow concentrations between 10 and 20 mg/L. The timing of the tracer response is also different with Si, DOC and $\delta^{18}O$ concentration responding rapidly to increasing discharge, but DOC concentration fall immediately while Si and $\delta^{18}O$ remains depleted for up to 24 hours after the event (Figure 4.5). The magnitude and timing of the stream concentrations reflect additional sources during the rainfall events.

Solute concentrations are also measured at different 'end-members' across the hillslope during the nine events (Figure 4.1 and Table 4.4). As mentioned previously, the rain and throughfall was enriched in $\delta^{18}O$ and had much lower concentrations of DOC and Si than the stream water. The PGW and SP1 water show the opposite chemistry, with more depleted $\delta^{18}O$ and higher concentrations of Si. The DOC concentrations vary significantly across the landscape, from less than 3 mg/L in spring waters, to 8 mg/L in the riparian groundwater and soil-water, and much higher (25.0 mg/L) in the near-stream saturated areas. The tracer concentrations are used subsequently to estimate the source areas of runoff using simple hydrograph separation techniques.

Table 4.3: Solute concentrations for the end members used in the mixing analysis. The end-members are averaged from multiple measurements during all nine storm events.

| End Member | Si (mg/L) | $\delta^{18}O$ (‰) | DOC (mg/L) |
|---|---|---|---|
| Mean rain and throughfall (standard deviation) | 0.06 (0.04) | -4.92 (0.87) | 1.03 (0.43) |
| Mean perennial GW (standard deviation) | 1.68 (0.15) | -9.73 (0.26) | 7.68 (1.56) |
| Mean spring GW (standard deviation) | 1.9 (0.11) | -10.91 (0.25) | 2.49 (1.03) |
| Mean saturated area (standard deviation) | 0.69 (0.16) | -8.84 (0.48) | 24.97 (3.05) |
| Mean soil water (standard deviation) | 0.92 (0.59) | -6.04 (1.87) | 7.06 (1.15) |

4.4.2.3 New Water Response

A simple two-component mixing model (Equation 3) is used to separate streamflow into event water (event rainwater) and pre-event water (baseflow water) contributions during nine storms. The contribution of event water was 14% to 37% of the runoff volume, with the maximum storm contribution from 18% to 49% usually near peak stream discharge (Table 4.5 and Figure 4.6a,c). The proportion of new water contributions is clearly a function of rainfall characteristics and antecedent conditions. For example, during three successively larger storms in September (Figure 4.3), the event water contributions increase from 14%, to 25%, and 37% as the system wets up (Table 4.5). The timing of the event water also becomes less lagged and more synchronized with stream discharge during the 9/11/07 storm. However, during the 10/19/07 storm, with very wet antecedent conditions, new water comprises only 33% of the total volume (Table 4.5), as groundwater contributions are larger due to greater baseflow (Figure 4.6). Overall, the event water contributions during these nine storms

are strongly explained by the rainfall volume ($r^2$=0.69), but less so by the 7-day or 21-day antecedent rainfall ($r^2$=0.20 and 0.41, respectively).

The event water reaches a consistent maximum of around 35% during the three largest events (9/11/07, 9/12/07, and 10/19/07) despite varying rainfall intensities and antecedent conditions. Across all of the events, the maximum event water contributions are more correlated to the length of the rainfall event and volume ($r^2$=0.70 and 0.79, respectively) than the mean or maximum 15-minute rainfall intensity ($r^2$=0.61 and -0.24, respectively). The error estimated with Equation 9 is shown for each stream sample in Figure 4.6a and 4.6c, with errors from 12.4% to 30.1% of the storm volume for the nine events. Overall, the two-component model demonstrates that event rainwater is an important source of runoff during summer storms.

Table 4.4: Results from mixing models and hydrograph separations for nine storm events.

Saturated areas are estimated for selected events via field surveys (Figure 4.2).

| | Event date | 7/4/07 | 7/23/07 | 9/8/07 | 9/9/07 | 9/11/07 | 9/27/07 | 10/9/07 | 10/10/07 | 10/19/07 |
|---|---|---|---|---|---|---|---|---|---|---|
| | Runoff coefficient % | 0.49 | 1.39 | 0.14 | 1.39 | 1.60 | 3.07 | 2.24 | 5.59 | 8.30 |
| | Saturated area % | N/A | N/A | 1.3 | 1.3 | 3.1 | N/A | 2.3 | N/A | N/A |
| 2-component model | Volume new water % | 14.9 | 15.2 | 13.6 | 25.0 | 36.9 | 36.4 | 21.7 | 26.6 | 33.1 |
| | Max proportion new water % | 22.5 | 23.2 | 17.5 | 28.1 | 45.6 | 49.0 | 26.6 | 28.0 | 49.2 |
| 3-component model | Volume rain and throughfall % | 15.8 | 7.0 | 3.6 | 6.5 | 14.5 | 18.9 | 11.3 | 13.1 | 24.8 |
| | Volume saturated areas % | 11.2 | 20.7 | 1.5 | 5.8 | 28.4 | 24.2 | 15.8 | 21.5 | 22.5 |
| | Volume groundwater % | 73.1 | 72.3 | 95.0 | 87.7 | 57.1 | 56.8 | 72.9 | 65.5 | 52.8 |
| | Max proportion rain and throughfall % | 21.5 | 16.9 | 5.8 | 10.1 | 22.2 | 29.3 | 16.7 | 15.6 | 31.6 |
| | Max proportion saturated areas % | 17.7 | 32.3 | 3.9 | 10.3 | 59.3 | 49.6 | 23.9 | 30.1 | 33.9 |

Figure 4.6: Hydrograph separations using simple mixing models for 9/8/07, 9/9/07, and 9/11/07 storms (4.6a, b) and 10/19/07 storm (4.6c, d). Top graphs show separation of new event water using the 2-component model and rain plus saturated areas from 3-component model. The bottom graphs show the contributions of the 3-component model using Si, DOC, and $\delta^{18}O$.

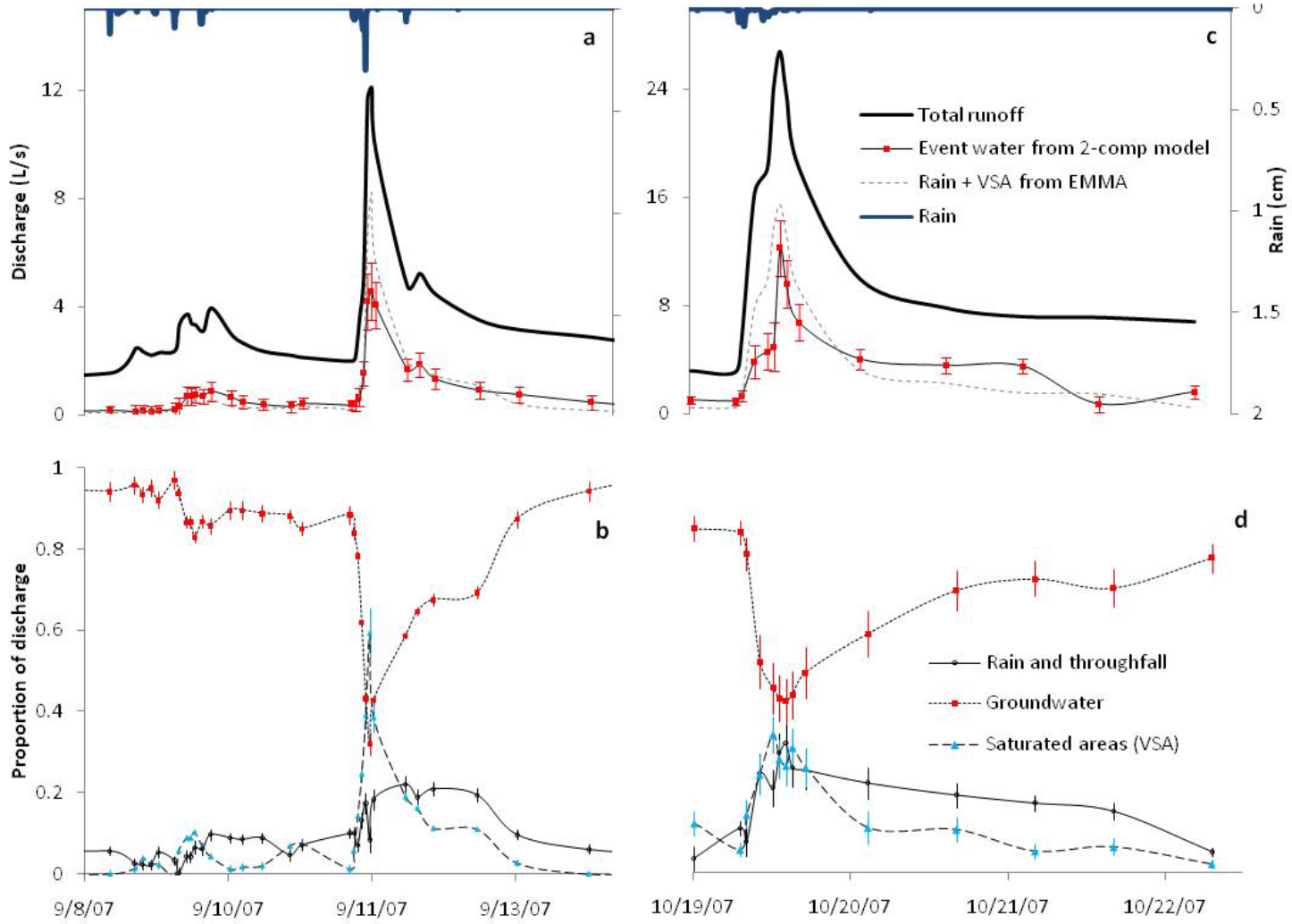
a
b
c
d
Discharge (L/s)
Proportion of discharge
Rain (cm)
Total runoff
Event water from 2-comp model
Rain + VSA from EMMA
Rain
Rain and throughfall
Groundwater
Saturated areas (VSA)
9/8/07
9/10/07
9/11/07
9/13/07
10/19/07
10/20/07
10/21/07
10/22/07

4.4.2.4 End-Member Response

The response of three solutes, Si, DOC, and $\delta^{18}O$, are used to identify water source areas using end-member mixing analysis (EMMA) and Equations 5 to 7. Viable end-members are selected using the concentration plots between the various solutes (Figure 4.6). A groundwater end-member is necessary to explain the high Si concentrations and depleted $\delta^{18}O$ over the entire event (Figure 4.7), particularly during baseflow. While more enriched $\delta^{18}O$ and lower Si stream concentrations are attributable to rain and throughfall sources (Figure 4.7). The depleted rainfall $\delta^{18}O$ did not change by more than 1.5‰ during any of the short rainfall events, with a mean of -4.92‰ and 1 standard deviation of 0.87‰ over all nine events (Table 4.4). Soil water from neither the A-horizon nor shallow groundwater can explain the DOC concentrations in the stream (Figure 4.7). Instead, saturated areas are the only source capable of producing high stream DOC concentrations (Figure 4.7), which can exceed 15 mg/L at peak storm flows (Figure 4.5). Soil water is excluded from the EMMA because the $\delta^{18}O$ is not distinguishable from rain water and the volume of water collected from the free-draining lysimeters was minimal and erratic, only producing runoff in four of nine events. Thus, the concentration plots suggest that a three end-member system are necessary to explain storm stream concentrations between groundwater (baseflow water), saturated areas, and rain water.

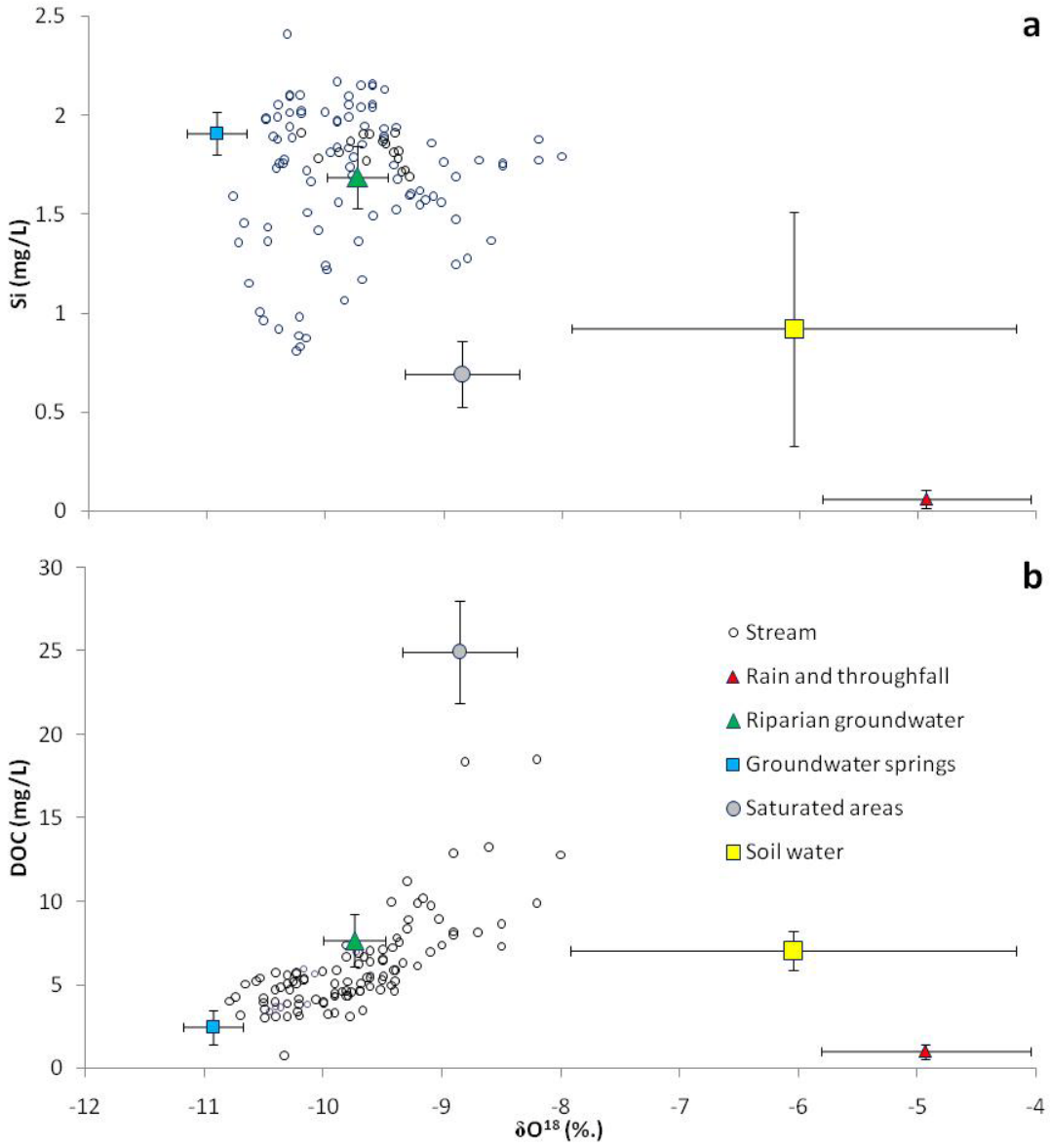


Figure 4.7: Solute concentrations for all nine storm events and average end-members concentration. Groundwater (spring and riparian waters) capture most of the stream concentrations, but a DOC-rich source, and enriched $\delta^{18}O$ source are necessary to capture all the variability.

Principal component analysis (PCA) was used to define a mixing space for the nine events using the three end-members for each event. This model explains 90% to 98% (depending on the storm) of the variability in Si, DOC, and $\delta^{18}O$ stream concentrations for the nine storm events, implying three end-members are necessary (Figure 4.8). The first principal component is controlled by the dilution of Si and $\delta^{18}O$; while the second is controlled by the flushing of DOC. The percent contribution for the three end-members over the nine storm events are shown in Table 4.5. The groundwater dominates the volume of stream water during storm events, producing 53% to 95% of total runoff volume (Table 4.5). The volume of rain water ranged from 4% to 25% and saturated areas between 2% and 24% of the total storm volume for the nine storm events (Table 4.5). The model was adequate in reproducing the measured values, with $r^2$ from 0.55 to 0.77 for Si, 0.76 to 0.97 for DOC, and 0.85 to 0.99 for $\delta^{18}O$. The error estimates made using Equation 8 are shown for select rain events in Figure 4.6b and d for all three end-members, and range from 8% to 31% for the total storm volumes during the nine events.

Figure 4.8: Principal component analysis used in the 3-component mixing model for 9/8/07, 9/9/07, and 9/11/07 (8a) and 10/19/07 storm (8b). The first principal component is mainly explained by Si and $\delta^{18}O$ concentrations, while the second is mostly explained by the DOC concentration.

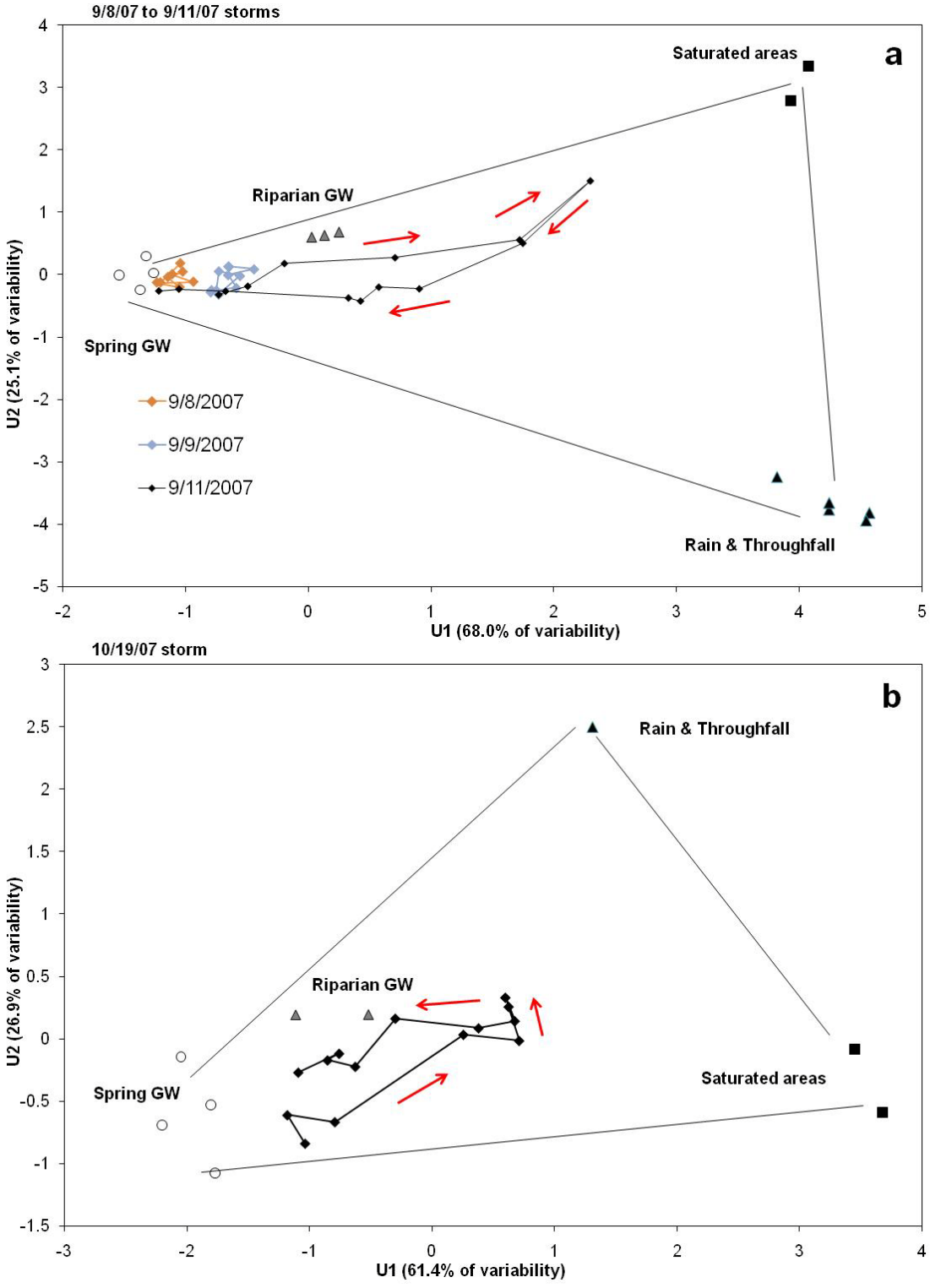
9/8/07 to 9/11/07 storms
a
Saturated areas
Riparian GW
Spring GW
9/8/2007
9/9/2007
9/11/2007
Rain & Throughfall
U2 (25.1% of variability)
U1 (68.0% of variability)
10/19/07 storm
b
Rain & Throughfall
Riparian GW
Spring GW
Saturated areas
U2 (26.9% of variability)
U1 (61.4% of variability)

Contributions from saturated areas reach their maximum during peak stream discharge and fall rapidly, while the contributions from rain water are more damped and lagged from the runoff peak (Figure 4.6). During the 9/11/07 storm event, maximum saturated area contributions exceed 59% of peak streamflow compared to a maximum of 22% from rain water coming after peak streamflow. This same trend is also evident from the PCA plot (Figure 4.8) that shows a rapid expression of saturated areas in the stream water followed by rain water during the falling limb of the hydrograph for both the 9/11/07 and 10/19/07 storm events. However, combining the saturated area and rain water contributions gives a runoff volume with similar timing and magnitude to the event water estimated with the two-component model (Equation 3) for both events in Figure 4.6a,c. The relative agreement between the two models suggests that the EMMA results are a plausible explanation for sources of event water.

## 4.5 Discussion

Saturation excess runoff is an important contributor to storm response in the Northeast U.S., but remains difficult to spatially and temporally quantify because of the lateral re-distribution of water due to subsurface heterogeneities and preferential flow. In Town Brook watershed, preferential flowpaths could potentially connect hill side areas to the stream, making predictions difficult with conventional variable saturated area (VSA) models.

### 4.5.1 Causes of Soil Saturation in Town Brook

The spatiotemporal patterns of surface saturation are different between valley-bottom areas and hill side areas far from stream channels (Figure 4.2f). After snowmelt on 4/12/07, saturated areas adjacent to stream channel (within 15 m)

represent about 80% of the total extent (Figure 4.2a). The near-stream saturation accounts for only around 55% of the saturation area during the driest survey on 9/5/07, with the remaining soil saturation occurring in isolated areas on the hill sides and is not connected to the stream (Figure 4.2d). Hill side saturation areas maintained by groundwater springs have been described throughout the Catskills (Burns et al. 1998; West et al. 2004; Siren 1963). The differing controls on saturation areas in the valley-bottoms versus the hill sides makes prediction difficult using common VSA conceptualizations.

Estimates of saturation areas made using surface topography and soil properties are not able to robustly reproduce the measured saturation areas. The topographic index or TI (Figure 4.2b) correctly identifies most hill side saturation areas using a 5 m by 5 m DEM, but even high-resolution LIDAR topography cannot detect the concentrated overland flow from the spring heads. Additionally, TI would predict that valley-bottom areas should remain saturated during drier conditions because of larger contributing areas than the upslope areas; however, the continuous spring discharge maintains hill side saturation areas, while valley-bottom decrease quickly after snowmelt (Figure 4.2a,b). The soil topographic index (STI) even more severely over-predicts valley-bottom saturation because the Onteora soils (Figure 4.1 and 4.2c) have lower hydraulic conductivity. This qualitative analysis shows that TI and STI generally over predict the extent of saturation area and underestimate the importance of concentrated flowpaths.

Previous studies in Town Brook have also shown that measured saturation areas are generally over predicted from models using surface topography. Working in adjacent north-facing Town Brook tributary, Mehta et al. (2004) showed that hill side saturation areas were concentrated and connected to the stream, but were poorly

predicted by their distributed model (see Figure 10 in Mehta et al. 2004). Even with inclusion of micro-topography, the model severely overpredicts the extent of saturated areas near the stream channels and does not capture small hill side areas caused by groundwater springs (see Mehta et al. 2004 Figure 4.12). Additionally, Lyon et al (2006a; 2006b) used 43 piezometers in a 120 m by 180 m area at the toe of the study hillslope (Figure 4.1) to estimate the shallow groundwater table. They found that STI had a relationship to probability of surface saturation during wet conditions (March to May), but not during dry conditions (June to August). A reanalysis of toe slope saturation patterns from Lyon et al. 2006b shows that during dry conditions (see Figure 5 in Lyon et al.) the most persistent saturation occurs at the outlet of the soil pipe in the northwest corner of the hillslope (Figure 4.1 and 4.2). The lack of agreement between the saturation predictions and measurements in Town Brook appears driven by preferential flowpaths, such as the springs and soil pipes, that are not well-described by the surface topography and soil surveys.

The role of preferential flowpaths is better examined in regards to the hillslope geomorphology and geology. The contact groundwater springs occur from bedding planes in the sandstone bedrock, but are not predictable by elevation or upslope area. Instead, the hill side saturation areas consistently emerge at the interface between the Willowmoc and Lackawanna soils (Figure 4.1), when vertical hydraulic conductivity decreases (see STI in Figure 4.2c) and the fragipan becomes more consistent. The hill side saturation areas rarely extend to the near-stream Onteora soils (Figure 4.2c) because the Willowmoc soils on the toe slope (Figure 4.1) have reduced slopes and increased soil depths. On the study hillslope, the Willowmoc soils also contain at least two measured soil pipes at depths of less than 0.75 m that extend to within 300 m of the stream. The soil pipe occur within the Willowmoc soils, but discharge into the

flat, poorly-draining Onteora soils and create one of the few consistent near-stream saturation area (Figure 4.2 and see also Lyon et al. 2006a). The near-stream saturation areas are influenced by the upslope preferential flowpaths, but their relative influence on watershed functioning remains to be explored.

The co-evolution of the soils in Town Brook watershed is likely responsible for the importance of preferential flowpaths on saturation area dynamics. Consistent preferential pathways persist because of the upslope springs and down slope fragipan layers. In general, these preferential pathways increase lateral runoff and reduce vertical infiltration (vary the typology); the most extreme case being the saturated soils, which transfer all rainfall to lateral runoff. The co-evolved drainage system found in Town Brook is similar to the glacial Cairngorm Mountains in Scotland described by Soulsby et al. (2006), Soulsby et al. (2008), and Hrachowitz (2009), where small amounts of responsive peats soils can dominate runoff sources in larger watersheds during rainfall events. Thus, the influence of hill side saturation patterns on the watershed response could have important new implications for the management of soil and water in this well-studied area.

### 4.5.2 Importance of Preferential Pathways to Storm Runoff Sources

Evaluating the impacts of preferential pathways on watershed functioning requires inferences from the hydrometric, chemical, and isotope data because direct, robust measurements are impractical. In Town Brook, preferential flow occurs both during low-flows and transiently during rainfall events due to a variety of causes, including bedrock heterogeneities, overland flowpaths, micro-topography, and soil piping. The preferential pathways accentuate lateral runoff and may reduce the role of topography and topology on runoff source areas if they connect to the stream.

Several hydrometric lines of evidence suggest that hill side saturation areas connect to the stream channel during rain events. First, GIS measurements made after snowmelt (Figure 4.2a) and within three hours of the 9/11/07 rain event (Figure 4.2f) show saturated connections from the spring head down to the stream channel. Second, the overland flow measurements at the springs and soil pipe respond faster to rainfall events than the stream (Figure 4.4c,d), implying they could be a source of peak storm runoff. Third, the transient NSGW also responds rapidly and stays within 10 cm of the surface, where the lateral conductivity in the organic horizon is much higher than the mineral soil (Figure 4.4b). This transmissivity feedback type response has been found in other studies in till soils (Bishop et al. 1990; Kendall et al. 1999) and is indicative of fast runoff pathways and high DOC concentrations (Kendall et al. 1999). In this study, the shallow flow in the top 5 cm to 10 cm is essentially overland because the vertical infiltration is near zero and these areas appear saturated using the 'boot-print' survey method shown in Figure 4.2. Finally, the deeper PGW and nearby TGW1 do not respond fast enough to contribute to the peak stream discharge (Figure 4.3a,c and 4.4a). The entirety of the hydrometric observations suggest that surface saturation in near-stream areas stay connected to the stream during rain events and act as flowpaths for hill side water to reach the stream.

The water chemistry is also used to estimate source areas via simple hydrograph separations. The simplest two-component model using $\delta^{18}O$ convincing shows that water supplied by the rain event (event water) is a significant source of runoff, especially during peak streamflow (Figure 4.6 and Table 4.5). This implies that source areas and flowpaths combine to rapidly contribute event water to the stream during the rising limb of the hydrograph. However, using several tracers ($\delta^{18}O$, Si, and DOC) the EMMA shows that stream contributions from rain water are lagged

and damped from the stream response (Figure 4.6b, d). The rapid contributions during the rising limb are instead supplied by saturated areas, which supply up to 24% of the runoff volume and 18% to 49% at peak streamflow. Combining the saturated area and rain contributions produces a similar hydrograph to the event water estimated using the two-component model (Figure 4.6a, c), but event water is slightly smaller (>10%) during peak streamflow. These results imply that event water is mobilized both by direct precipitation onto the stream channel, but also from water that mixes in the saturated areas during peak flows. The EMMA relies on DOC to act as tracer for saturated areas to be accurately predicted (Figure 4.5).

The large flush of DOC during the rising limb of the hydrograph can only be explained by concentrations in the near-stream saturated areas (Figure 4.7a). Other studies have found that the variability of DOC concentrations in streamwater may be an effective indicator of flowpaths during storm runoff (Moore 1989; McDowell and Fisher 1976; Fiebig et al. 1990; Brown et al. 1999). Fiebig et al. (1990) suggested that DOC indicated flushing from preferential flowpaths further from the stream channel that did not contribute during baseflow. The consistent trend of higher DOC concentrations on the rising limb versus falling limb of the hydrograph (Figure 4.5) is similar to trends in Maimai, New Zealand (Moore 1989) and in a small hardwood watershed in Massachusetts (McDowell and Fisher 1976). Brown et al. (1999) also found that shallow soils were the most important source of DOC and a possible source of quick runoff in the Catskill Mountains. The EMMA suggests that the DOC is rapidly mobilized through shallow layers and/or preferential flowpaths, while more dilute rain water dominates after peak streamflow.

Contributions from rain water (event water that does not mix in the saturated areas) reach their maximum of 5.8% to 31.6% of the instantaneous discharge during

the falling limb of the hydrograph (Figure 4.6b, d). Similar dilution effects have been attributed to direct precipitation onto riparian saturated areas (Eshleman et al. 1993, Wels et al. 1991). However, Buttle and Peters (1997) found that hill slopes were capable of generating event runoff from preferential pathways that was often attributed to direct precipitation onto saturated areas. Buttle and Peters (1997) also suggested preferential pathways could invalidate common assumptions in hydrograph separation techniques without consideration of hydrometric response. The results presented here concur with Buttle and Peters (1997) that preferential flowpaths are capable of transporting rain water far from the stream channel without considerable mixing, which could have been attributed to direct precipitation on valley-bottom saturation areas (e.g. Wels et al. 1991) if the intensive hydrometric measurements had not been collected. Although the results cannot not preclude contribution of rain (event) water via subsurface preferential flowpaths as well, occurring on the transient perched water table.

Separately the hydrometric and water chemistry results suggest that water supplied to saturated areas during peak storm runoff may come from hill-side sources, but an integration of these data sets could further corroborate this runoff mechanism. The rainfall events shown in Figure 4.3a and 4.3b during several September rain events are used to further illustrate hill side contributions. The 9/5/2007 (Figure 4.2d) survey was made during summer low flow and the total saturated area in the study watershed was 1.1%, but 0.21% was connected to the stream via surface saturation (essentially only the stream channel). Correspondingly, the rainfall event on 9/8/07 has a very small runoff coefficient (0.14%) and runoff was generated principally from direct precipitation onto the stream channel and not from saturated areas (3.6% versus 1.5% of the total runoff volume, respectively). As a result of this storm event the

water table heights increased (Table 4.3 and Figure 4.3b) and the saturation extents likely increased. The subsequent 9/9/07 storm had roughly equal contributions from rain and saturation areas (6.5% versus 5.8 % of the total runoff volume, respectively), but saturation contributions could still be explained by a small near-stream area (<0.10% of the watershed area). However, during the larger event on 9/11/07, when the hill side saturation areas connect to the stream, the volume contributed by saturation areas jumps to 28.4% of the total and 59.3% at peak streamflow. The near-stream saturation areas are not of sufficient size to generate this volume of runoff, which suggests that water from the hill side areas was quickly transported to the stream via preferential pathways under certain conditions. The changing saturation areas during these September storms are an example of how antecedent conditions and rainfall characteristics act to influence runoff sources.

### 4.5.3 Conceptualizing Runoff Source Areas during Varying Summer Storms

The antecedent conditions and rainfall characteristics have uneven controls on the hydrometric response between differing parts of the watershed. The rate of groundwater rise at the NSGW and PGW is significantly correlated ($r^2$ = 0.89 and 0.90, respectively) to the 7-day antecedent rainfall conditions. In contrast, the upslope transient groundwater (TGW1 and TGW2) is more strongly explained by total amount of rainfall ($r^2$ = 0.65 and 0.65) than 7-day antecedent rainfall ($r^2$= 0.45 and 0.35). The same is true for overland flow at SPO, SP1, SP2, and SP3, where the increase in discharge is more correlated to storm rainfall volumes ($r^2$ = 0.60, 0.57, 0.77, and 0.78, respectively) than 7-day antecedent rainfall ($r^2$ = 0.29, 0.26, 0.54, and 0.23, respectively). The difference in response likely reflects the redistribution of water in near-stream areas, while hill side features have a more limited memory of past rain events.

The differences in hydrometric response across antecedent conditions manifest into differing runoff sources to the stream during the storm events. The volume and maximum instantaneous event water contributions are much more correlated to rainfall volume ($r^2$=0.69 and 0.79, respectively) than the 7-day antecedent rainfall ($r^2$= 0.20 and 0.30, respectively). The rainfall contributions from EMMA also show more correlation to total rainfall volumes ($r^2$=0.60) than 7-day antecedent rainfall ($r^2$=0.10). However, the total and maximum contributions from the saturated areas show similar positive correlation to rainfall amounts ($r^2$= 0.57 and 0.68, respectively) and 7-day antecedent rainfall ($r^2$=0.68 and 0.63, respectively). As a result of these controls, the three rainfall events larger than 8 mm produce a similar volume of saturated area runoff (22.5% to 28.4% of the total), while rain water contributions are more variable (14.5% to 25.8%) and increase more linearly with rainfall volume. The complicated controls on source area contributions are not easily parameterized using conventional VSA runoff models (Figure 4.2b,c) that rely on surface topography to redistribute water down slope.

From a synthesis of these results we propose a conceptual model capable of predicting the source areas across antecedent conditions and under different rainfall characteristics. During smaller events and drier conditions, the upslope saturation areas remain disconnected, near-stream saturation areas are minimal, and most storm runoff is generated by direct precipitation onto the stream. A similar storm would generate more saturation excess overland flow in wet antecedent conditions, when the PGW and NSGW respond faster and near-stream saturation areas are more easily connected. For storms with more 8 mm of total rainfall, the additional sources and timing of overland flow can only be explained by the connection of hill side saturation areas. However, the hill side saturation areas have a maximum spatial extent that they

quickly reach in wet antecedent conditions due to the limited upslope expansion of the preferential flowpaths (Figure 4.2e, f and measurements from SP1 corroborate this). Larger rain storms thus produce similar amount of runoff volume from saturated areas, but larger relative amounts of rain water. The lagged contribution of the rain and event water (Figure 4.6) implies that direct precipitation onto the stream channel is not the only source of rain water to the stream and that preferential flowpaths could move rain water from further up the hill sides. This conceptual framework reinforces the idea that isolated areas in the landscape can contribute the majority of storm runoff through saturation excess processes.

### 4.5.4 Implications for Modeling and Management of VSA Hydrology

These results add to the growing body of evidence that highly responsive soils on the hill sides can be important contributors to storm runoff in co-evolved glacial soils (Buttle 2006; Soulsby et al. 2006; Soulsby and Tetzlaff 2008). It is clear that predicting the exact positions of saturated contributing areas is not possible because of heterogeneities in the geology and soils. We believe that these heterogeneities are responsible for the overland saturation patterns and become a major source of storm runoff during larger summer and fall events. However, we also acknowledge this method does not rule out other sources or runoff, including subsurface-flow caused by saturation on the perched water table. Although the stream chemistry would suggest a more shallow soil source, the mixing overland flow and subsurface waters in near-stream area means this cannot be excluded as a possible source. What is apparent is that watershed sources and flowpaths rapidly deliver water mixed in the saturated soils and slowly supply event (rain) water during the stream recession.

The spatial patterns of runoff source areas in Town Brook are influenced by

rapid lateral flow by select areas in the landscape. Thus, conventional VSA theories do in general apply and are capable for supporting management decisions, but in general the models fail to capture the isolated flowpaths on the hill sides and over predict near-stream saturation extents (Mehta et al. 2004; Lyon et al. 2006b). This means that water gets to the stream faster and from sources further than what is predicted by the surface topography or the drainage network (topology). In other areas, hydrologic soil classification schemes have been developed (e.g. HOST classifications from Scotland, website: http://www.macaulay.ac.uk/host/) to better predict landscape typology. Developing these surveys by hand would be too resource intensive, but so far remote-sensing (de Alwis et al. 2007) and geophysical measures (Dahlke et al. 2009) have proved impractical for widespread applications. Therefore, at present surface topography and SSURGO soil maps remain the most robust means for managing soil and water in the near-term, a more concerted effort should however be made to better integrate differences typology in future VSA models.

## 4.6 Conclusions

The variable source areas (VSA) concepts proposed over 40 years ago (e.g. Betson 1964 and Dunne and Black 1970) for Northeastern watersheds have been subject to few updates and improvements. However, there is a growing body of literature from other glacial areas (e.g. Soulsby and Tetzlaff, 2008) suggesting that differences in the lateral and vertical distribution of water can cause hill side features to control overall watershed functioning. Therefore, we more closely considered the effects of lateral redistribution of water via saturation-excess overland flow in a 2.51 $km^2$ watershed using hydrometric, chemical, and isotopic data. The intensive surveys revealed that hill sides have saturation areas maintained by spring heads that can connect to the stream via overland flow in larger events. These results are supported

by the hydrometric measurements, which showed a rapid response of overland flowpaths and transient near-stream saturation during the event. Finally, hydrograph separations using isotope and geochemicals confirm that a signature of shallow overland flow supplies up to 59% at peak streamflow and event (rain) water has maximum contributions to the stream the falling limb of the hydrograph.

Overall these results would be difficult to predict with conventional VSA models because the saturated areas are not well-captured by the soil or topographic information. For example, near-stream areas do not saturate as readily as predicted by the upslope topography or drainage network (topology). The presence of lateral preferential flowpaths suggest that water is transported more quickly and from sources further from the stream channel than current VSA theories would predict. Although this does not preclude the use of conventional models, which although overpredict the extent of saturated areas, but do delineate the measured runoff areas and as hydrologically sensitive areas for management purposes. For VSA models to 'get the right answers for the right reasons' will require more validation of internal watershed processes with regard to the lateral redistribution of water due to preferential flowpaths in glaciated Northeastern U.S. watersheds.

# REFERENCES


Beven, K.J. 1986. Runoff production and flood frequency in catchment of order n: an alternative approach. in Scaling Problems in Hydrology. Eds: V.K Gupta, I. Rodriguez-Iturbe, and E.F. Wood. Reidel: Dordrecht. 107-131.

Betson, R.P. 1964. Water is watershed runoff? Journal of Geophysical Research 69(8):1541-1552.

Beven, K. and J. Feyen. 2002. The Future of Distributed Modeling. Hydrological Processes. 16: 169-172.

Beven, K. and M.J. Kirkby, 1979. A physically based variable contributing are model of basin hydrology. Hydrological Sciences Bulletin, 24(1): 43-69.

Bishop, K.H., Grip, H., O'Neill, A., 1990. The origins of acid runoff in a hillslope during storm events. J. Hydrology. 116, 35–61.

Brown, V.A., J.J. McDonnell, D.A. Burns, C. Kendall. 1999. The role of event water, a rapid shallow flow component, and catchment size in summer stormflow. Journal of Hydrology. 217:171-190.

Broxton, P.D., P.A. Troch, and S.W. Lyon. 2009. On the role of aspect to quantify water transit times in small mountainous catchments. Water Resources Research. <in press>

Burns, D.A., P.S.Murdoch, G.B. Lawrence, and R.L. Michel. 1998. The effect of groundwater springs on $NO3^-$ concentrations during summer in Catskill Mountain streams: Water Resources Research, v. 34, p. 1987-1996.

Burns, D.A., J.J. McDonnell, R.P. Hooper, N.E. Peters, J.E. Freer, C. Kendall, and K. Beven. 2001. Quantifying contributions to storm runoff through end-member mixing analysis and hydrologic measurements at the Panola Mountain Research Watershed (Georgia, USA). Hydrological Processes. 15(10): 1903-1924.

Buttle, J.M. and D. Peters. 1997. Inferring hydrological processes in a temperate basin using isotopic and geochemical hydrograph separation a re-evaluation. Hydrological Processes. 11: 557-573.

Buttle, J.M. 2006. Mapping first-order controls on streamflow from drainage basins: the $T^3$ template. Hydrological Processes. 20(15):3415-3422.

Christopherson N., and R.P. Hooper. 1992. Multivariate analysis of stream water chemical data: the use of principal components analysis for the end-member mixing problem. Water Resources Research 28: 99–107.

Dahlke, H.E., Easton, Z.M., Fuka, D.R., Lyon, S.W. and, T. S. Steenhuis. 2009. Modeling Variable Source Area Dynamics in a CEAP Watershed. Ecohydrology. <published online June 2009>

de Alwis, D.A., Z.M. Easton, H.E. Dahlke, W.D. Philpot, and T. S. Steenhuis. 2007. Unsupervised classification of saturated areas using a time series of remotely sensed images. Hydrol. Earth Syst. Sci., 11, 1609-1620, 2007.

Dunne, T., and R.D. Black. 1970. Partial area contributions to storm runoff in a small New England watershed. Water Resources Research 6:1296-1311.

Dunne, T. Moore, T.R., and Taylor, C.H. 1975. Recognition and prediction of runoff-producing zones in humid regions. Hydrological Sciences Bulletin. 20(3):305-327.

Engman, E.T. 1974. Partial area hydrology and its application to water resources. Water Resources Bulletin. 10:512-521

Eshleman, K.N., J.S. Pollard, A.N. O'Brien. 1993. Determination of contributing areas for saturation overland flow from chemical hydrograph separations. Water Resources Research. 29(10): 3577-3587.

Fiebig, D.M., Lock, M.A., Neal, C., 1990. Soil water in the riparian zone as a source of carbon for a headwater stream. J. Hydrology.116: 217–237.

Genereux DP. 1998. Quantifying uncertainty in tracer-based hydrograph separations. Water Resources Research 34: 915–919.

Hewlett, J.D. and Hibbert, A.R. 1967. Factors affecting the response of small watersheds to precipitation in humid regions. IN Forest Hydrology (eds. W.E. Sopper and H.W. Lull). Pergamon Press, Oxford. pp. 275-290

Hrachowitz M., C. Soulsby, D. Tetzlaff, J.C. Dawson, S.M. Dunn, and I.A. Malcom. 2009. Using longer-term data sets to understand transit times in contrasting headwater catchments. Journal of Hydrology. DOI:10 1029/2004JF000249.

Inamdar, S.P. and M.J. Mitchell. 2007. Contributions of riparian and hillslope waters to storm runoff across multiple catchments and storm events in a glaciated forested watershed. Journal of Hydrology 341: 116-130.

Kendall KA, Shanley JB, McDonnell JJ. 1999. A hydrometric and geochemical approach to test the transmissivity feedback hypothesis during snowmelt. Journal of Hydrology 219: 188–205.

Kirchner, J.W., X.H. Feng and C. Neal. 2000. Fractal stream chemistry and its

implications for contaminant transport in catchments, Nature. 403: 524-527.

Kurdish, M. 2002. Catskill Forests. Purple Mountain Press: Fleischmanns, NY.

Laudon, H., V. Sjoblom, I. Buffam, J. Seibert, and M. Morth. 2007. The role of catchment scale and landscape characteristics for runoff generation of boreal streams. Journal of Hydrology. 344:198-209.

Lin, H. 2006. Temporal stability of soil moisture spatial pattern and subsurface preferential flow pathways in the Shale Hill catchment. Vadose Zone Journal. 5:317-340.

Lin, H.S., and X.B. Zhou. 2008. Evidence of Subsurface Preferential Flow Using Soil Hydrologic Monitoring in the Shale Hills Catchment. European J. of Soil Science 59:34–49.

Lis, G., L. Wassenaar, and M.J. Hendry. 2008. High-precision laser spectroscopy D/H and $^{18}O/^{16}$ O measurements of microliter natural water samples, *Anal. Chem*, 80: 287-293.

Lyon S.W, M.T. Walter, P. Gerard-Marchant, T.S. Steenhuis. 2004. Using a topographic index to distribute variable source area runoff predicted with the SCS curve-number equation. Hydrology Process. 18 (15): 2757-2771.

Lyon, S.W., A.J. Lembo, M. T. Walter, T.S. Steenhuis. 2006a. Defining probability of saturation with indicator kriging on hard and soft data. Advances in Water Resources 29(2006):181-193.

Lyon, S.W., J. Seibert, A.J. Lembo, M.T. Walter, T.S. Steenhuis. 2006b. Geostatistical investigation into the temporal evolution of spatial structure in a shallow water table. Hydrol. Earth Sys. Sci. 10: 113-125.

Lyon, S.W., S.L.E. Desilets, and P.A. Troch. 2009. A tale of two isotopes: Differences in hydrological separation for a runoff event when using δD vs. $\delta^{18}O$. Hydrological Processes, doi:10.1002/hyp.7326.

McDonnell, J.J., M. Sivapalan. K. Vache, S. Dunn, G. Grant, R. Haggerty, C. Hinz, R. Hooper, J. Kirchner, M.L. Roderick, J. Selker, and M. Weiler. 2007. Moving beyond heterogeneity and process complexity: A new vision for watershed hydrology. Water Resources Research. 43. W07301 Doi:10.1029/2006WR005467.

McDowell, W.H., Fisher, S.G., 1976. Autumnal processing of dissolved organic matter in a small woodland stream ecosystem. Ecology 57, 561–569.

McGlynn, B.L., J.J. McDonnell, J. Seibert, and C. Kendall. 2004. Scale effects on headwater catchment runoff timing, flow sources, and groundwater-streamflow relations. Water Resources Research. 40. doi:10.1029/2003WR002494.

McGuire, K.J., J. J. McDonnell, M. Weiler, C. Kendall, B. L. McGlynn, J. M. Welker, and J. Seibert (2005). The role of topography on catchment-scale water residence time. Water Resources Research. 41, doi:10.10292004WR003657.

Mehta, V.K., M.T. Walter, E.S. Brooks, T.S. Steenhuis, M.F. Walter, M. Johnson, J. Boll, and D. Thongs. 2004. Application of SMR to modeling watersheds in the Catskill Mountains. Environmental Modeling and Assessment. 9:77-89.

Moore, T., 1989. Dynamics of dissolved organic carbon in forested and disturbed

catchments, Westland, New Zealand, 1. Maimai. Water Resources Research 25:1321–1330.

Reynolds, R.J. 2000. Hydrogeology of the Beaver Kill Basin in Sullivan, Delaware, and Ulster Counties, NY. USGS Water-Resources Report 00-4034.

Rich, J.L. 1934. Glacial Geology of the Catskills. New York State Bulletin, 299. University of the State of New York, Albany. 180 pp.

Sklash, M.G. and R.N. Farvolden. 1979. The role of groundwater in storm runoff. Journal of Hydrology 43:45-65.

Soren, J. 1963. The ground-water resources of Delaware County, New York: New York State Department of Conservation Bulletin GW-50, 66p.

Soulsby C, Tetzlaff D, Dunn SM, Waldron S. 2006. Scaling up and out in runoff process understanding: insights from nested experimental catchment studies. Hydrological Processes 20:2461–2465.

Soulsby, C. and D. Tetzlaff. 2008. Towards simple approaches for mean residence time estimation in ungauged basins using tracers and soil distributions. Journal of Hydrology. 363(1-4): 60-74.

Steenhuis, T.S., M. Winchell, J. Rossing, J.A. Zollweg, and M.F. Walter. 1995. SCS runoff equation revisited for variable source runoff areas. ASCE Journal of Irrigation and Drainage Engineering 121:234-238.

USDA. 2007. Soil survey of Delaware County, New York. NRCS: Washington, D.C.

Teztlaff, D. J. Seibert, and C. Soulsby. 2009. Inter-catchment comparison to assess the

influence of topography and soils on catchment transit times in a geomorphologic province; the Cairngorm Mountains, Scotland. Hydrological Processes. 23: 1874-1886.

Troch, P.A., G.A. Carrillo, I. Heidbuchel, S. Rajagopal, M. Switanek, T.H.M. Volkmann, and M. Yaeger. 2008. Dealing with landscape heterogeneity in watershed hydrology: a review of recent progress toward new hydrological theory. Geography Compass. 2:10.1111/j.1749-8198.2008.00186

Tromp-van Meerveld, H.J. and J.J. McDonnell (2006) Threshold relations in subsurface stormflow 1. A 147 storm analysis of the Panola hillslope, Water Resources Research 42, W02410, doi:10.1029/2004WR003778.

Waddington, J.M., N.T. Roulet, and A.R. Hill. 1993. Runoff mechanism in a forest groundwater discharge wetland. Journal of Hydrology. 147: 37-60.

Walter, M.T., V.K. Mehta, A.M. Marrone, J. Boll, T.S. Steenhuis, M.F. Walter, C.A. Scott. 2002. A simple estimation of the prevalence of Hortonian flow in the New York City watersheds. ASCE Journal of Hydrological Engineering.

Wels, C., Cornett, R.J., LaZerte, B.D., 1991. Hydrograph separation: A comparison of geochemical and isotopic tracers. J. Hydrol. 122, 253–274.

West, A.J., S.E. Findlay, D.A. Burns, K.C. Weathers, and G.M. Lovett. 2004. Catchment-scale variation in the nitrate concentrations of groundwater seeps in the Catskill Mountains, New York, U.S.A. Water, Air, & Soil Pollution. 132(3-4):389-400.

# Chapter 5

# CONCLUSIONS

The goal of this dissertation was to evaluate whether 'hydrogeomorphologic' properties can be effective predictors of stream chemistry and aquatic biota in two Catskill watersheds: Neversink (176.0 $km^2$) and Town Brook (2.5 $km^2$). This goal was met by analyzing hydrometric, chemical, and isotopic data using a variety of statistical and graphical methodologies. Overall, the dissertation demonstrated that hydrogeomorphologic 'properties', such as watershed slope and channel network, are coupled to some stream chemistry measures (acid neutralizing capacity ANC and $Ca^{2+}$), corresponding aquatic biota (i.e. macroinvertebrate and fish), and spatial runoff patterns.

The Neversink represented an ideal place to explore hydrogeomorphologic relationships because sufficient nested monitoring data exists and spatial patterns in stream chemistry are not well-explained. The lack of a theoretical or even conceptual model for differences in acid buffering chemistry (ANC and $Ca^{2+}$) indicated that a simple regression analysis was sufficient. The regression analysis yielded a relationship that predicted over 80% of the variability in mean baseflow ANC values and $Ca^{2+}$ concentrations using the *Runoff Ratio*, or the mean ratio of 'quickflow' runoff to precipitation during twenty storm events. It was further shown that watersheds with steeper slopes and more stream channels had greater mean *Runoff Ratios* and reduced baseflow ANC values and $Ca^{2+}$ concentrations.

Applying the relationship between mean *Runoff Ratio* and baseflow ANC

values, estimated using drainage density and mean slope, we predicted the spatial distribution of aquatic biota in the Neversink. The study tested hydrogeomorphologic controls on macroinvertebrate, periphytic diatom, and fish inventories from three previous studies (Ernst et al., 2008; Burns et al., 2008; Baldigo and Lawrence, 2000) in 28 Neversink sub-watersheds (0.2 to 176 $km^2$). The hyrdogeomorphologic relationship was more effective in predicting macroinvertebrate than fish or diatom populations because our 'static' properties could not capture the episodic changes in stream chemistry that affected fish and diatom inventories.

In Town Brook we investigated how hillslope-scale hydrogeomorphologic properties can affect hydrological sources and flowpaths at the outlet of a 2.5 $km^2$ watershed. The end-member mixing analysis and hydrometric measurements suggested that saturated areas supply much of the 'new water' during runoff events. Maps of the saturated areas also indicated that hill sides likely connect to the stream and contribute runoff when precipitation exceeded 1 cm. In Town Brook, 'small-scale' features (springs and pipes) caused hill side saturation features that were difficult to replicate with topographic or soil properties.

All of these findings are consistent with a fairly simple conceptualization of the Catskills as a system controlled by watershed geomorphology. For example, we showed that geomorphology (slope and drainage density) was a strong control on hydrology (mean *Runoff Ratio*) in the Neversink. This meant that hydrology and geomorphology were combined controls on a watershed's ability to buffer diffuse sources of acidity. The hydroeomorphologic controls on stream chemistry (i.e. ANC values) had obvious implications for predicting aquatic habitat in the Neversink. Working in Town Brook watershed, spatial geomorphologic properties were less effective in estimating the extent of saturated areas on smaller scales (<0.01 $km^2$) that

corresponded to sources of stream solutes during high-flows. Limitations to hydrogeomorphologic approaches exist in areas without sufficient spatial data and/or where subsurface properties are more variable. Another limitation of this approach is that it is not necessarily clear that the hydrogeomorphologic properties are mechanistically related to the stream chemistry or aquatic habitat.

These limitations aside, the understanding of hydrogeomorphologic controls in the two study watersheds allowed for estimates of some stream solutes (i.e. ANC, $Ca^{2+}$, DOC, etc.) and some aquatic biota (i.e. macroinvertebrate and fish) using widely-available spatial data. The success of hydrogeomorphologic properties in estimating watershed response under select conditions suggests that simple alternatives to traditional Darcy-based predictions may exist for certain water management applications.

## 5.1 Future Research

Despite the long-held recognition of variable saturated area (VSA) runoff generation in Northeastern U.S. watersheds (Betson, 1964), relatively few studies have related this to watershed geomorphology in quantitative ways. As a result, we have limited tools for predicting the saturation patterns observed in Town Brook a priori or estimating how widespread these runoff processes are in other parts of the Catskills. These questions require new remote measurement techniques for quantifying saturation areas, coupled to field validation similar to Chapter 4. Collecting event runoff data across a wider range of conditions (besides the growing-season) may also help verify the conceptualization for hydrological flowpaths and sources. The potential to connect baseflow measurements to the event data in Chapter 4 may be a potential way to verify these concepts.

There appears to be considerable research potential in the Neversink for applying the relationships developed in this dissertation to other data sets, particularly as a tool for predictions in ungauged watersheds. For example, expanding the knowledge of sand and gravel aquifers to low-flows at different and larger Catskill watersheds is merited. We are also interested in a more quantitative analysis of the factors that suggested 'self-similar' discharge (i.e. Shaman et al., 2004) in larger watersheds. The stream chemistry models also have the potential to predict acid buffering chemistry and stream biota in other Catskill watersheds. Further, the connections demonstrated between event-scale processes and baseflow chemistry is being investigated using 20+ year data sets from the Neversink. This future work has the potential to isolate the influences of changing precipitation patterns and emission trends on stream acidity in the Catskills. Overall, this dissertation has tapped into a rich research field that has the potential to help protect and manage the water and ecological resources of the Catskill Mountains.

# REFERENCES

Baldigo, B.P. and G.B. Lawrence. 2000. Composition of fish communities in relation to stream acidification and habitat in the Neversink River, New York. Transactions of the American Fisheries Society. 129: 60-76.

Betson, R.P. 1964. Water is watershed runoff? Journal of Geophysical Research 69(8):1541-1552.

Burns, D.A., K. Riva-Murray, R.W. Bode, S. Passy. 2008. Changes in stream chemistry and biology in response to reduces levels of acid deposition during 1987-2003 in the Neversink River Basin, Catskill Mountains. Ecological Features. 8(3): 191-203.

Ernst, A.G., B.P. Baldigo, G.E. Schuler, C.D. Apse, J.L. Carter, and G.T. Lester. 2008, Effects of habitat characteristics and water quality on macroinvertebrate communities along the Neversink River in southeastern New York, 1991-2001. USGS Scientific Investigation Report, 2008-5024, 15p.

Shaman, J. M. Stieglitz, and D. Burns. 2004. Are big basins just the sum of small catchments?. Hydrological Processes. 18:3195-3206.

# APPENDIX

## A.1 Chapter 2 raw data

Table 1: Bi-weekly/monthly data used to calculate summer water chemistry averages.

| Winnisook | ANC | Ca |
|---|---|---|
| 6/4/1991 | -20 | 29 |
| 7/2/1991 | -22 | 28 |
| 7/16/1991 | -21 | 28 |
| 7/30/1991 | -20 | 31 |
| 8/13/1991 | -20 | 30 |
| 8/27/1991 | -19 | 31 |
| 9/10/1991 | -18 | 28 |
| 9/24/1991 | -14 | 29 |
| 6/2/1992 | -22 | 20 |
| 6/16/1992 | -21 | 18 |
| 6/30/1992 | -18 | 17 |
| 7/14/1992 | -20 | 16 |
| 7/31/1992 | -19 | 21 |
| 8/11/1992 | -19 | 20 |
| 8/25/1992 | -20 | 20 |
| 9/9/1992 | -21 | 22 |
| 9/22/1992 | -18 | 22 |
| 6/1/1993 | -14 | 35 |
| 6/15/1993 | -25 | 25 |
| 6/29/1993 | -16 | 22 |
| 7/13/1993 | -18 | 27 |
| 7/27/1993 | -18 | 27 |
| 8/3/1993 | -21 | 25 |
| 8/17/1993 | -22 | 25 |
| 8/31/1993 | -23 | 22 |
| 9/21/1993 | -18 | 15 |
| average | -20 | 25 |
| st. dev | 3 | 5 |

| High Falls | ANC | Ca |
|---|---|---|
| 6/18/1991 | 139 | 74 |
| 7/2/1991 | 147 | 77 |
| 8/20/1991 | 151 | 140 |
| 9/18/1992 | 175 | 111 |
| 6/23/1992 | 96 | 100 |
| 7/21/1992 | 119 | 102 |
| 8/18/1992 | 132 | 105 |
| 9/17/1992 | 146 | 107 |
| 7/8/1993 | 143 | 127 |
| 8/18/1993 | 179 | 132 |
| average | 138 | 107 |
| st. dev | 21 | 21 |

| Biscuit | ANC | Ca |
|---|---|---|
| 6/14/1991 | 32 | 68 |
| 6/27/1991 | 23 | 68 |
| 7/9/1991 | 29 | 69 |
| 7/30/1991 | 29 | 81 |
| 8/8/1991 | 29 | 83 |
| 8/13/1991 | 30 | 74 |
| 8/27/1991 | 32 | 76 |
| 9/3/1991 | 30 | 78 |
| 9/25/1991 | 33 | 84 |
| 6/2/1992 | 18 | 59 |
| 6/16/1992 | 27 | 58 |
| 6/26/1992 | 32 | 68 |
| 7/9/1992 | 36 | 70 |
| 7/21/1992 | 36 | 77 |
| 8/9/1992 | 38 | 79 |
| 8/25/1992 | 28 | 65 |
| 9/15/1992 | 42 | 89 |
| 6/2/1993 | 36 | 56 |
| 6/8/1993 | 28 | 58 |
| 6/22/1993 | 14 | 61 |
| 7/27/1993 | 33 | 62 |
| 8/3/1993 | 31 | 60 |
| 8/24/1993 | 32 | 74 |
| 9/21/1993 | 33 | 75 |
| average | 30 | 71 |
| st. dev | 6 | 9 |

| Wildcat | ANC | Ca |
|---|---|---|
| 6/4/1991 | 17 | 56 |
| 6/18/1991 | 19 | 56 |
| 7/2/1991 | 21 | 57 |
| 7/16/1991 | 21 | 53 |
| 7/30/1991 | 22 | 54 |
| 8/13/1991 | 21 | 55 |
| 8/19/1991 | 23 | 59 |
| 8/27/1991 | 26 | 59 |
| 9/10/1991 | 22 | 57 |
| 9/24/1991 | 23 | 54 |
| 6/2/1992 | 16 | 47 |
| 6/16/1992 | 21 | 55 |
| 6/30/1992 | 24 | 32 |
| 7/14/1992 | 22 | 50 |
| 8/11/1992 | 22 | 40 |
| 8/25/1992 | 28 | 52 |
| 9/22/1992 | 29 | 42 |
| 6/8/1993 | 23 | 40 |
| 7/6/1993 | 24 | 50 |
| average | 22 | 51 |
| st. dev | 3 | 7 |

| Tisons | ANC | Ca |
|---|---|---|
| 6/18/1991 | -11 | 31 |
| 7/2/1991 | -10 | 30 |
| 7/9/1991 | -9 | 32 |
| 7/16/1991 | -9 | 29 |
| 7/30/1991 | -10 | 33 |
| 8/7/1991 | -8 | 31 |
| 8/20/1991 | -15 | 31 |
| 9/10/1991 | -8 | 29 |
| 9/20/1991 | -6 | 30 |
| 6/2/1992 | -24 | 27 |
| 6/16/1992 | -10 | 28 |
| 6/30/1992 | -5 | 19 |
| 7/7/1992 | -15 | 31 |
| 7/21/1992 | -11 | 19 |
| 8/4/1992 | -10 | 27 |
| 8/17/1992 | -6 | 25 |
| 8/27/1991 | -11 | 26 |
| 9/8/1992 | -11 | 26 |
| 9/27/1992 | -8 | 25 |
| 9/29/1992 | -6 | 25 |
| 6/8/1993 | -6 | 29 |
| 6/15/1993 | -11 | 27 |
| 7/13/1993 | -2 | 25 |
| 7/27/1993 | -4 | 25 |
| 8/10/1993 | -6 | 27 |
| 8/31/1993 | -7 | 23 |
| 9/9/1993 | -16 | 19 |
| 9/28/1993 | -11 | 29 |
| average | -10 | 27 |
| st. dev | 4 | 4 |

| Otter Pool | ANC | Ca |
|---|---|---|
| 7/2/1991 | 83 | 82 |
| 7/16/1991 | 88 | 82 |
| 7/30/1991 | 89 | 92 |
| 8/13/1991 | 89 | 84 |
| 8/27/1991 | 95 | 87 |
| 9/10/1991 | 90 | 81 |
| 9/24/1991 | 86 | 85 |
| 6/2/1992 | 32 | 62 |
| 6/30/1992 | 73 | 52 |
| 7/14/1992 | 80 | 77 |
| 8/11/1992 | 69 | 62 |
| 9/22/1992 | 82 | 65 |
| 6/8/1993 | 83 | 85 |
| 7/6/1993 | 82 | 87 |
| 8/3/1993 | 88 | 62 |
| average | 81 | 77 |
| st. dev | 15 | 12 |

Table 1 (Continued)

| West Br. | ANC | Ca |
|---|---|---|
| 7/2/1991 | 115 | 107 |
| 7/16/1991 | 126 | 107 |
| 7/30/1991 | 133 | 108 |
| 8/13/1991 | 129 | 104 |
| 8/27/1991 | 134 | 111 |
| 9/10/1991 | 159 | 112 |
| 9/24/1991 | 181 | 107 |
| 6/2/1992 | 43 | 77 |
| 6/16/1992 | 71 | 85 |
| 6/30/1992 | 90 | 75 |
| 7/14/1992 | 99 | 87 |
| 8/11/1992 | 85 | 72 |
| 8/25/1992 | 107 | 95 |
| 9/22/1992 | 110 | 95 |
| 6/8/1993 | 90 | 82 |
| 7/6/1993 | 118 | 107 |
| 8/3/1993 | 126 | 75 |
| 8/31/1993 | 147 | 95 |
| average | 115 | 95 |
| st. dev | 33 | 14 |

| New Hill | ANC | Ca |
|---|---|---|
| 7/2/1991 | 8 | 42 |
| 7/16/1991 | 10 | 41 |
| 7/30/1991 | 11 | 47 |
| 8/13/1991 | 9 | 42 |
| 8/27/1991 | 7 | 42 |
| 9/10/1991 | 11 | 43 |
| 9/24/1991 | 12 | 41 |
| 6/2/1992 | -4 | 32 |
| 6/16/1992 | 2 | 47 |
| 6/30/1992 | 9 | 47 |
| 7/14/1992 | 9 | 50 |
| 8/11/1992 | 3 | 32 |
| 8/25/1992 | 11 | 45 |
| 9/22/1992 | 7 | 32 |
| 6/8/1993 | 14 | 42 |
| 7/6/1993 | 17 | 47 |
| average | 9 | 42 |
| st. dev | 5 | 5 |

| East Br. | ANC | Ca |
|---|---|---|
| 7/2/1991 | 17 | 45 |
| 7/16/1991 | 24 | 52 |
| 7/30/1991 | 20 | 47 |
| 8/13/1991 | 18 | 44 |
| 8/27/1991 | 17 | 46 |
| 9/10/1991 | 22 | 60 |
| 9/24/1991 | 45 | 45 |
| 6/2/1992 | 2 | 40 |
| 6/16/1992 | 12 | 42 |
| 6/30/1992 | 16 | 27 |
| 7/14/1992 | 17 | 45 |
| 8/11/1992 | 15 | 37 |
| 8/13/1992 | 24 | 37 |
| 8/25/1992 | 27 | 52 |
| 9/22/1992 | 17 | 37 |
| 6/8/1993 | 15 | 32 |
| 7/6/1993 | 20 | 45 |
| 8/3/1993 | 20 | 40 |
| 8/31/1993 | 22 | 37 |
| average | 19 | 43 |
| st. dev | 8 | 7 |

| Main Br. | ANC | Ca |
|---|---|---|
| 7/2/1991 | 65 | 76 |
| 7/16/1991 | 68 | 76 |
| 7/30/1991 | 70 | 82 |
| 8/13/1991 | 66 | 75 |
| 8/27/1991 | 71 | 75 |
| 9/10/1991 | 71 | 74 |
| 9/24/1991 | 72 | 78 |
| 6/2/1992 | 32 | 60 |
| 6/30/1992 | 60 | 47 |
| 7/14/1992 | 64 | 70 |
| 8/11/1992 | 61 | 60 |
| 8/25/1992 | 68 | 82 |
| 9/22/1992 | 76 | 60 |
| 6/8/1993 | 67 | 65 |
| 7/6/1993 | 75 | 80 |
| 8/3/1993 | 80 | 57 |
| 8/31/1993 | 85 | 60 |
| 9/10/1993 | 73 | 76 |
| average | 68 | 70 |
| st. dev | 11 | 10 |

Table 2: Runoff ('quickflow') data from twenty storm events used to derive *Runoff Ratios*

| | | Runoff (m) | | | | | | | | | |
|---|---|---|---|---|---|---|---|---|---|---|---|
| start date | stopdate | WS | WC | OP | WB | MB | HF | BB | TS | NH | EB |
| 8/18/1991 | 9/10/1991 | 1.51E-02 | 3.12E-03 | 2.70E-03 | 2.91E-03 | 3.70E-03 | 1.77E-03 | 2.78E-03 | 8.62E-03 | 6.91E-03 | 5.74E-03 |
| 9/25/1991 | 10/2/1991 | 3.90E-03 | 1.82E-03 | 2.27E-03 | 2.40E-03 | 2.07E-03 | 2.20E-04 | 3.16E-03 | 3.24E-03 | 2.03E-03 | 2.22E-03 |
| 10/17/1991 | 10/29/1992 | 1.26E-02 | 7.17E-03 | 3.04E-03 | 2.57E-03 | 3.38E-03 | 9.69E-04 | 4.33E-03 | 8.28E-03 | 5.20E-03 | 4.45E-03 |
| 11/22/1991 | 12/5/1991 | 2.47E-02 | 2.69E-02 | 1.70E-02 | 2.42E-02 | 2.67E-02 | 1.55E-02 | 6.56E-02 | 1.83E-02 | 1.89E-02 | 1.88E-02 |
| 3/26/1992 | 4/6/1991 | 5.10E-02 | 2.61E-02 | 1.25E-02 | 1.38E-02 | 1.86E-02 | 2.46E-03 | 1.36E-02 | 2.92E-02 | 2.25E-02 | 1.91E-02 |
| 5/31/1992 | 6/5/1992 | 4.04E-02 | 2.65E-02 | 1.88E-02 | 2.43E-02 | 3.29E-02 | 8.97E-03 | 1.72E-02 | 3.44E-02 | 2.65E-02 | 2.87E-02 |
| 6/5/1992 | 6/13/1992 | 4.61E-02 | 3.65E-02 | 2.26E-02 | 3.19E-02 | 4.11E-02 | 2.28E-02 | 2.18E-02 | 6.67E-02 | 3.98E-02 | 4.24E-02 |
| 8/9/1992 | 8/17/1992 | 4.91E-03 | 7.74E-03 | 7.07E-03 | 7.14E-03 | 6.25E-03 | 4.37E-03 | 4.81E-03 | 6.11E-03 | 6.29E-03 | 6.62E-03 |
| 8/17/1992 | 8/21/1992 | 4.64E-05 | 3.43E-04 | 2.16E-04 | 2.60E-04 | 3.85E-04 | 1.10E-03 | 3.03E-04 | 4.67E-04 | 4.91E-04 | 4.86E-04 |
| 9/10/1992 | 9/18/1992 | 4.25E-04 | 1.51E-03 | 1.52E-03 | 1.43E-03 | 1.35E-03 | 1.23E-03 | 1.49E-03 | 8.74E-04 | 1.36E-03 | 1.17E-03 |
| 9/22/1992 | 9/26/1992 | 7.62E-04 | 1.14E-03 | 1.07E-03 | 1.07E-03 | 1.19E-03 | 1.02E-03 | 1.30E-03 | 1.17E-03 | 1.49E-03 | 1.27E-03 |
| 9/26/1992 | 10/8/1992 | 1.02E-02 | 1.98E-03 | 1.20E-03 | 1.21E-03 | 1.81E-03 | 1.14E-03 | 1.15E-03 | 5.22E-03 | 3.50E-03 | 2.61E-03 |
| 10/24/1992 | 10/30/1992 | 1.02E-04 | 7.17E-04 | 4.98E-04 | 5.02E-04 | 4.85E-04 | 2.87E-04 | 1.09E-03 | 4.25E-04 | 5.53E-04 | 4.77E-04 |
| 11/2/1992 | 11/5/1992 | 2.56E-03 | 3.88E-03 | 3.38E-03 | 3.23E-03 | 3.60E-03 | 3.12E-03 | 3.78E-03 | 4.11E-03 | 4.76E-03 | 4.38E-03 |
| 11/12/1992 | 11/16/1992 | 2.40E-02 | 2.17E-02 | 2.03E-02 | 1.75E-02 | 1.74E-02 | 1.47E-02 | 2.21E-02 | 1.59E-02 | 1.45E-02 | 1.43E-02 |
| 5/5/1993 | 5/20/1993 | 2.19E-03 | 1.67E-03 | 1.11E-03 | 1.22E-03 | 1.75E-03 | 6.30E-04 | 1.10E-03 | 3.87E-03 | 3.09E-03 | 2.88E-03 |
| 5/20/1993 | 5/26/1993 | 6.24E-04 | 1.37E-03 | 1.05E-03 | 9.71E-04 | 1.04E-03 | 6.16E-04 | 1.11E-03 | 1.76E-03 | 1.45E-03 | 1.32E-03 |
| 6/9/1993 | 6/15/1993 | 1.19E-04 | 2.46E-04 | 2.49E-04 | 2.83E-04 | 2.19E-04 | 3.24E-04 | 3.86E-04 | 3.18E-04 | 2.45E-04 | 2.92E-04 |
| 7/19/1993 | 7/23/1993 | 1.78E-04 | 2.44E-04 | 3.19E-04 | 3.99E-04 | 4.51E-04 | 2.98E-04 | 4.15E-04 | 6.60E-04 | 5.28E-04 | 6.00E-04 |
| 9/3/1993 | 9/6/1993 | 4.18E-04 | 3.16E-04 | 4.67E-04 | 6.02E-04 | 6.88E-04 | 7.60E-04 | 4.17E-04 | 9.51E-04 | 8.53E-04 | 9.19E-04 |

Table 3: Precipitation from twenty storm events used to derive *Runoff Ratios*

| | | Precip (m) | | | | | | | | | |
|---|---|---|---|---|---|---|---|---|---|---|---|
| start date | stopdate | WS | WC | OP | WB | MB | HF | BB | TS | NH | EB |
| 8/18/1991 | 9/10/1991 | 5.32E-02 | 5.44E-02 | 5.54E-02 | 5.59E-02 | 5.63E-02 | 5.50E-02 | 5.44E-02 | 5.39E-02 | 5.53E-02 | 5.58E-02 |
| 9/25/1991 | 10/2/1991 | 3.24E-02 | 3.33E-02 | 3.41E-02 | 3.45E-02 | 3.48E-02 | 3.38E-02 | 3.33E-02 | 3.29E-02 | 3.40E-02 | 3.44E-02 |
| 10/17/1991 | 10/29/1992 | 3.59E-02 | 3.22E-02 | 2.96E-02 | 2.79E-02 | 2.70E-02 | 3.06E-02 | 3.24E-02 | 3.40E-02 | 2.98E-02 | 2.85E-02 |
| 11/22/1991 | 12/5/1991 | 8.31E-02 | 8.22E-02 | 8.16E-02 | 8.12E-02 | 8.10E-02 | 8.19E-02 | 8.23E-02 | 8.26E-02 | 8.17E-02 | 8.14E-02 |
| 3/26/1992 | 4/6/1991 | 9.38E-02 | 8.58E-02 | 8.00E-02 | 7.64E-02 | 7.43E-02 | 8.23E-02 | 8.61E-02 | 8.95E-02 | 8.05E-02 | 7.75E-02 |
| 5/31/1992 | 6/5/1992 | 8.04E-02 | 8.03E-02 | 8.02E-02 | 8.01E-02 | 8.01E-02 | 8.02E-02 | 8.03E-02 | 8.03E-02 | 8.02E-02 | 8.02E-02 |
| 6/5/1992 | 6/13/1992 | 8.97E-02 | 8.94E-02 | 8.91E-02 | 8.90E-02 | 8.89E-02 | 8.92E-02 | 8.94E-02 | 8.95E-02 | 8.92E-02 | 8.90E-02 |
| 8/9/1992 | 8/17/1992 | 1.97E-02 | 3.46E-02 | 4.54E-02 | 5.21E-02 | 5.60E-02 | 4.11E-02 | 3.40E-02 | 2.77E-02 | 4.43E-02 | 5.00E-02 |
| 8/17/1992 | 8/21/1992 | 1.11E-02 | 1.09E-02 | 1.08E-02 | 1.07E-02 | 1.06E-02 | 1.08E-02 | 1.09E-02 | 1.10E-02 | 1.08E-02 | 1.07E-02 |
| 9/10/1992 | 9/18/1992 | 1.83E-02 | 1.80E-02 | 1.78E-02 | 1.77E-02 | 1.77E-02 | 1.79E-02 | 1.80E-02 | 1.81E-02 | 1.79E-02 | 1.78E-02 |
| 9/22/1992 | 9/26/1992 | 2.85E-02 | 2.82E-02 | 2.79E-02 | 2.77E-02 | 2.76E-02 | 2.80E-02 | 2.82E-02 | 2.83E-02 | 2.79E-02 | 2.78E-02 |
| 9/26/1992 | 10/8/1992 | 1.98E-02 | 2.01E-02 | 2.03E-02 | 2.04E-02 | 2.05E-02 | 2.02E-02 | 2.01E-02 | 2.00E-02 | 2.03E-02 | 2.04E-02 |
| 10/24/1992 | 10/30/1992 | 8.94E-03 | 8.61E-03 | 8.37E-03 | 8.22E-03 | 8.14E-03 | 8.47E-03 | 8.63E-03 | 8.77E-03 | 8.40E-03 | 8.27E-03 |
| 11/2/1992 | 11/5/1992 | 2.60E-02 | 2.67E-02 | 2.73E-02 | 2.76E-02 | 2.78E-02 | 2.71E-02 | 2.67E-02 | 2.64E-02 | 2.72E-02 | 2.75E-02 |
| 11/12/1992 | 11/16/1992 | 5.55E-02 | 5.13E-02 | 4.81E-02 | 4.62E-02 | 4.51E-02 | 4.94E-02 | 5.14E-02 | 5.32E-02 | 4.84E-02 | 4.68E-02 |
| 5/5/1993 | 5/20/1993 | 1.56E-02 | 1.63E-02 | 1.68E-02 | 1.71E-02 | 1.73E-02 | 1.66E-02 | 1.63E-02 | 1.60E-02 | 1.67E-02 | 1.70E-02 |
| 5/20/1993 | 5/26/1993 | 2.06E-02 | 2.11E-02 | 2.15E-02 | 2.17E-02 | 2.19E-02 | 2.13E-02 | 2.11E-02 | 2.09E-02 | 2.15E-02 | 2.17E-02 |
| 6/9/1993 | 6/15/1993 | 9.68E-03 | 1.16E-02 | 1.29E-02 | 1.38E-02 | 1.43E-02 | 1.24E-02 | 1.15E-02 | 1.07E-02 | 1.28E-02 | 1.35E-02 |
| 7/19/1993 | 7/23/1993 | 1.15E-02 | 1.22E-02 | 1.28E-02 | 1.31E-02 | 1.33E-02 | 1.26E-02 | 1.22E-02 | 1.19E-02 | 1.27E-02 | 1.30E-02 |
| 9/3/1993 | 9/6/1993 | 1.16E-02 | 1.09E-02 | 1.03E-02 | 9.98E-03 | 9.78E-03 | 1.05E-02 | 1.09E-02 | 1.12E-02 | 1.04E-02 | 1.01E-02 |

Table 3: (continued)

| | | Runoff Ratio (m/m) | | | | | | | | |
|---|---|---|---|---|---|---|---|---|---|---|
| startdate | stopdate | WS | WC | OP | WB | MB | HF | BB | TS | NH |
| 8/18/1991 | 9/10/1991 | 0.28 | 0.06 | 0.05 | 0.05 | 0.07 | 0.03 | 0.05 | 0.16 | 0.12 |
| 9/25/1991 | 10/2/1991 | 0.12 | 0.05 | 0.07 | 0.07 | 0.06 | 0.01 | 0.09 | 0.10 | 0.06 |
| 10/17/1991 | 10/29/1992 | 0.35 | 0.22 | 0.10 | 0.09 | 0.13 | 0.03 | 0.13 | 0.24 | 0.17 |
| 11/22/1991 | 12/5/1991 | 0.30 | 0.33 | 0.21 | 0.30 | 0.33 | 0.19 | 0.80 | 0.22 | 0.23 |
| 3/26/1992 | 4/6/1991 | 0.54 | 0.30 | 0.16 | 0.18 | 0.25 | 0.03 | 0.16 | 0.33 | 0.28 |
| 5/31/1992 | 6/5/1992 | 0.50 | 0.33 | 0.23 | 0.30 | 0.41 | 0.11 | 0.21 | 0.43 | 0.33 |
| 6/5/1992 | 6/13/1992 | 0.51 | 0.41 | 0.25 | 0.36 | 0.46 | 0.26 | 0.24 | 0.62 | 0.45 |
| 8/9/1992 | 8/17/1992 | 0.25 | 0.22 | 0.16 | 0.14 | 0.11 | 0.11 | 0.14 | 0.22 | 0.14 |
| 8/17/1992 | 8/21/1992 | 0.00 | 0.03 | 0.02 | 0.02 | 0.04 | 0.10 | 0.03 | 0.04 | 0.05 |
| 9/10/1992 | 9/18/1992 | 0.02 | 0.08 | 0.09 | 0.08 | 0.08 | 0.07 | 0.08 | 0.05 | 0.08 |
| 9/22/1992 | 9/26/1992 | 0.03 | 0.04 | 0.04 | 0.04 | 0.04 | 0.04 | 0.05 | 0.04 | 0.05 |
| 9/26/1992 | 10/8/1992 | 0.52 | 0.10 | 0.06 | 0.06 | 0.09 | 0.06 | 0.06 | 0.26 | 0.17 |
| 10/24/1992 | 10/30/1992 | 0.01 | 0.08 | 0.06 | 0.06 | 0.06 | 0.03 | 0.13 | 0.05 | 0.07 |
| 11/2/1992 | 11/5/1992 | 0.10 | 0.15 | 0.12 | 0.12 | 0.13 | 0.12 | 0.14 | 0.16 | 0.17 |
| 11/12/1992 | 11/16/1992 | 0.43 | 0.42 | 0.42 | 0.38 | 0.39 | 0.30 | 0.43 | 0.30 | 0.30 |
| 5/5/1993 | 5/20/1993 | 0.14 | 0.10 | 0.07 | 0.07 | 0.10 | 0.04 | 0.07 | 0.24 | 0.18 |
| 5/20/1993 | 5/26/1993 | 0.03 | 0.06 | 0.05 | 0.04 | 0.05 | 0.03 | 0.05 | 0.08 | 0.07 |
| 6/9/1993 | 6/15/1993 | 0.01 | 0.02 | 0.02 | 0.02 | 0.02 | 0.03 | 0.03 | 0.03 | 0.02 |
| 7/19/1993 | 7/23/1993 | 0.02 | 0.02 | 0.02 | 0.03 | 0.03 | 0.02 | 0.03 | 0.06 | 0.04 |
| 9/3/1993 | 9/6/1993 | 0.04 | 0.03 | 0.05 | 0.06 | 0.07 | 0.07 | 0.04 | 0.08 | 0.08 |
| | average | 0.21 | 0.15 | 0.11 | 0.12 | 0.15 | 0.08 | 0.15 | 0.19 | 0.15 |
| | standard dev | 0.20 | 0.14 | 0.10 | 0.12 | 0.14 | 0.08 | 0.18 | 0.15 | 0.11 |

Table 4: Step-wise regression data

| | Runoff Ratio fraction | L/G m | Measured ANC ueq/L | Regression Constants | | Predicted Ca ueq/L |
|---|---|---|---|---|---|---|
| HF | 0.09 | 2.15 | 108 | $a_1$ | -1157 | 141 |
| BB | 0.15 | 2.43 | 73 | $a_2$ | -49 | 55 |
| WS | 0.21 | 2.44 | 22 | $b_0$ | 347 | -17 |
| WC | 0.15 | 3.08 | 53 | | | 17 |
| OP | 0.11 | 2.69 | 77 | | | 85 |
| WB | 0.12 | 2.53 | 95 | | | 79 |
| TS | 0.19 | 3.06 | 27 | | | -26 |
| NH | 0.15 | 3.06 | 41 | | | 26 |
| EB | 0.15 | 2.87 | 43 | | | 34 |
| MB | 0.15 | 2.52 | 70 | | | 55 |

Table 4 (Continued)

| | Runoff Ratio fraction | L/G m | Measured Ca umol/L | Regression Constants | | Predicted Ca umol/L |
|---|---|---|---|---|---|---|
| HF | 0.09 | 2.15 | 108 | $a_1$ | -712 | 106 |
| BB | 0.15 | 2.43 | 73 | $a_2$ | -29 | 54 |
| WS | 0.21 | 2.44 | 22 | $b_0$ | 230 | 9 |
| WC | 0.15 | 3.08 | 53 | | | 31 |
| OP | 0.11 | 2.69 | 77 | | | 72 |
| WB | 0.12 | 2.53 | 95 | | | 69 |
| TS | 0.19 | 3.06 | 27 | | | 5 |
| NH | 0.15 | 3.06 | 41 | | | 37 |
| EB | 0.15 | 2.87 | 43 | | | 41 |
| MB | 0.15 | 2.52 | 70 | | | 54 |

A.2 Chapter 3 raw data

Table 1: Data from Ernst et al. (2008)

| Watershed | Total richness | EPT richness |
|---|---|---|
| WB1 | 35 | 12 |
| WB2 | 34 | 18 |
| EB1 | 21 | 5 |
| EB2 | 23 | 6 |
| EB3 | 32 | 11 |
| NV15 | 32 | 9 |
| WB3 | 27 | 12 |
| WB5 | 44 | 24 |
| WB6 | 43 | 21 |
| WB7 | 44 | 19 |
| WB8 | 44 | 20 |
| EB4 | 13 | 0 |
| EB5 | 23 | 5 |
| EB6 | 25 | 8 |
| NV16 | 37 | 13 |
| WB4 | 22 | 7 |

Table 2: Data from Burns et al. (2008)

| Watershed | DATI | Acid BAP 1987 | Acid BAP 2003 |
|---|---|---|---|
| TS | 56 | 0 | 2.08 |
| NH | 88 | N/A | 3.63 |
| EB | 83 | 8.04 | 9.06 |
| WS | 93 | 2.47 | 3.63 |
| BB | 16 | 8.24 | 6.72 |
| WC | 47 | 7.37 | 7.58 |
| WB | 2 | 9.27 | 9.25 |
| MB | 13 | 6.99 | 8.85 |
| B1 | 76 | 0 | 1.92 |
| NE7 | 74 | 0.65 | 1.88 |
| NE9 | 80 | N/A | 5.28 |
| NE10 | 88 | 7.83 | 7.35 |
| NW8 | 5 | 7.58 | 9.22 |

Table 3: Data from Baldigo and Lawrence (2000 & 2001)

| Watershed | Total fish density (#/$m^2$) | Fish species richness |
|---|---|---|
| BB | 0.6 | 3.0 |
| WS | 0.0 | 0.0 |
| WC | 0.5 | 3.0 |
| OP | 0.7 | 5.0 |
| WB | 1.0 | 5.0 |
| TS | 0.1 | 1.0 |
| NH | 0.1 | 2.0 |
| EB | 0.5 | 4.0 |
| MB | 1.6 | 6.0 |
| DC | 0.1 | 1.0 |
| UT | 0.0 | 0.0 |
| B2 | 0.1 | 1.0 |
| O1 | 0.4 | 2.0 |
| B1 | 0.3 | 1.0 |
| SM | 0.2 | 2.0 |
| O2 | 1.7 | 2.0 |

A.3 Chapter 4 raw data

Table 1. Stream chemistry used in hydrograph separations (data in bold was used in EMMA)

| Collect Date | Collect Time | Cl | Ca | **Si** | **O18** | **DOC** | $SO^{4-}$ | $NO^{3-}$ |
|---|---|---|---|---|---|---|---|---|
| 7/4/2007 | 13:00 | 0.34 | 5.17 | **1.89** | **-10.45** | **3.44** | 1.52 | 0.17 |
| 7/4/2007 | 19:15 | 0.26 | 3.02 | **1.51** | **-10.16** | **5.94** | 1.42 | 0.26 |
| 7/4/2007 | 21:30 | 0.21 | 3.64 | **1.42** | **-10.06** | **5.69** | 1.52 | 0.22 |
| 7/5/2007 | 0:30 | 0.14 | 2.16 | **1.36** | **-9.72** | **6.96** | 1.75 | 0.08 |
| 7/5/2007 | 4:30 | 0.20 | 3.82 | **1.49** | **-9.60** | **5.59** | 1.61 | 0.08 |
| 7/5/2007 | 6:30 | 0.21 | 4.26 | **1.56** | **-9.89** | **4.36** | 1.38 | 0.05 |
| 7/5/2007 | 9:30 | 0.20 | 4.72 | **1.67** | **-10.13** | **3.89** | 1.29 | 0.05 |
| 7/5/2007 | 12:30 | 0.30 | 4.02 | **1.76** | **-10.39** | **3.71** | 1.34 | 0.03 |
| 7/5/2007 | 18:30 | 0.32 | 5.23 | **1.77** | **-10.35** | **3.69** | 1.46 | 0.03 |
| | | | | | | | | |
| 7/19/2007 | 0:00 | 0.46 | 5.31 | **1.48** | **-10.78** | **3.54** | 1.18 | 0.21 |
| 7/23/2007 | 9:00 | 0.17 | 5.25 | **1.59** | **-10.79** | **4.01** | 1.38 | 0.38 |
| 7/23/2007 | 12:15 | 0.32 | 4.56 | **1.36** | **-10.74** | **4.27** | 1.22 | 0.77 |
| 7/23/2007 | 13:15 | 0.34 | 3.31 | **1.15** | **-10.65** | **5.03** | 1.22 | 0.49 |
| 7/23/2007 | 14:15 | 0.49 | 3.03 | **1.01** | **-10.56** | **5.21** | 1.20 | 0.41 |
| 7/23/2007 | 15:15 | 0.28 | 2.53 | **0.97** | **-10.53** | **5.40** | 1.08 | 0.38 |
| 7/23/2007 | 16:15 | 0.22 | 2.91 | **0.92** | **-10.40** | **5.74** | 1.15 | 0.14 |
| 7/23/2007 | 17:15 | 0.51 | 2.19 | **0.89** | **-10.22** | **5.68** | 1.16 | 0.14 |
| 7/23/2007 | 18:15 | 0.39 | 2.45 | **0.83** | **-10.22** | **5.71** | 1.12 | 0.13 |
| 7/23/2007 | 20:15 | 0.27 | 2.41 | **0.88** | **-10.16** | **5.29** | 1.09 | 0.15 |
| 7/23/2007 | 21:15 | 0.34 | 1.86 | **0.81** | **-10.25** | **5.19** | 1.22 | 0.11 |
| 7/23/2007 | 22:15 | 0.32 | 1.95 | **0.99** | **-10.22** | **5.09** | 1.24 | 0.09 |
| 7/24/2007 | 0:15 | 0.25 | 2.00 | **1.07** | **-9.84** | **4.59** | 1.24 | 0.10 |
| 7/24/2007 | 2:45 | 0.41 | 2.21 | **1.17** | **-9.68** | **4.63** | 1.25 | 0.18 |
| 7/24/2007 | 8:45 | 0.35 | 3.17 | **1.24** | **-10.00** | **3.98** | 1.22 | 0.26 |
| 7/24/2007 | 12:45 | 0.27 | 3.59 | **1.22** | **-9.99** | **3.89** | 1.29 | 0.31 |
| 7/24/2007 | 20:30 | 0.21 | 4.07 | **1.37** | **-10.49** | **3.55** | 1.16 | 0.34 |
| 7/25/2007 | 16:30 | 0.22 | 4.17 | **1.44** | **-10.49** | **3.02** | 1.16 | 0.39 |
| 7/26/2007 | 9:15 | 0.23 | 4.47 | **1.46** | **-10.69** | **3.19** | 1.17 | 0.41 |

| Collect Date | Collect Time | Cl | Ca | **Si** | **O18** | **DOC** | SO4- | NO3- |
|---|---|---|---|---|---|---|---|---|
| 9/5/2007 | 14:30 | 0.38 | 6.28 | **1.85** | **-10.80** | **2.81** | 1.50 | 0.20 |
| 9/8/2007 | 18:15 | 0.37 | 7.57 | **2.02** | **-10.20** | **3.84** | 1.57 | 0.16 |
| 9/9/2007 | 0:30 | 0.88 | 8.53 | **1.98** | **-10.50** | **3.94** | 1.60 | 0.19 |
| 9/9/2007 | 2:30 | 0.75 | 8.65 | **1.99** | **-10.40** | **4.69** | 1.57 | 0.42 |
| 9/9/2007 | 4:30 | 0.61 | 8.30 | **1.98** | **-10.50** | **4.21** | 1.70 | 0.24 |
| 9/9/2007 | 6:30 | 0.62 | 7.10 | **1.88** | **-10.40** | **3.96** | 1.33 | 0.35 |

Table 1 (Continued)

| | | | | | | | | |
|---|---|---|---|---|---|---|---|---|
| 9/9/2007 | 10:30 | 0.57 | 6.94 | **2.10** | **-10.30** | **3.86** | 1.54 | 0.42 |
| 9/9/2007 | 11:30 | 0.78 | 8.56 | **2.10** | **-10.30** | **5.56** | 1.48 | 0.40 |
| 9/9/2007 | 13:30 | 0.96 | 7.80 | **2.10** | **-9.80** | **6.67** | 1.63 | 0.25 |
| 9/9/2007 | 14:30 | 1.10 | 8.17 | **2.15** | **-9.70** | **6.89** | 1.58 | 0.22 |
| 9/9/2007 | 15:30 | 1.07 | 7.91 | **2.06** | **-9.60** | **7.06** | 1.39 | 0.19 |
| 9/9/2007 | 17:30 | 0.72 | 8.80 | **2.16** | **-9.60** | **6.40** | 1.55 | 0.17 |
| 9/9/2007 | 19:30 | 0.76 | 8.05 | **2.04** | **-9.60** | **5.42** | 1.58 | 0.17 |
| 9/10/2007 | 0:30 | 0.49 | 7.58 | **2.15** | **-9.60** | **4.89** | 1.68 | 0.17 |
| 9/10/2007 | 3:30 | 0.61 | 7.62 | **2.05** | **-9.80** | **4.65** | 1.88 | 0.25 |
| 9/10/2007 | 8:30 | 0.49 | 7.61 | **1.97** | **-9.90** | **4.46** | 2.02 | 0.20 |
| 9/10/2007 | 15:30 | 0.34 | 7.83 | **2.02** | **-10.00** | **5.81** | 1.93 | 0.16 |
| 9/10/2007 | 18:30 | 0.49 | 7.90 | **2.04** | **-9.70** | **6.22** | 1.93 | 0.14 |
| 9/11/2007 | 6:30 | 0.46 | 7.50 | **1.99** | **-9.80** | **4.35** | 1.82 | 0.14 |
| 9/11/2007 | 7:30 | 0.49 | 7.09 | **1.84** | **-9.90** | **5.05** | 1.90 | 0.15 |
| 9/11/2007 | 8:30 | 0.68 | 6.97 | **1.84** | **-9.80** | **7.38** | 1.87 | 0.15 |
| 9/11/2007 | 9:30 | 0.52 | 5.91 | **1.62** | **-9.20** | **9.91** | 1.85 | 0.17 |
| 9/11/2007 | 10:30 | 0.88 | 1.05 | **1.25** | **-8.90** | **12.90** | 1.64 | 0.14 |
| 9/11/2007 | 11:30 | 0.96 | 4.70 | **1.28** | **-8.80** | **18.43** | 1.89 | 0.14 |
| 9/11/2007 | 12:30 | 0.79 | 2.18 | **1.37** | **-8.60** | **13.27** | 1.62 | 0.14 |
| 9/11/2007 | 20:30 | 0.40 | 1.02 | **1.48** | **-8.90** | **8.18** | 1.59 | 0.14 |
| 9/11/2007 | 23:30 | 0.51 | 3.00 | **1.69** | **-8.90** | **8.01** | 1.41 | 0.15 |
| 9/12/2007 | 3:30 | 0.61 | 2.05 | **1.55** | **-9.20** | **6.13** | 1.68 | 0.15 |
| 9/12/2007 | 14:30 | 0.49 | 3.16 | **1.52** | **-9.40** | **5.88** | 1.64 | 0.20 |
| 9/13/2007 | 0:30 | 0.52 | 8.48 | **2.13** | **-9.50** | **5.30** | 1.45 | 0.14 |
| 9/13/2007 | 18:30 | 0.51 | 6.34 | **2.17** | **-9.90** | **4.31** | 1.35 | 0.19 |
| 9/14/2007 | 12:30 | 0.56 | 10.47 | **2.10** | **-10.21** | **3.37** | 1.32 | 0.19 |

| Collect Date | Collect Time | Cl | Ca | **Si** | **O18** | **DOC** | SO4- | NO3- |
|---|---|---|---|---|---|---|---|---|
| 9/27/2007 | 19:30 | 1.99 | 6.69 | **1.88** | **-9.50** | **7.15** | 3.98 | 2.36 |
| 9/27/2007 | 21:30 | 1.82 | 7.51 | **1.88** | **-8.20** | **18.58** | 4.06 | 0.42 |
| 9/27/2007 | 22:30 | 1.94 | 8.78 | **1.79** | **-8.00** | **12.82** | 4.59 | 2.11 |
| 9/27/2007 | 23:30 | 1.79 | 8.68 | **1.77** | **-8.20** | **9.91** | 4.48 | 1.35 |
| 9/28/2007 | 0:30 | 1.29 | 6.78 | **1.76** | **-8.50** | **8.66** | 2.07 | 0.23 |
| 9/28/2007 | 1:30 | 1.13 | 7.26 | **1.78** | **-8.70** | **8.14** | 2.12 | 0.15 |
| 9/28/2007 | 2:30 | 1.05 | 7.93 | **1.75** | **-8.50** | **7.31** | 2.17 | 0.15 |
| 9/28/2007 | 3:30 | 0.96 | 7.14 | **1.76** | **-9.00** | **7.40** | 1.97 | 0.16 |
| 9/28/2007 | 5:30 | 1.15 | 7.24 | **1.86** | **-9.10** | **6.99** | 1.71 | 0.17 |
| 9/28/2007 | 7:30 | 1.20 | 7.34 | **1.90** | **-9.50** | **6.56** | 1.89 | 0.18 |

Table 1 (Continued)

| | | | | | | | | |
|---|---|---|---|---|---|---|---|---|
| 9/28/2007 | 9:30 | 1.32 | 6.94 | **1.93** | **-9.50** | **6.47** | 1.43 | 0.54 |
| 9/28/2007 | 12:30 | 1.81 | 7.14 | **1.94** | **-9.40** | **4.63** | 1.50 | 0.95 |
| 9/28/2007 | 16:30 | 1.53 | 7.14 | **1.85** | **-9.69** | **4.65** | 1.28 | 0.38 |
| 9/28/2007 | 18:45 | 1.10 | 7.51 | **1.95** | **-9.67** | **3.46** | 1.81 | 0.19 |
| 9/28/2007 | 21:00 | 1.36 | 7.29 | **1.97** | **-9.90** | **3.33** | 1.53 | 0.94 |
| 9/28/2007 | 23:30 | 1.51 | 7.23 | **2.01** | **-10.20** | **3.15** | 1.78 | 0.15 |
| 9/29/2007 | 16:30 | 1.42 | 6.24 | **1.95** | **-10.30** | **3.12** | 1.65 | 1.24 |
| 10/1/2007 | 17:00 | 1.07 | 5.77 | **2.06** | **-10.40** | **3.09** | 3.87 | 1.73 |

| Collect Date | Collect Time | Cl | Ca | **Si** | **O18** | **DOC** | SO4- | NO3- |
|---|---|---|---|---|---|---|---|---|
| 10/8/2007 | 21:30 | 0.67 | 5.90 | **1.79** | **-10.06** | **4.14** | 1.60 | 0.21 |
| 10/8/2007 | 22:30 | 1.11 | 4.16 | **1.81** | **-9.88** | **5.89** | 1.85 | 0.19 |
| 10/8/2007 | 23:30 | 0.82 | 4.85 | **1.77** | **-9.65** | **6.71** | 1.91 | 0.19 |
| 10/9/2007 | 2:30 | 0.90 | 5.18 | **1.82** | **-9.38** | **7.82** | 1.92 | 0.18 |
| 10/9/2007 | 7:30 | 0.94 | 5.26 | **1.86** | **-9.49** | **5.51** | 1.92 | 0.16 |
| 10/9/2007 | 12:30 | 0.87 | 5.16 | **1.91** | **-9.68** | **5.10** | 1.92 | 0.14 |
| 10/9/2007 | 18:30 | 0.61 | 5.98 | **1.91** | **-9.62** | **5.46** | 1.67 | 0.17 |
| 10/9/2007 | 20:30 | 0.86 | 4.21 | **1.91** | **-9.41** | **7.24** | 2.01 | 0.16 |
| 10/9/2007 | 21:30 | 0.81 | 3.66 | **1.72** | **-9.35** | **7.58** | 1.96 | 0.18 |
| 10/9/2007 | 23:30 | 1.05 | 4.95 | **1.69** | **-9.29** | **8.37** | 1.98 | 0.14 |
| 10/10/2007 | 1:30 | 0.93 | 5.19 | **1.73** | **-9.32** | **6.32** | 1.96 | 0.14 |
| 10/10/2007 | 2:30 | 0.86 | 5.45 | **1.79** | **-9.39** | **5.89** | 2.04 | 0.14 |
| 10/10/2007 | 4:30 | 0.93 | 5.50 | **1.82** | **-9.42** | **4.98** | 2.07 | 0.15 |
| 10/10/2007 | 9:30 | 0.79 | 5.39 | **1.87** | **-9.51** | **4.75** | 1.65 | 0.17 |
| 10/10/2007 | 18:30 | 0.95 | 6.03 | **1.87** | **-9.79** | **4.39** | 1.95 | 0.23 |

| Collect Date | Collect Time | Cl | Ca | **Si** | **O18** | **DOC** | SO4- | NO3- |
|---|---|---|---|---|---|---|---|---|
| 10/19/2007 | 17:00 | 0.556 | 4.621 | **1.891** | **-10.28** | **4.73** | 1.545 | 0.685 |
| 10/19/2007 | 18:00 | 0.737 | 4.638 | **1.721** | **-10.15** | **5.39** | 1.548 | 0.623 |
| 10/19/2007 | 20:00 | 1.118 | 5.15 | **1.749** | **-9.42** | **10.01** | 1.791 | 0.431 |
| 10/19/2007 | 22:00 | 1.041 | 3.747 | **1.594** | **-9.285** | **11.24** | 1.692 | 0.224 |
| 10/19/2007 | 23:00 | 1.083 | 3.937 | **1.59** | **-9.088** | **9.76** | 1.932 | 0.245 |
| 10/20/2007 | 0:00 | 1.227 | 4.665 | **1.559** | **-9.019** | **8.99** | 2.031 | 0.226 |
| 10/20/2007 | 1:00 | 1.007 | 4.526 | **1.571** | **-9.157** | **10.23** | 2.082 | 0.22 |
| 10/20/2007 | 3:00 | 0.868 | 4.654 | **1.603** | **-9.276** | **8.93** | 2.048 | 0.29 |
| 10/20/2007 | 12:30 | 0.937 | 4.943 | **1.677** | **-9.388** | **5.26** | 1.8 | 0.533 |
| 10/21/2007 | 2:00 | 0.529 | 5.997 | **1.742** | **-9.788** | **5.22** | 1.404 | 0.525 |
| 10/21/2007 | 14:00 | 0.614 | 5.558 | **1.698** | **-9.768** | **3.12** | 1.708 | 0.709 |
| 10/22/2007 | 2:00 | 0.526 | 5.704 | **1.789** | **-9.757** | **4.59** | 1.705 | 0.744 |
| 10/22/2007 | 17:00 | 0.567 | 5.484 | **1.815** | **-9.954** | **3.29** | 1.626 | 0.767 |

Table 2. End-members used in hydrograph separations

| Location | Date | Time | Cl | Ca | Si | O18 | DOC | $SO^{4-}$ | $NO^{3-}$ |
|---|---|---|---|---|---|---|---|---|---|
| VSA | 7/4/2007 | 17:00 | 0.35 | 3.57 | 0.86 | -8.69 | 24.98 | 1.62 | 0.23 |
| Lysimeter | 7/5/2007 | 10:00 | 0.64 | 14.56 | 2.53 | -8.56 | 8.51 | 2.59 | 0.30 |
| R+TF | 7/4/2007 | 20:00 | 0.06 | 0.77 | 0.11 | -5.94 | 0.65 | 0.84 | 0.09 |
| R+TF | 7/5/2007 | 10:00 | 0.19 | 0.12 | 0.10 | -4.29 | 0.37 | 1.55 | 0.25 |
| VGW | 7/4/2007 | 17:00 | 0.69 | 22.18 | 1.44 | -9.80 | 8.15 | 0.68 | 0.02 |
| VGW | 7/5/2007 | 11:30 | 0.60 | 18.56 | 1.50 | -9.63 | 7.73 | 1.16 | 0.01 |
| SP1 | 7/4/2007 | 17:00 | 0.40 | 3.63 | 2.14 | -11.55 | 3.21 | 1.71 | 0.35 |
| SP2 | 7/5/2007 | 11:30 | 0.35 | 3.25 | 1.85 | -11.10 | 2.81 | 1.63 | 0.10 |

| Location | Date | Time | Cl | Ca | Si | O18 | DOC | SO4- | NO3- |
|---|---|---|---|---|---|---|---|---|---|
| VSA | 7/5/2007 | 10:30 | 0.27 | 0.33 | 0.43 | -7.16 | 18.12 | 1.81 | 0.24 |
| Lysimeter | 7/24/2007 | 18:45 | 0.64 | 11.26 | 2.79 | -8.10 | 11.53 | 3.55 | 0.41 |
| R+TF | 7/23/2007 | 18:00 | 0.40 | 0.26 | 0.06 | -4.30 | 1.20 | 0.22 | 0.19 |
| R+TF | 7/24/2007 | 14:45 | 0.43 | 0.16 | 0.07 | -3.70 | 1.60 | 0.21 | 0.20 |
| VGW | 7/23/2007 | 9:15 | 0.37 | 10.24 | 1.30 | -9.39 | 6.48 | 1.53 | 0.56 |
| VGW | 7/23/2007 | 19:00 | 0.32 | 33.16 | 0.72 | -9.60 | 5.96 | 1.56 | 0.53 |
| VGW | 7/24/2007 | 14:45 | 0.23 | 22.06 | 0.77 | -9.10 | 5.25 | 1.86 | 0.01 |
| SP1 | 7/23/2007 | 9:35 | 0.25 | 3.87 | 1.63 | -11.69 | 2.13 | 1.71 | 0.35 |
| SP1 | 7/23/2007 | 18:00 | 0.32 | 4.88 | 1.71 | -11.09 | 1.98 | 1.63 | 0.12 |
| SP1 | 7/24/2007 | 14:55 | 0.21 | 3.13 | 1.44 | -11.39 | 3.10 | 1.61 | 0.32 |

| Location | Date | Time | Cl | Ca | Si | O18 | DOC | SO4- | NO3- |
|---|---|---|---|---|---|---|---|---|---|
| VSA | 9/11/2007 | 12:30 | 2.03 | 5.19 | 0.54 | -9.34 | 28.23 | 1.46 | 0.12 |
| VSA | 9/15/2007 | 12:00 | 1.11 | 9.48 | 0.56 | -9.10 | 25.78 | 2.02 | 0.13 |
| Lysimeter | 9/15/2007 | 12:00 | 0.50 | 15.76 | 1.12 | -5.97 | 12.43 | 3.95 | 0.48 |
| R+TF | 9/15/2007 | 12:00 | 0.26 | 1.48 | 0.10 | -5.13 | 1.02 | 1.60 | 0.42 |
| R+TF | 9/8/2007 | 18:30 | 0.25 | 1.41 | 0.00 | -4.90 | 1.53 | 1.48 | 0.54 |
| R+TF | 9/9/2007 | 13:30 | 0.15 | 0.59 | 0.00 | -6.20 | 1.12 | 0.96 | 0.34 |
| R+TF | 9/10/2007 | 18:30 | 0.05 | 0.49 | 0.02 | -4.80 | 1.09 | 1.60 | 0.42 |
| R+TF | 9/11/2007 | 8:30 | 0.06 | 0.55 | 0.00 | -5.40 | 1.03 | 0.29 | 0.24 |
| VGW | 9/8/2007 | 18:30 | 0.26 | 19.47 | 1.69 | -9.90 | 10.12 | 0.61 | 0.03 |
| VGW | 9/9/2007 | 15:45 | 0.37 | 19.87 | 1.69 | -10.10 | 9.10 | 0.57 | 0.15 |
| VGW | 9/10/2007 | 18:30 | 0.23 | 19.37 | 1.59 | -10.20 | 9.14 | 0.96 | 0.06 |
| VGW | 9/11/2007 | 13:00 | 0.10 | 15.90 | 1.49 | -9.80 | 7.13 | 0.64 | 0.05 |
| SP1 | 9/8/2007 | 18:30 | 0.49 | 5.73 | 1.79 | -11.06 | 3.02 | 1.73 | 1.25 |
| SP1 | 9/9/2007 | 15:30 | 0.55 | 6.37 | 1.94 | -11.03 | 4.40 | 1.44 | 0.76 |
| SP1 | 9/11/2007 | 12:30 | 0.26 | 4.21 | 1.80 | -10.98 | 1.71 | 1.40 | 0.70 |
| SP3 | 9/11/2007 | 12:30 | 0.49 | 5.45 | 1.84 | -11.28 | 2.13 | 1.34 | 2.39 |

| Location | Date | Time | Cl | Ca | Si | O18 | DOC | SO4- | NO3- |
|---|---|---|---|---|---|---|---|---|---|
| VSA | 9/28/2007 | 13:00 | 0.54 | 5.60 | 0.74 | -7.70 | 23.56 | 2.02 | 0.13 |
| Lysimeter | 9/29/2007 | 12:00 | 0.64 | 11.26 | 2.79 | -8.10 | 11.53 | 3.55 | 0.41 |

Table 2 (Continued)

| | | | | | | | | | |
|---|---|---|---|---|---|---|---|---|---|
| R+TF | 9/27/2007 | 19:00 | 0.50 | 0.31 | 0.09 | -5.10 | 1..00 | 0.61 | 0.36 |
| R+TF | 9/28/2007 | 13:00 | 0.11 | 0.72 | 0.08 | -4.30 | 1.25 | 0.81 | 0.26 |
| R+TF | 9/28/2007 | 18:00 | 0.25 | 0.61 | 0.11 | -5.60 | 1.37 | 3.27 | 1.12 |
| R+TF | 9/29/2007 | 16:30 | 0.26 | 0.12 | 0.14 | -5.10 | 1.45 | 1.27 | 0.56 |
| VGW | 9/27/2007 | 12:00 | 1.51 | 18.80 | 1.96 | -9.80 | 6.51 | 1.92 | 1.26 |
| VGW | 9/28/2007 | 13:00 | 1.83 | 13.84 | 1.68 | -9.50 | 8.02 | 1.24 | 0.11 |
| VGW | 9/28/2007 | 16:45 | 0.66 | 16.93 | 1.60 | -9.60 | 8.16 | 0.95 | 0.32 |
| VGW | 9/29/2007 | 16:30 | 0.75 | 13.13 | 1.80 | -9.40 | 8.52 | 1.02 | 0.31 |
| VGW | 10/1/2007 | 17:00 | 0.34 | 14.08 | 1.38 | -9.70 | 8.25 | 0.84 | 0.05 |
| SP1 | 9/27/2007 | 12:00 | 0.51 | 6.64 | 2.34 | -10.90 | 3.27 | 1.40 | 0.93 |
| SP1 | 9/28/2007 | 13:30 | 0.47 | 6.26 | 2.29 | -10.90 | 3.20 | 1.22 | 0.65 |
| SP1 | 10/1/2007 | 17:00 | 0.47 | 6.12 | 2.16 | -10.80 | 2.51 | 1.31 | 0.85 |
| SP3 | 9/27/2007 | 12:00 | 0.85 | 6.77 | 2.41 | -10.80 | 1.24 | 2.82 | 0.73 |

| Location | Date | Time | Cl | Ca | Si | O18 | DOC | SO4- | NO3- |
|---|---|---|---|---|---|---|---|---|---|
| VSA | 10/10/2007 | 13:10 | 0.36 | 6.96 | 0.61 | -8.06 | 19.90 | 0.06 | 2.94 |
| VSA | 10/11/2007 | 13:40 | 0.33 | 5.55 | 0.62 | -7.07 | 18.61 | 0.12 | 2.55 |
| Lysimeter | 10/11/2007 | 14:00 | 0.53 | 8.90 | 2.22 | -8.17 | 10.15 | 2.91 | 0.32 |
| R+TF | 10/8/2007 | 12:00 | 0.47 | 0.30 | 0.04 | -5.62 | 1.55 | 0.68 | 1.35 |
| R+TF | 10/9/2007 | 9:30 | 0.41 | 0.06 | 0.02 | -3.92 | 0.58 | 0.51 | 1.16 |
| R+TF | 10/10/2007 | 8:00 | 0.34 | 0.34 | 0.03 | -3.62 | 0.92 | 0.43 | 0.84 |
| R+TF | 10/10/2007 | 13:30 | 0.37 | 0.71 | 0.05 | -3.50 | 1.28 | 0.64 | 0.93 |
| VGW | 10/8/2007 | 12:00 | 0.55 | 16.66 | 1.82 | -9.89 | 5.68 | 0.37 | 1.10 |
| VGW | 10/11/2007 | 13:00 | 0.58 | 13.94 | 1.83 | -9.75 | 5.35 | 0.33 | 1.06 |
| SP1 | 10/8/2007 | 12:15 | 0.48 | 6.13 | 2.06 | -11.15 | 4.18 | 1.02 | 1.68 |
| SP1 | 10/11/2007 | 13:35 | 0.79 | 5.95 | 2.14 | -10.99 | 2.61 | 1.00 | 1.67 |
| SP3 | 10/11/2007 | 13:45 | 0.53 | 6.96 | 2.12 | -11.05 | 0.96 | 2.63 | 1.31 |

| Location | Date | Time | Cl | Ca | Si | O18 | DOC | SO4- | NO3- |
|---|---|---|---|---|---|---|---|---|---|
| VSA | 10/20/2007 | 13:00 | 0.35 | 3.57 | 1.20 | -8.39 | 24.98 | 1.62 | 0.23 |
| VSA | 10/19/2007 | 10:00 | 0.38 | 4.59 | 1.43 | -8.25 | 20.89 | 2.01 | 0.25 |
| Lysimeter | 10/20/2007 | 12:00 | 0.64 | 14.56 | 2.53 | -8.56 | 8.51 | 2.59 | 0.30 |
| R+TF | 10/20/2007 | 13:00 | 0.43 | 0.27 | 1.42 | -6.26 | 0.10 | 0.27 | 0.22 |
| VGW | 10/22/2007 | 17:00 | 0.53 | 10.11 | 1.80 | -9.40 | 6.95 | 1.11 | 0.04 |
| VGW | 10/20/2007 | 13:00 | 0.19 | 9.16 | 1.77 | -9.50 | 4.66 | 1.01 | 0.16 |
| SP1 | 10/19/2007 | 10:00 | 0.43 | 4.98 | 1.86 | -11.00 | 2.54 | 1.55 | 1.25 |
| SP2 | 10/19/2007 | 10:00 | 0.44 | 0.47 | 1.99 | -10.90 | 2.12 | 1.54 | 1.84 |
| SP2 | 10/19/2007 | 18:00 | 0.53 | 6.96 | 2.12 | -10.50 | 0.96 | 1.31 | 2.63 |
| SP3 | 10/22/2007 | 17:00 | 0.72 | 3.89 | 1.95 | -10.60 | 3.06 | 1.54 | 1.89 |